ACTA UNIVERSITATIS SZEGEDIENSIS

ACTA MINERALOGICA-PETROGRAPHICA

Tomus XXXII

SZEGED, HUNGARIA

1991

NOTE TO CONTRIBUTORS

General

The Acta Mineralogica—Petrographica publishes original studies on the field of geochemistry mineralogy and petrology, first of all studies of Hungarian researchers, papers resulted in by cooperation of Hungarian researchers and those of other countries and, in a limited volume, papers from abroad on topics of global interest.

Manuscripts should be written in English and submitted to the Editor-in-chief, Institute of Mineralogy, Geochemistry and Petrography, Attila József University, H-6701 Szeged, Pf. 651 Hungary.

The authors are responsible for the accuracy of their data, references and quotations from other sources.

Manuscript

Manuscripts should be typewritten with double spacing, 25 lines on a page and space for 50 letter, in a line. Each new paragraph should begin with an indented line. Underline only words that should be typed in italics.

Manuscripts should generally be organized in the following order:

Title
Name(s) of author(s) and their affiliations, in foot-note the address of the author to whom the correspondence should be sent.
Abstract
Introduction
Methods, techniques, material studied, description of the area investigated, etc.
Results
Discussion or conclusions
Acknowledgement
Explanation of plates (if any)
Tables
Captions of figures (drawings, photomicrographs, etc.)

Abstract

The abstract cannot be longer than 500 words.

Tables

The tables should be typewritten on separate sheets and numbered according to their sequence in the text, which refers to all tables.

The title of the table as well as the column headings must be brief, but sufficiently explanatory.

The tables generally should not exceed the type-area of the journal, i.e. 12.5x18.5 cm. Foldouts can only exceptionally be accepted.

(continuation on the inner side of verso)

ACTA UNIVERSITATIS SZEGEDIENSIS

ACTA MINERALOGICA-PETROGRAPHICA

Tomus XXXII

SZEGED, HUNGARIA

1991

HU ISSN 0365—8066
HU ISSN 0324—6523

SERIES NOSTRA AB INSTITUTIS MINERALOGICIS, GEOCHIMICIS PETROGRAPHICIS UNIVERSITATUM HUNGARICUM ADIUVATUR

Nota

Acta Miner. Petr., Szeged

Kiadja

a József Attila Tudományegyetem Ásványtani, Geokémiai és Kőzettani Tanszéke
H-6722 Szeged, Egyetem u. 2—6

Kiadványunk címének rövidítése
Acta Miner. Petr., Szeged

SOROZATUNK A MAGYARORSZÁGI EGYETEMEK ROKON TANSZÉKEINEK TÁMOGATÁSÁVAL JELENIK MEG

CONTENTS

Acta Mineralogica-Petrographica, Szeged, XXXII, 5—19, 1991

Figaro (misurando)
Cinque... dieci... venti... trenta...
Trentasei... quarantatrè...
LORENZO DA PONTE (1786):
Le nozze di Figaro (musica di W. A. MOZART)

AQUEOUS SOLUBILITY OF MAGNESIAN CALCITES WITH DIFFERENT ENDMEMBERS*

FRIEDRICH LIPPMANN

Mineralogisch-Petrographisches Institut der Universität Tübingen**

ABSTRACT

The aqueous solubility of magnesian calcites has been studied on the basis of the total solubility product (LIPPMANN, 1980) for magnesite, dolomite, and huntite as possible endmembers. Deviations from ideal solid solubility were estimated in terms of excess lattice energies calculated from interionic distances for magnesite and huntite. In the case of the dolomite endmember, a value obtained by extrapolation of experimental high-temperature data could be used to describe deviations from ideal behaviour.

Solid solubility is limited, at 25 °C, by the spinodal points which were calculated for the endmembers magnesite, dolomite, and huntite to amount to 6, 3, and 18.3 mole percent Mg, respectively. Accordingly, huntite is the endmember that accounts for the full range of compositions observed in low-temperature magnesian calcites.

For the endmembers dolomite and huntite, new formulae are presented that express the total solubility product as the sum of partial solubility products and as functions of solid and aqueous compositions in the system $CaCO_3$—$MgCO_3$. The resulting phase diagrams depicting the aqueous solubility of magnesian calcites may serve as guidelines in experiments where such mixed crystals are to be equilibrated with suitably composed aqueous solutions.

KEYWORDS: Magnesian calcites, solubility (aqueous), solid solution, endmembers, magnesite, dolomite, huntite, spinode, phase diagram.

INTRODUCTION

Magnesian calcites (Mg calcites) are known to form in two different ranges of temperature. Quenchable mixed crystals (solid solutions) are in equilibrium with (calcian) dolomites in synthetic systems related to dolomitic marbles, i.e. in the system calcite-dolomite (*Fig. 1*). Solid solubility becomes noticeable from about 300 °C upwards to increase rapidly toward the upper critical point near 1100 °C above which solid solubility is complete between calcite and dolomite.

* A lecture on the same subject was held by the author in the Hungarian Academy of Sciences, Budapest, on 23 Sep. 1991

**D—72074 Tübingen, Wilhelmstrasse 56. Germany

Near earth-surface temperature, magnesian calcites occur in the submarine lithification of carbonate sediments with up to 18 mole percent Mg (MACINTYRE 1985) and as hard parts of certain organisms up to similar mole percentages.

Low-temperature magnesian calcites have been subjected to aqueous dissolution studies by a number of authors. Although all pertinent publications are unsatisfactory, because both experimental conditions and evaluation of results have been based on objectionable thermodynamic premises (LIPPMANN 1977, 1982), interesting qualitative information may be gleaned from some of the publications.

WALTER and MORSE (1984) have found that dissolution behaviour varies with the initial Mg/Ca ratio in the dissolving water. This result may be taken to discredit pure water as the unique solvent in experiments with magnesian calcites. However, it is interesting nonetheless that low-temperature and synthetic high-temperature magnesian calcites of comparable compositions behave in distinctly different ways when dissolved in destilled water (BISCHOFF, MACKENZIE and BISHOP 1987).

The main objection to the publications mentioned in the preceding paragraph is that aqueous solubilities of solid solutions are recalculated to unique solubility products involving activities risen to fractional powers. This practice has been criticised by LIPPMANN (1977, 1982), for it is in contradiction to the proof of the constancy of the solubility product at saturation, viz. that solid solutions be excluded (see e.g. PRIGOGINE and DEFAY 1954, p. 442; DENBIGH 1971, p. 308). In view of the experience that ionic interdiffusion is completely inhibited in solid solutions at ordinary temperature, it is strange that authors attribute so much importance to the "stoichiometric" character of the dissolution of magnesian calcites and propagate the concept of "stoichiometric saturation".

The latter term is a misnomer anyhow, because magnesian calcites are good examples for non-stoichiometric compositions as far as calcium and magnesium are concerned. Their initial dissolution behaviour is more appropriately described as "isochemical dissolution".

THE CONCEPT OF THE TOTAL SOLUBILITY PRODUCT

For a quantitative description of aqueous solubility of solid solutions within the framework of chemical thermodynamics, i.e. under equilibrium conditions, the solubility-product concept can be extended to solid solutions in the form of the total solubility product $\Sigma\Pi$, which is defined as the sum of partial solubility products Π_i contributed by the individual endmembers i of the solid solution (LIPPMANN 1980). Different from the ordinary solubility product valid only for pure endmember minerals, the total solubility product $\Sigma\Pi$ is not constant but is a function of the composition or mole fraction X_i of the solid solution. In a more complicated fashion, $\Sigma\Pi$ is a function also of the activity fraction X_{fi} of the component ions in the aqueous solution.

The graphical representation of $\Sigma\Pi$ as functions of the solid and aqueous compositions yields a variety of phase diagrams, depending on the degree of deviation from ideal behaviour in the solid solution. For example, in binary systems of carbonate minerals, the diagrams obtained show features familiar from vapour-pressure diagrams of binary liquid mixtures (LIPPMANN 1980, 1982).

The formulae derived by LIPPMANN (1980) may be applied to magnesian calcite in a straightforward way, if magnesite is assumed to be the endmember. This may appear unrealistic, since *Fig. 1* shows that dolomite is the magnesian component at elevated temperature.

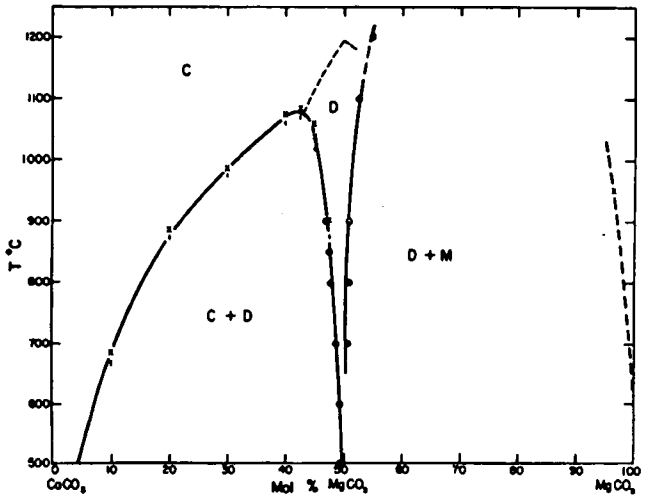

Fig. 1. Phase diagram of the system $CaCO_3$-$MgCO_3$ at elevated temperatures from GOLDSMITH and HEARD (1961). The diagram is polybaric, i.e. with increasing temperature, the pressure was increased to such a degree as to avoid the thermal decomposition of the carbonates.
C = calcitic phase, D = dolomitic phase, M = magnesite.
Notice that the meaning of these capital letters is different here from what it is in the text and in the explanations of the other figures. The region in which dolomite occurs as an ordered compound is delimited by a dashed line.

However, if we consider solid solutions quenched from above 1200 °C, we may choose magnesite as well, because dolomite is completely disordered above this temperature (GOLDSMITH and HEARD 1961). Aqueous solubility of such mixed crystals is governed by two partial solubility products:

$$[Ca^{2+}][CO_3^{2-}] = C[CaCO_3] \quad (1)$$

$$[Mg^{2+}][CO_3^{2-}] = M[MgCO_3] \quad (2)$$

The square brackets on the left-hand side denote the activities of the component ions in the aqueous solution. C and M are the solubility-product constants of pure calcite and magnesite, respectively. The square brackets on the right-hand side are the activities of the endmember in the solid solution which may be expressed by the product of the mole fraction X_i and the activity coefficient γ_i:

$$[Ca^{2+}][CO_3^{2-}] = CX_{Ca}\gamma_{Ca} \quad (1a)$$

$$[Mg^{2+}][CO_3^{2-}] = MX_{Mg}\gamma_{Mg} \quad (2a)$$

By analogy to the case of liquid mixtures, where partial pressures of the components are added to express the total vapour pressure, the sum of the partial

solubility products may be regarded as the total solubility product ΣΠ which represents the measure of the total solubility of the solid solution in water:

$$\Sigma\Pi = [Ca^{2+}][CO_3^{2-}]+[Mg^{2+}][CO_3^{2-}] \quad (3)$$

or

$$\Sigma\Pi = CX_{Ca}\gamma_{Ca} + MX_{Mg}\gamma_{Mg} \quad (3a)$$

and, with $X_{Ca} = 1-X_{Mg}$

$$\Sigma\Pi = C(1 - X_{Mg})\gamma_{Ca} + MX_{Mg}\gamma_{Mg} \quad (3b)$$

These equations for ΣΠ are consistent with the normal solubility product, which becomes apparent when one of the components is assumed to be absent from the system.

The activity coefficients γ_i are rendered, with fair approximation, (PRIGOGINE and DEFAY 1954, Eq. (16.48)) by:

$$\gamma_{Ca} = \exp(aX_{Mg}^2) \quad (4)$$

$$\gamma_{Mg} = \exp\{a(1 - X_{Mg})^2\} \quad (5)$$

Substitution in (**3b**) then yields ΣΠ as a function of the mole fraction X_{Mg}:

$$\Sigma\Pi = C(1 - X_{Mg}) \exp(aX_{Mg}^2) + MX_{Mg} \exp\{a(1 - X_{Mg})^2\} \quad (6)$$

According to a MADELUNG-VEGARD approach, which is based on the rigid-sphere model of lattice energy and is explained by LIPPMANN (1980), we have a=8.76 for calcite-magnesite mixed crystals assumed to form regular solid solutions, at 25 °C.

Evaluation of (**6**) involves the calculation of (**1a**) and (**2a**), i.e. the partial solubility products, which may be used to determine the composition of the aqueous solution in equilibrium with mixed crystals of solid mole fraction X_{Mg} in terms of mole fraction in the liquid phase or aqueous activity fraction, X_{lMg}:

$$X_{lMg} = \frac{[Mg^{2+}][CO_3^{2-}]}{[Ca^{2+}][CO_3^{2-}] + [Mg^{2+}][CO_3^{2-}]} = \frac{[Mg^{2+}]}{[Ca^{2+}] + [Mg^{2+}]} \quad (7)$$

In this way, each value of ΣΠ is dependent not only on its X_{Mg} according to (**6**) but is characterised in addition by the variable X_{lMg}, although no equation can be found expressing ΣΠ explicitly as a function of X_{lMg}, except in the case of ideal solid solutions (LIPPMANN 1980). On the one hand, ΣΠ may thus be plotted depending on X_{Mg}, and the resulting trace should be referred to as the *solidus* as in melting diagrams of solid solutions. On the other hand, the trace of ΣΠ versus X_{lMg} is named the *solutus* in a self-explanatory fashion. These traces are shown in *Fig. 2.*

In the solidus, ΣΠ rises steeply, from the solubility-product constant of pure calcite, for more than two orders of magnitude to a maximum near $X_{Mg}^{sp} = 0.06$ which is determined by:

$$X^{sp} = \frac{1}{2} \pm \sqrt{\frac{1}{4} - \frac{1}{2a}} \qquad (8)$$

(cf. PRIGOGINE and DEFAY 1954, Eq. (16.52); LIPPMANN 1980, Eq. (20); LIPPMANN 1982 Eq. (11)).

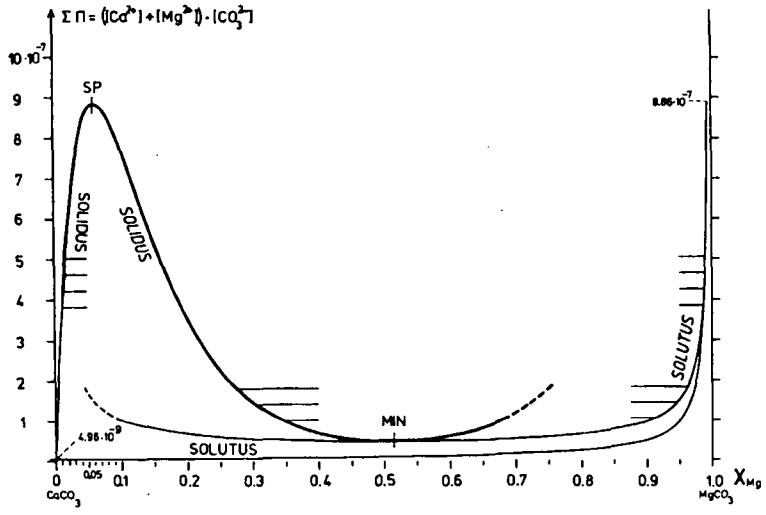

Fig. 2. Phase diagram depicting aqueous solubility of magnesian calcites with magnesite as the endmember. The spinodal point of the solidus is marked SP, that of the solutus is characterised by $\Sigma\Pi^{sp}=8.86 \cdot 10^{-7}$. The horizontal tie line connecting both spinodal points, i.e. both maximum compositions in equilibrium, has not been drawn.
The beginning and end points of four tie lines for solid compositions between 0.0125 and 0.0175 are indicated. They are supposed to connect these solid compositions with the aqueous ones in equilibrium.
Three tie lines for X_{Mg} = 0.275, 0.305 and 0.35, i.e. for values beyond the spinode, are indicated tentatively in order to illustrate the spinodal paradox, viz. that higher Mg in the solid would require lower Mg in the aqueous solution. Consequently solid solutions exceeding the spinodal point are unstable.
The values for the solubility-product constants of calcite $C = 4.96 \cdot 10^{-9}$ and magnesite $M = 6.37 \cdot 10^{-9}$ have been calculated from the data of ROBIE *et al.* (1978).
According to Eq.(16) of LIPPMANN (1982), a minimum of solubility, marked MIN, is located at X_{Mg}=0.514, a value exceeding the spinode. If M were smaller than C, which is possible within the limits of error, MIN would be below X_{Mg}=0.5 and thus fall into the range of calcian dolomites ("protodolomites"). It appears possible that MIN represents the only solid exceeding the spinode that can precipitate nonetheless. For, according to the theorem of GIBBS and KONOVALOV (see LIPPMANN 1980. p. 13), the aqueous solution in equilibrium has the same composition as the solid in this point.

Starting also from pure calcite, the solutus first runs almost horizontally to about X_{Mg} = 0.9 to rise steeply, near X^{sp}_{Mg} = 0.995, to the same maximum $\Sigma\Pi$ as the solidus. In chemical thermodynamics, the maximum is referred to as the spinode or the spinodal point. Solid solutions more concentrated than the spinodal compositions should be unstable on the basis of physical-chemical reasoning. In *Fig.* 2, the traces were continued beyond the spinodal point nonetheless, in order to show that solid compositions on either side of the spinode are characterised by

nearly the same X_{lMg}. This already shows, without any deeper reasoning, that hyperspinodal solid solutions are very unlikely to form.

The position of $\Sigma\Pi^{MIN}$ near X_{Mg}=0.5 might explain the formation of disordered phases near dolomite composition in rapid precipitations from concentrated solutions (SIEGEL 1961; ERENBURG 1961).

Even the magnesian calcites below the spinodal composition (X^{sp}_{Mg} = 0.06) are by no means stable solutions. The unusually high value of a=8.763 determines a miscibility gap fromX^{gap}_{Mg} = 0.000157 upwards according to:

$$\ln (1 - X^{gap}) - \ln X^{gap} = a (1 - 2X^{gap}) \qquad (9)$$

(cf. PRIGOGINE and DEFAY 1954, Eq.(**16.59**); LIPPMANN 1980, Eq.(**21**); LIPPMANN 1982, Eq.(**8**))

Therefore, in the system calcite-magnesite, the only stable phases, at ordinary temperature, are the practically pure endmembers. Moderately magnesian calcites, up to the spinodal composition, represent at most metastable phases, whereas more highly magnesian calcites are unstable. From this point of view, it is unlikely that low-temperature magnesian calcites, with up to X_{Mg}=0.18, are mixed crystals between calcite and magnesite. Even so, *Fig. 2* predicts that moderately magnesian calcites quenched from above 1200 °C may be in metastable equilibrium, at 25 °C, with aqueous solutions slightly belowX^{sp}_{lMg}= 0.995.

MAGNESIAN CALCITES WITH DOLOMITE AS THE ENDMEMBER

This choice of the endmember is suggested by *Fig. 1* for temperatures below 1100 °C. The miscibility gap between magnesian calcites and dolomite is characterised by an asymmetry which increases with temperature. According to GOTTSCHALK (1990), this is caused by thermal disorder in the dolomite phase. At ordinary temperature, where ordered dolomite is in equilibrium with disordered magnesian calcites, the gap is symmetrical so that the solid activity coefficients may be expressed by the one-term equations (**4**) and (**5**). The value for a = 8.774 has been extrapolated by GOTTSCHALK (1990) from experimental high-temperature data.

The partial solubility product of the dolomite component then is:

$$P_{1D} = X_{sD} D \exp (a(1 - X_{sD})^2) = [Ca^{2+}][Mg^{2+}][CO_3^{2-}]^2 \qquad (10)$$

where X_{sD} varying between zero and unity is the solid mole fraction, with X_{sD}=1 corresponding to X_{Mg}=0.5, and D is the solubility-product constant of dolomite.

The partial product of the calcite component must be written for the same number of Ca^{2+} ions as the preceding product, i.e. the square of the solubility product C of calcite must be used, in order to make both partial products dimensionally equivalent:

$$P_{2D} = (1 - X_{sD}) C^2 \exp (aX^2_{sD}) = [Ca^{2+}]^2[CO_3^{2-}]^2 \qquad (11)$$

Because in (**10**) the aqueous activity of Mg^{2+} is factored with that of Ca^{2+} there is no straightforward way of obtaining the activity fraction X_{lMg} in the aqueous solution as defined by (**7**).

A hypothetical aqueous mole fraction X_{lMg} must be written in terms of P_{1D} and P_{2D} which have to be factored with undetermined coefficients. The factors of P_{1D} are determined by putting P_{2D} = 0. The derivation of $\Sigma\Pi$ is similar to that of

$\Sigma\Pi_{dol}$ (LIPPMANN 1980, Eq. (27)) for pure dolomite. For $X_{Mg} = X_{lMg} = 0.5$, both products must be identical. The factor of P_{2D} turns out to be unity, and we obtain the total product for disordered magnesian calcites supposed to be in equilibrium, exactly at the miscibility gap (see below), with an ordered dolomitic phase:

$$\Sigma\Pi = \frac{2P_{1D} + P_{2D}}{\sqrt{P_{1D} + P_{2D}}} \tag{12}$$

It is the sum of two "pure" partial solubility products:

$$\Pi_{1D} = [Mg^{2+}][CO_3^{2-}] = \frac{P_{1D}}{\sqrt{P_{1D} + P_{2D}}} \tag{13}$$

and

$$\Pi_{2D} = [Ca^{2+}][CO_3^{2-}] = \frac{P_{1D} + P_{2D}}{\sqrt{P_{1D} + P_{2D}}} \tag{14}$$

Finally, determination of the factored coefficients yields the aqueous activity fraction as defined by (7):

$$X_{lMg} = \frac{P_{1D}}{2P_{1D} + P_{2D}} \tag{15}$$

which implies:

$$(1 - X_{lMg}) = X_{lCa} = \frac{P_{1D} + P_{2D}}{2P_{1D} + P_{2D}}$$

The latter equation is of essential importance in the derivation of (12), (13), and (14), before the factor of P_{2D} is known to be unity.

The resulting phase diagram (*Fig. 3*) is very similar to that for calcite-magnesite (*Fig. 2*) in that the abscissa $X_{Mg}=X_{lMg}=1$ in the latter seems to be replaced by $X_{Mg}=X_{lMg}=0.5$ in *Fig. 3*.

The spinodal maximum solubility is located at $X_{sD}^{sp} = 0.06$ according to (8), i.e. $X_{Mg}^{sp} = 0.03$. This means that low-temperature magnesian calcites, at any rate those with more than 3 mole percent Mg, must be regarded to be completely unstable and would not be able to form in the environments in which they are found, if dolomite would indeed be the endmember. The conclusion is that dolomite is definitely not eligible as the endmember of the more highly magnesian mixed crystals known, e.g., from sea urchins, coralline algae, and submarine lithifications.

The spinodal aqueous composition is $X_{lMg}^{sp} = 0.4948$. Consequently, magnesian calcites quenched from higher temperatures may be expected to equilibriate metastably, at 25 °C, when immersed in aqueous solutions close to that composition. Metastability even for compositions below 3 mole percent Mg is indicated by the miscibility gap calculated according to (9) to extend from $X_{sD} = 0.000155$, or $X_{Mg} = 0.0000775$ upwards. The position of this gap is still closer to pure calcite than for magnesite as the endmember. This is another expression of the experience that dolomite is the endmember for temperatures below 1200 °C. At first sight, it appeared tempting to prepare the complementary phase diagram for calcian

dolomites ("protodolomites") on the basis of the same endmembers and formulae. However, "protodolomites" are known to be disordered, which speaks in favour of magnesite as their endmember. Moreover, many calcian dolomites contain less Mg than the spinodal limit of $X_{Mg}^{sp} = 0.47$ in the system calcite-ordered dolomite. Finally, the spinodal aqueous composition in equilibrium of $X_{lMg}^{sp} = 0.0023$ is so low in Mg^{2+} that the formation of calcian dolomites from such a solution appears impossible from a kinetic point of view.

In this situation, it is felt that the conditions of formation of "protodolomites" are appropriately described by $\Sigma\Pi^{MIN}$ in *Fig. 2*. Variable Mg contents are probably due to the difference in temperature dependence of *C* and *M* to be substituted in Eq. (**16**) of LIPPMANN (1982). If this temperature dependence could be calibrated by precipitations in the laboratory, Mg contents in "protodolomites" might serve as sensitive geological thermometers.

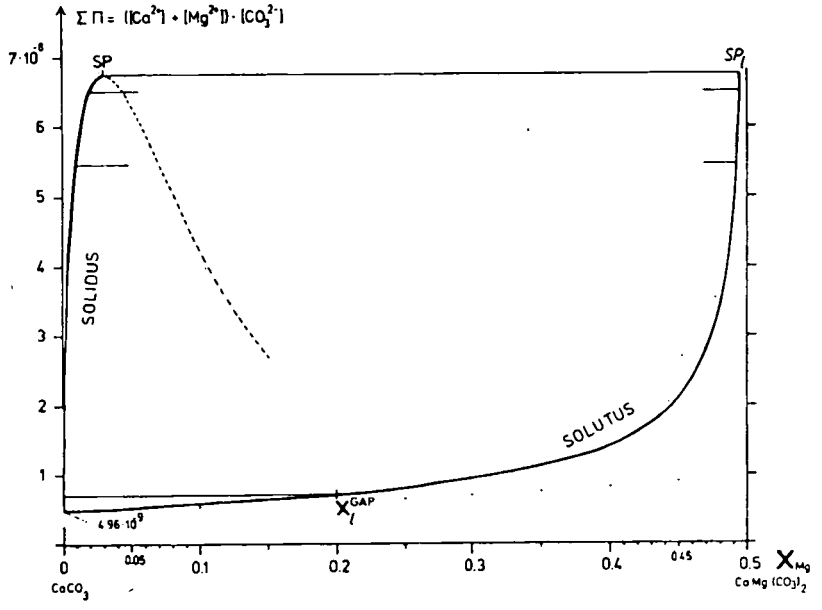

Fig. 3. Phase diagram depicting aqueous solubility of magnesian calcites with dolomite as the endmember. The spinodal point of the solidus is marked SP, that of that solutus SP_l. Both spinodal points are connected by the spinodal tie line which delimits the maximum compositions ($X_{Mg} = 0.03$ and $X_{lMg} = 0.495$) in metastable equilibrium. It is characterised by $\Sigma\Pi^{sp} = 6.76 \cdot 10^{-8}$.

Below this line, any number of horizontal tie lines might be drawn to connect any desired solid composition with its pertaining aqueous equilibrium composition and vice versa. Accordingly, tie lines for $X_{Mg} = 0.01$ and 0.02 and the aqueous equilibrium activity fractions $X_{lMg} = 0.492$ and 0.494, respectively, are indicated as examples. In addition, the complete tie line for the miscibility gap $X_{Mg}^{gap} = 0.0000775$ has been drawn ending at $X_{lMg}^{gap} = 0.20$.

The unstable part of the solidus is continued beyond the spinodal point by a dashed line. Two dots above the solutus indicate its unstable branch. The dots below the solutus show the eutectic solubility curve of pure calcite. Based on $C = 4.96 \cdot 10^{-9}$ and $D = 8.18 \cdot 10^{-18}$ as calculated from the data of ROBIE *et al.* (1978).

After the failure of a dolomite component to account for the full range of composition of low-temperature magnesian calcites, the only possibility left is to try huntite, $CaMg_3(CO_3)_4$, as the endmember. This is a strictly low-temperature mineral which has never been found to form in hydrothermal experiments with the system $CaCO_3$—$MgCO_3$. It is indeed one of the few minerals that have not been synthesized so far. At 25 °C, huntite is metastable with regard to magnesite and dolomite. This is indicated by the solubility diagram of huntite, (LIPPMANN 1980, 1982), where its solubility curve runs distinctly higher than the solutus curves of the other two carbonates.

The occurrences of huntite (see e.g. LIPPMANN 1973, p. 38-39) clearly attest to low formation temperatures. An instructive locality has been described by VEEN and ARNDT (1973) in a vertisol in N Australia, where huntite has formed along with aragonite in the same soil horizon.

The partial solubility product of the huntite component in magnesian calcites is:

$$P_{1H} = X_{sH} H \exp(a(1 - X_{sH})^2) = [Ca^{2+}][Mg^{2+}]^3[CO_3^{2-}]^4 \qquad \textbf{(16)}$$

$\mathbf{X_{sH}}$ varies between zero and unity and is the solid mole fraction. $\mathbf{X_{sH}}$=1 corresponds to X_{Mg} = 3/4 = 0.75. **H** = $3.44 \cdot 10^{-31}$ is the solubility-product constant of huntite as calculated from the thermochemical data of ROBIE *et al.* (1978). It is hoped to be internally consistent with the other solubility constants **C**, **M** and **D** taken from the same source.

The partial product of the calcite component must be written for four formula units for reasons analogous to the case of the dolomite endmember (**11**), and the fourth power of **C** must be used:

$$P_{2H} = (1 - X_{sH})C^4 \exp(aX_{sH}^2) = [Ca^{2+}]^4[CO_3^{2-}]^4 \qquad \textbf{(17)}$$

Information on the value of *a* can be derived from the crystal structure of huntite as determined by GRAF and BRADLEY (1962) and the refinement of DOLLASE and REEDER (1986). The structure is rhombohedral like that of calcite, both structures being based ultimately on the NaCl pattern. Huntite is ordered with respect to Ca and Mg. However, different from dolomite where Ca and Mg are segregated in alternate layers, the cations in huntite are ordered within individual cation layers. In this way, although huntite has an ordered structure, the cations are more evenly distributed throughout the lattice than they are in dolomite. In a way, the arrangement of the cations in huntite is thus closer to disorder than it is in dolomite.

Because the cation-anion distances calculated for huntite are remarkably uniform and individual values are rather close to an average of about 3.06 Å (Table 1), the MADELUNG-VEGARD approach of LIPPMANN (1980) could be used to estimate *a* for the system calcite-huntite. It comes as a surprise that the spinodal compositions obtained by substituting *a*(25 °C) in (**8**) fall into the range of maximum Mg contents known for low-temperature magnesian calcites when recalculated for the system $CaCO_3$—$MgCO_3$ (Table 1). The value derived from the model of GRAF and BRADLEY X_{Mg}^{sp}=0.173 is low and that from DOLLASE and REEDER X_{Mg}^{sp}= 0.196 is high in comparison to the maximum X_{Mg} values between 0.18 and 0.19 given by MACINTYRE for submarine magnesian calcite. Since the spinodal composition varies with temperature anyhow and formation temperatures appear to be difficult to determine, and so are rarely given by authors, the following

discussion will be based on $a(25\ °C) = 2.71$ as calculated from the mean interionic distance of both structure models.

TABLE 1.

$Ca^{2+} - CO_3^{2-}$ *distances in huntite structure (in Å)*
GRAF and BRADLEY (1962) DOLLASE and REEDER (1986)

Ca—C_{II}	3.060		3.069
Mg—C_I	3.063		3.066
Mg—C_{II}	3.076		3.051
Mg—C_{II}'	3.047		3.084
average	3.0615		3.0675
mean		3.0645	
$a(25\ °C)$	2.82	2.71	2.59
X_{sH}^{sp}	0.230	0.244	0.261
$X_{Mg}^{sp} = \frac{3X_{sH}^{sp}}{4}$	0.173	0.183	0.196

The near coincidence of calculated and observed maximum Mg contents would also justify the converse strategy of calculating values for a from maximum Mg contents, if formation temperatures were well documented for any occurrences of inorganic magnesian calcites. The derivation of the formula for $\Sigma\Pi$ as the sum of two "pure" partial solubility products and the expression for X_{lMg}, the aqueous activity fraction, is more involved than it is in the case of dolomite as the endmember but proceeds along with similar lines. A hypothetical aqueous mole fraction X_{lMg} is written in terms of P_{1H} and P_{2H} factored by undetermined coefficients. The factors of P_{1H} are determined by putting $P_{2H}=0$. We then have $X_{lMg} = 3/4$. $\Sigma\Pi$ is derived in an analogous fashion as $\Sigma\Pi_{hunt}$ (LIPPMANN 1980, Eq. (**29**)). By approaching $X_{Mg} = X_{lMg} = 3/4$, both products become equal. The factor of P_{2H} is found to be a complicated algebraic function of both P_{1H} and P_{2H}. After substitution and suitable algebraic transformations the total solubility product is expressed by:

$$\Sigma\Pi = \frac{4P_{1H}^{1/3} + 3P_{2H}^{1/3}}{\sqrt[4]{3^3\,(P_{1H}^{1/3} + 3P_{2H}^{1/3})}} \qquad (18)$$

It is the sum of the two "pure" partial solubility products:

$$\Pi_{1H} = [Mg^{2+}][CO_3^{2-}] = \frac{3P_{1H}^{1/3}}{\sqrt[4]{3^3\,(P_{1H}^{1/3} + 3P_{1H}^{1/3})}} \qquad (19)$$

and

$$\Pi_{2H} = [Ca^{2+}][CO_3^{2-}] = \frac{P_{1H}^{1/3} + 3P_{2H}^{1/3}}{\sqrt[4]{3^3\,(P_{1H}^{1/3} + 3P_{2H}^{1/3})}} \qquad (20)$$

It is remarkable that the cube roots of P_{1H} and P_{2H} figure in these equations and not the products themselves. With this knowledge, the derivation becomes easier by building the hypothetical aqueous mole fractions not only with undeter-

mined factors but by applying an undetermined exponent in addition. When this exponent is put 1/3, the desired formulae become shorter and simpler than for any other values, and the same expressions result for **(18)**, **(19)**, and **(20)**.

Both methods of derivation also yield the aqueous activity fraction as defined by **(7)**:

$$X_{lMg} = \frac{3P_{1H}^{1/3}}{4P_{1H}^{1/3} + 3P_{2H}^{1/3}} \qquad \textbf{(21)}$$

along with:

$$(1 - X_{lMg}) = X_{lCa} = \frac{P_{1H}^{1/3} + 3P_{2H}^{1/3}}{4P_{1H}^{1/3} + 3P_{2H}^{1/3}}$$

While they are still encumbered by the unknown factor of P_{2H} (and the unknown exponent), these aqueous activity fractions are of essential importance in the derivation of the preceding formulae.

The plot of $\Sigma\Pi$ versus X_{Mg} (solidus) and X_{lMg} (solutus) represents the phase diagram depicting the aqueous solubility of magnesian calcites with huntite as the endmember. It is shown in *Fig. 4*. The solidus starts to rise steeply from the solubility of pure calcite. It finally bends to run almost horizontally into the spinodal point SP determined by X_{lMg}^{sp}=0.183. Starting also from pure calcite, the solutus runs upward with increasing gradient, to end at the spinodal point of the aqueous solution *SP* characterised by X_{lMg}^{sp} = 0.692. In *Fig.4,* both spinodal points are connected by a horizontal straight line which represents the spinodal conode or tie line. It delimits the maximum metastable compositions.

According to **(9)**, a = 2.71 yields the mole fraction at the miscibility gap X_{sH}^{gap} = 0.1053. Multiplying this by 3/4=0.75, we obtain X_{Mg}^{gap} = 0.079 in the system $CaCO_3$—$MgCO_3$ for magnesian calcites at the gap between calcite and huntite. The aqueous activity fraction in equilibrium is X_{lMg}^{gap} = 0.688. The horizontal line connecting these mole fractions in equilibrium is the second conode shown in full in *Fig. 4*. It is remarkable that the aqueous equilibria of the more highly magnesian calcites are resricted to the relatively small area between these two tie lines.

Compositions with less than X_{Mg}^{gap} = 0.079 form stable solid solutions, whereas higher Mg contents, up to the spinodal composition, are only metastable in the system calcite-huntite. Since huntite itself is metastable already with respect to dolomite and magnesite, magnesian calcites below X_{Mg}^{gap} are also metastable from an absolute point of view. Compositions between the gap an the spinode may therefore be referred to as meta-metastable. This usage is followed in *Fig. 4*.

Like in the case of the endmembers magnesite and dolomite, magnesian calcites are subdivided by the gap into (meta)stable and (meta-)metastable solid solutions. However, in the latter cases, this difference in thermodynamic status is of minor importance, because X_{Mg}^{gap} merely defines extremely pure calcites. By contrast, in the case of huntite solid solutions, calcites containing sizeable amounts of Mg are subdivided into two classes of different thermodynamic status. It is felt that X_{Mg}^{gap} of about 0.08 might be accepted as the natural divide between highly and moderately magnesian calcites, provided it becomes possible to confirm this limit by suitable experimental methods.

The gradient of the solutus, when approaching the spinode, is not as steep as it is for magnesite or dolomite as the endmembers. The Mg content in the calcites

is nevertheless very sensitive to variations in the aqueous solution. This is illustrated by the three tie lines indicated in *Fig. 4* below the tie line of the gap for X_{Mg}=0.05, 0.03 and 0.02 which are in equilibrium with the aqueous activity fractions $X_{/Mg}$=0.682, 0.678 and 0.665, respectively.

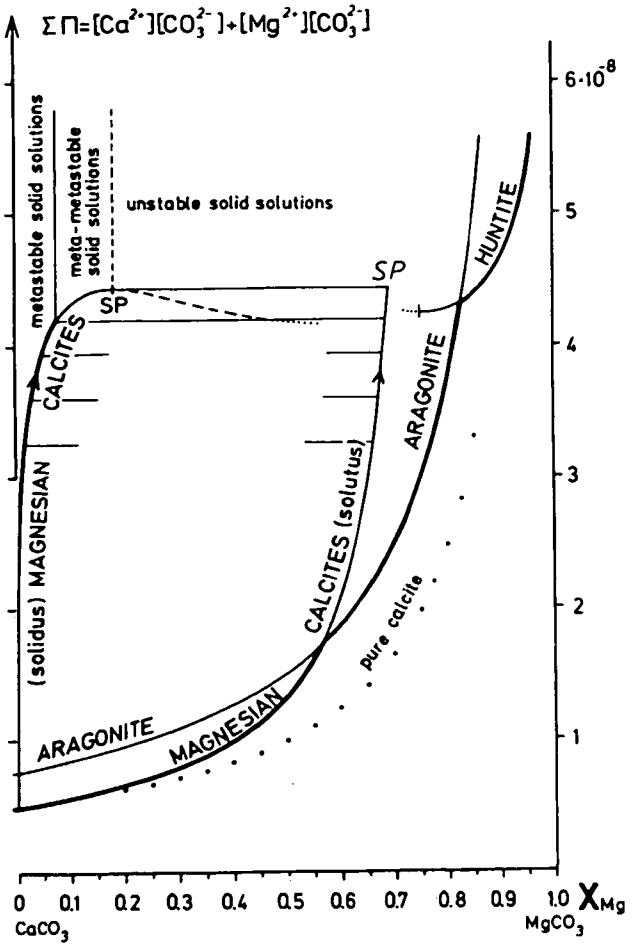

Fig. 4. Phase diagram depicting aqueous solubility of magnesian calcites with huntite as the endmember. In addition to the ΣΠ traces and the limits of solid solubility of the mixed crystals described in the text, the eutectic solubility curves of pure calcite (dotted) and aragonite are shown, as well as the peritectic saturation line of pure huntite.
The solutus is intersected by the solubility curve of aragonite between $X_{/Mg}$ = 0.5 and 0.6. This is in harmony with the observation that in slow precipitations of $CaCO_3$ from Mg bearing solutions, calcite forms below this range, whereas aragonite crystallises at higher values of $X_{/Mg}$ (LIPPMANN 1973, p.109 ff.).
The intersection of the saturation lines of aragonite and huntite may serve to characterise the solution in the soils where both minerals appear to have formed side by side (VEEN and ARNDT 1973).
Solid solutions on the huntite side of the diagram have been disregarded, because calcian huntites have not become known.

The conclusion is that organisms secreting magnesian calcites must be capable of stabilising the Mg/Ca ratio in their body fluids to a considerable degree, in order to precipitate a specific composition. It is conceivable that the required aqueous activity fraction is buffered by organic complexing agents originating from biochemical processes. Because the solubility of most magnesian calcites is higher than that of aragonite, the presence of organic surface "poisons" suppressing aragonite is required as well.

As for inorganically precipitated magnesian calcites, *Fig. 4* shows that formation from ordinary sea water characterised by $X_{/Mg}$=0.865 is not possible. Besides dilution with fresh water, another likely process to change the aqueous activity fraction to about 0.69 in interstitial sea water could be the production of CO_2 by decay of organic matter which could enhance the dissolution of $CaCO_3$ contained in the sediment.

SUMMARY AND IMPLICATIONS

The first reason to exclude magnesite as the endmember of low-temperature magnesian calcites has been the spinodal limit of 6 mole percent Mg. Moreover, the spinodal aqueous activity fraction of more than 99 mole percent Mg is highly unlikely to occur in the body fluids of organisms secreting magnesian calcites. Although $\Sigma\Pi^{SP} = 8.86 \cdot 10^{-7}$ is extremely high, it would be worth trying to equilibrate solids quenched from above 1200 °C with an aqueous solution of spinodal composition, because $\Sigma\Pi^{SP}$ is distinctly lower than the saturation line of aragonite, which runs near $1.5 \cdot 10^{-6}$ in the critical region. Reprecipitation of aragonite will thus not take place.

TABLE 2.

Summary of numerical results. Characteristic values calculated for magnesian calcites with different endmembers at 25 °C

Endmember:		magnesite $MgCO_3$	dolomite $CaMg(CO_3)_2$	huntite $CaMg_3(CO_3)_4$
The constant in (4) and (5)	a (25 °C)	8.763	8.774	2.71
		Values characterising miscibility gap		
Solid mole fraction	X_{Mg}^{gap}	0.000157	0.0000775	0.079
Aqueous equilibrium activity fraction	X_{lMg}^{gap}	0.563	0.200	0.688
Total solubility product	$\Sigma\Pi^{gap}$	$1.13 \cdot 10^{-8}$	$7.15 \cdot 10^{-9}$	$4.20 \cdot 10^{-8}$
		Values characterising spinode		
Solid mole fraction	X_{Mg}^{sp}	0.0608	0.0303	0.183
Aqueous equilibrium activity fraction	X_{lMg}^{sp}	0.9946	0.4948	0.6925
Total solubility product	$\Sigma\Pi^{sp}$	$8.86 \cdot 10^{-7}$	$6.76 \cdot 10^{-8}$	$4.435 \cdot 10^{-8}$

The main contribution of *Fig. 2* to carbonate petrology might be to explain the formation of calcian dolomites or "protodolomites" at ordinary temperatures by the minimum of solubility (MIN) near $X_{Mg} = 0.5$. By mapping this region of the diagram by rapid precipitations from solutions of slightly varying compositions and temperatures, our understanding of the mode of formation of "protodolomites" might be furthered.

Fig. 3 is certainly not helpful either in explaining the origin of magnesian calcites at earth-surface temperatures, because with the upper spinodal limit of 3 mole percent Mg for dolomite as the endmember, the range of metastable solids is still narrower than for magnesite. The only practical use of *Fig. 3* may be to serve as guide line in experiments where quenched high-temperature phases formed in equilibrium with dolomite are to be equilibrated with aqueous solutions near $X_{lMg} = 0.49$.

The main argument speaking in favour of huntite as the endmember is that it accounts for the full range of compositions of low-temperature magnesian calcites and that the spinodal point coincides very nearly with the maximum Mg contents observed in such phases. Additional arguments are the location of the spinodal aqueous composition at the intermediate value of $X_{lMg} = 0.69$, not too far from sea water, and the moderate value of the spinodal total solubility product $\Sigma\Pi^{SP} = 4.44 \cdot 10^{-8}$, which is only one order of magnitude higher than the solubility of pure calcite.

The diagram in *Fig. 4* should be tested by dissolving magnesian calcites in water containing Mg^{2+} and Ca^{2+} near the predicted spinodal aqueous composition, and in general with variable X_{fMg}. Because of the large number of possibilities, exploratory tests tried by the present writer have not yet yielded any definite results.

A different strategy would be to locate the spinodal points by suitable precipitation experiments. The exact position of the spinode depends, of course, on the accuracy of the constants to be substituted in **(16)** and **(17)**. However, since the cube roots of these partial products figure in **(21)**, the actual aqueous spinode may reasonably be expected to be rather close to 0.69. It is hoped that experiments as sketched above will finally lead to an empirical version of *Fig. 4*.

NOTE CONCERNING NOMENCLATURE

Because of the frequent occurrence of the term "magnesian calcites" in the text, the question naturally poses itself why the abbreviated form "Mg calcites" was not used for sake of brevity. Experience has shown that this is often read "magnesium calcite(s)". SCHALLER (1930) has pointed out the ambiguities that may arise from such usage. In the present case, "magnesium calcite" may be misunderstood as $MgCO_3$ for which the name magnesite has been defined, not to speak of "giobertite", an alternative name relegated to synonymy. Moreover, the use of "Mg calcites" has lead to such solecisms as "high magnesium calcite" and "low magnesium calcite", i.e. to expressions that are objectionable from the mere standpoint of grammar. SCHALLER's proposal to remedy the situation ("magnesian calcite") continues to be mandatory in mineralogical nomenclature (NICKEL and MANDARINO 1987).

REFERENCES

BISCHOFF, W. D., MACKENZIE, F. T. and BISHOP, F. C. (1987): Stability of synthetic magnesian calcites in aqueous solutions: comparison with biogenic materials. Geochim. Cosmochim. Acta **51**, 1413—1423.

DENBIGH, K. (1971): The principles of chemical equilibrium. 3rd ed. Cambridge University Press.

DOLLASE, W. A. and REEDER, R. J. (1986): Crystal structure refinement of huntite, $CaMg_3(CO_3)_4$, with X-ray powder data. Amer. Miner. **71**, 163—166.

ERENBURG, B. G. (1961): Artificial mixed carbonates in the $CaCO_3$-$MgCO_3$ series. Zhurnal Strukt. Khim. **2**, 178—182.

GOLDSMITH, J. R. and HEARD, H. C. (1961): Subsolidus phase relations in the system $CaCO_3$-$MgCO_3$. J.Geol. **69**, 45—74.

GOTTSCHALK, M. (1990): Internally consistent thermodynamic data in the system SiO_2-Al_2O_3-CaO-MgO-Na_2O-K_2O-H_2O-CO_2. Dissertation Tübingen (in German).

GRAF, D. L. and BRADLEY, W. F. (1962): The crystal structure of huntite, $Mg_3Ca(CO_3)_4$. Acta Cryst. **15**, 238—242.

LIPPMANN, F. (1973): Sedimentary carbonate minerals. Berlin, Heidelberg, New York: Springer.

LIPPMANN, F. (1977): The solubility products of complex minerals, mixed crystals, and three-layer clay minerals. N. Jb. Miner. Abh. **130**, 243—263.

LIPPMANN, F. (1980): Phase diagrams depicting aqueous solubility of binary carbonate systems. N. Jb. Miner. Abh. **139**, 1—25.

LIPPMANN, F. (1982): Stable and metastable solubility diagrams for the system $CaCO_3$-$MgCO_3$-H_2O. Bull. Minéral. **105**, 273—279.

MACINTYRE, I. A. (1985): Submarine cements — the peloidal question. Soc. Econ. Paleont. Mineral. Spec. Publ. No. 36: 109—116.

NICKEL, E. H. and MANDARINO, J. A. (1987): Procedures involving the IMA commission on new minerals and mineral names, and guidelines on mineral nomenclature. Can. Mineral. **25**, 353—377.

PRIGOGINE, I. and DEFAY, R. (1954): Chemical thermodynamics; transl. by EVERETT, D. H. London: Longman.
ROBIE, R. A., HEMINGWAY, B. S. and FISHER, J. R. (1978): Thermodynamic properties of minerals and related substances at 298.15 °K and 1 bar (10^5 Pascals) pressure and higher temperatures. U. S. Geol. Surv. Bull. **1259.**
SCHALLER, W. T. (1930): Adjectival ending of chemical elements used as modifiers to mineral names. Amer.Mineral. **15**, 566—574.
SIEGEL, F. R. (1961): Factors influencing the precipitation of dolomitic carbonates. State Geol. Survey Kansas Bull. **152**, 127—158.
VEEN, A. W. L. and ARNDT, T. W. (1973): Huntite and aragonite nodules in a vertisol near Katherine, Northern Territory, Australia. Nature Physical Sci. **241**, 37—40.
WALTER, L. M. and MORSE, J. W. (1984): Magnesian calcite stabilities: a reevaluation. Geochim. Cosmochim.Acta **48**, 1059—1070.

Manuscript received, 31 October, 1991

Acta Mineralogica-Petrographica, Szeged, XXXII, 21—36, 1991

GEOCHEMICAL FACIES ANALYSIS OF QUATERNARY PELITIC SEDIMENTS OF THE NORTH-EASTERN PARTS OF THE GREAT HUNGARIAN PLAIN (ALFÖLD)

G. SZÖÖR, I. BARTA, P. SÜMEGI

Department of Mineralogy and Geology, Kossuth Lajos University*

L. KUTI

Hungarian Geological Survey**

ABSTRACT

Within the framework of the geological mapping of the Great Hungarian Plain in the scale 1:100,000 mineralogical-geochemical analysis of sediments have been carried out from 94 boreholes of 30 m depth on the section of Nyírség-Szatmár Plain-Bodrogköz. Primarily, pelitic sediments exposed and their underlying and overlying beds were in the focus of the investigations. In this paper, the most important results are reviewed. On the basis of the detailed sedimentological, mineralogical and geochemical studies, it has become possible to characterize the formations from a mineralogical-geochemical point of view and distinguish the facies groups; in this way, the eolic and fluvial environments of the sedimentation are distinguishable from each other. The further aim of the authors is to suggest a new geochemical facies analysis model for the development of knowledge of Quaternary lithostratigraphical formations.

INTRODUCTION

In course of the complex geological mapping of the Great Hungarian Plain (RÓNAI 1985), most of the loose near-surface sediments were prospected by shallow boreholes, typically 10 m deep, planted in a network of 1.5·1.5 kms. This depth and density was adequate on the regions lying to the East of the Tisza (Tiszántúl) and the Danube-Tisza interfluvial region (Duna-Tisza köze). These regions were formerly investigated in details by previous mapping and, consequently, quite a number of data were already available on them. Opposed to this, on the North-Eastern parts of the Alföld we had deficient information on near-surface layers. For a more profound and detailed knowledge on these parts, apart from the shallow boreholes planted in a network, there were 94 boreholes more planted along five sections with 30 m depth (*Fig. 1*). Most of the cores from these boreholes were subjected to, apart from routine analyses generally practiced in mapping, a more detailed mineralogical, sedimentological, geochemical and palaeontological analysis. The reports on these analyses are deposited in the archives of the Hungarian Geological Survey.

* H—4010 Debrecen, P.O.Box. 4, Hungary
**H—1442 Budapest, P.O.Box. 106, Hungary

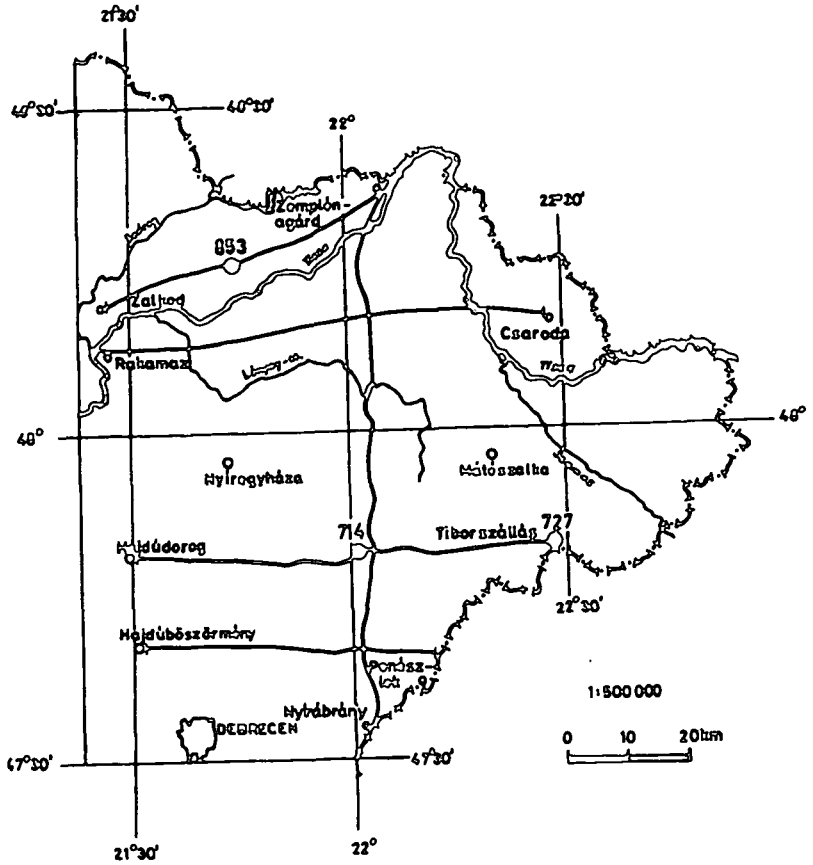

Fig. 1. Sketch map of the geological sections (o—o) and type-exposures (boreholes o 714, 727, 853).

One of the most important elements of these series of examinations has been the comparative geochemical analysis of the pelitic sediments, rich in fine grain fraction (BARTA and SZÖÖR 1983; BARTA *et al.* 1985). The mineralogical and geochemical analyses were focused on the determination of the mineral paragenesis which were not determinable by petrological microscopy, as well as the classification of the chemical character of the constituent formations. The clay mineral and carbonate paragenesis, amorphous and organic constituents were defined with thermoanalytical method, X-ray analysis and IR-spectroscopy.

Traditional wet chemical methods were used for the determination of the basic components of the sediments, its organic-, total sulphur- and lime content. Optical emission spectroscopy and atomic absorption spectroscopy were used for trace element analysis. From 28 components determined,13 were evaluated in details. The total U and Th content of the samples were determined lately (DARÓCZI *et al.* 1990), namely the so-called U-ekv value, that was also utilized in this paper.

The numerous data in our examination series enabled us to make a geochemical facies analysis on the samples (on the concept of "geochemical facies", see KEITH and DEGENS 1959; KREJCI-GRAF 1966; ERNST 1970). The primary aim of

this was the facies classification of the formation by geochemical methods. A more profound knowledge on the lithofacies and the chemofacies can result in tracing relations in the processes of denudation, sedimentation and diagenesis.

The importance of geochemical analysis is further stressed by the lack of fossils, or scarcity of fossils in most of the samples (both vertebrate and malacological material), therefore their traditional biostratigraphical evaluation was impossible to accomplish. Moreover, on a considerable part of their grained sediments (sands) on this area, opened by these boreholes as well, sedimentological, palaeogeographical and litho-faciological analysis has already been performed (BORSY *et al.* 1981, 1985, 1988; CSONGOR and FÉLEGYHÁZI 1987; MOLNÁR *et al.* 1988), whereas no report on the intercalated pelitic formations has been published as yet.

The volume of this paper does not allow a detailed presentation of the mineralogical and geochemical analyses; therefore, results will be presented on the basis of the three sections examined in the most detailed way. Interpretation of the results will be complemented by experiences on other boreholes as well.

LITHOFACIOLOGICAL DESCRIPTION

The three 30 m deep boreholes selected for presentation here were deepened at three spots with different geological construction. Borehole Nr. 714 was situated in the Nyírség region, East of the village Kisléta, borehole Nr. 727 to the North-East of Tiborszállás on the Szatmár Plain, while borehole Nr. 853 was planted to the South of Karcsa in the Bodrogköz region (*Fig. 1.*). The boreholes transsected formations of similar age (Holocene and Upper Pleistocene) and different genetics and geological history. It is a common feature in the section with different layer sequence that fine and coarse grain sediments are alternating in them several times (independent and different from each other) and, the formations are void fossils.

In the sequence of borehole Nr. 714, Late Pleistocene eolic sediments dominate (eolian sand, loessy sand, loess; *Fig. 2.)* Different genetics can only be supposed for the densely alternating layers transsected at 12.6—15.6 m. These grey, dark grey sandy rocks, silty sand layers of a few cms width were formed in the depressions of the former sandmoulds. Their formation was possibly similar to those observable on recent surface as well: depressions getting damp and marshy in wet seasons and drying out in the dry season. Increasing sandy fraction indicates more dry, increasing pelitic fraction, dark colour and considerable organic content denotes more humid periods. This alternating layer complex was overlain by light yellow loess, loessy sand and, later, eolic sand. Under the alternating layer there was 2 metres of sand and below this, 10 m thick layer of loess. These deeper lying layers are already all grey. The sand varieties of the section are dominantly small grained, with roughly equal medium- and fine grain fraction (10—20%). In the loesses exposed, apart from coarse silt, the fine silt and clay content can reach 30—50 %, while sand content can occasionally exceed 30 %. The carbonate content of the sediment is small, enriching to some extent in the phase between 18.5—19.0 m.

In the section of borehole Nr. 727 (*Fig. 3.*) we can find silty layers with considerable amount of pelitic fraction and organic matter till 10 metres from the surface, probably the result of freshwater-riparian sediments. Starting from the surface, the colour of the layers is black, yellow, yellowish grey, grey, blackish-grey and brown. The light yellow sediments at the depth of 1.5—3.0 m are lime concretions. Probably the whole silty complex, or at least its upper meters are of

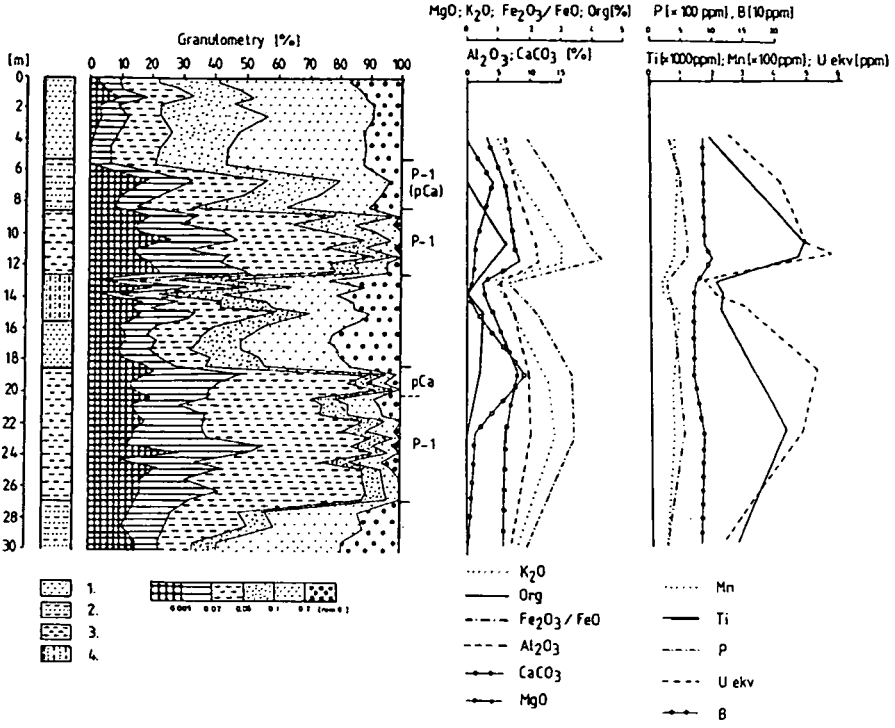

Fig. 2. Stratigraphy, lithological and geochemical facies of the borehole Nr. 714. 1=sand; 2=silty sand; 3=clayey silt; 4=sand and silty sand. P-1 and pCa=subfacies.

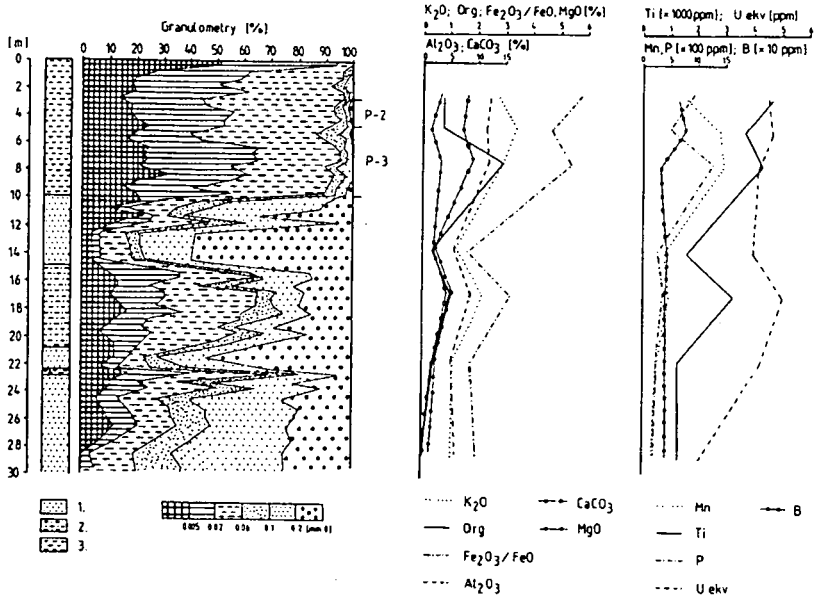

Fig. 3. Stratigraphy, lithological and geochemical facies of the borehole Nr. 727. 1=sand; 2=sandy silt and silty sand; 3=clayey silt. P-2 and P-3=subfacies.

Holocene age but there are no fossil or other time-indicating proofs of that. Deeper lying sediments are of Upper Pleistocene age. Under the near-surface silt of 10 meters, the sequence is composed of alternating layers of grey sand and grey sandy silt in different thickness. The composition of grains and macroscopic features (e.g., unperfectly worn grains) denote riverine-riparian environment of sedimentation.

In the sequence of borehole Nr. 853 (*Fig. 4.*), till 22.5 meter depth we can find clay and fine silt, under it, sand is dominating. Along the whole sequence, grey colour is dominating with the exception of the top soil layer (30 cms) which is brown. Small-grained sand between 3.4—6.0 m is yellowish grey, the clayey silt between 9.0—25.0 m is greenish grey with spots stained by vivianite. Towards the bottom (till 24 m) the sands get more coarse; at 24.0 m reaching medium grain sand and, after it, getting again finer. As opposed to sand, layers of silt get finer towards the bottom with increasing clay content.

On the basis of the grain composition and macroscopic features as well as alternating amount of organic matter we can suppose that the borehole exposed variable riverine, riparian and marshy sediment. Under 21.7 m the genetics of the sand layers are uncertain, comprising features denoting riparian and eolic origin as well.

There are no proofs concerning the age of the layers. Probably the upper meters were deposited already in the Holocene, while deeper lying layers belong to the Upper Pleistocene.

GEOCHEMICAL FACIES DIVISION

Analysis of the geochemical facies can be performed by several methods like suitable facies indicators — classification of mineral paragenesis, determination of elements, comparison of elements, organic and non-organic compunds, ratio of stabile isotopes etc. For the characterization of the variable clayey formations with different genetics, determination of mineral phases based on thermal analysis was used (mineral paragenesis classification). Thermoanalytical parameters based on characteristic run-off of **DTA** curves and corresponding temperature values as well as **DTG—TG** curves represent well the quality and quantity clay minerals and carbonates in the sample. The elements and pairs of elements seemingly most suited for facies indications were selected from the chemical data by computer-aided investigation. The pelitic formations in the near-surface Quaternary sediments of the North—Eastern parts of the Great Hungarian Plain were separated into geochemical groups presented below.

CARBONATIC PELITE FACIES GROUP

This facies group comprises clayey silts and silty clay varieties where the total amount of carbonate exceeds 10 percent.

Carbonates are present in the sediments in the form of coating to mineral grains forming sometimes this lime silt veins or small concretions (some mms large). There are also some Molluscan shell fragments as well.

Sediments of this type are light yellow in air dry state, sometimes stained by ochre. The constituents found by our analyses were calcite, aragonite (in Molluscan shells only), magnesito-calcite, calcium carbonate with Mg content in the form of amorphous precipitates, siderite, dioctahedric clay mica (illite), illite-smectite

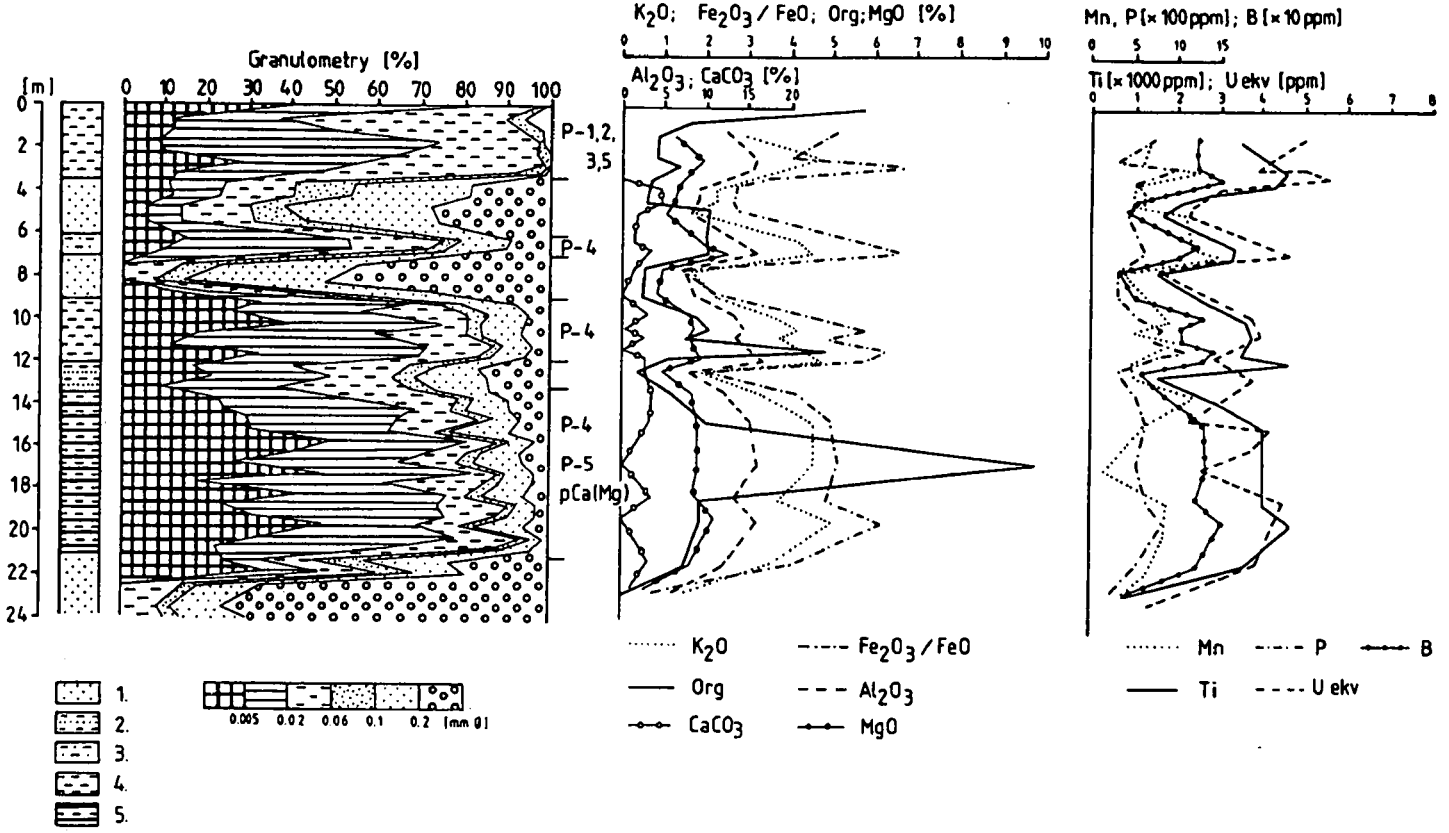

Fig. 4. Stratigraphy, lithological and geochemical facies of the borehole Nr. 853.
1=sand; 2=silty sand; 3=sandy silt; 4=clayey silt and silt; 5=silty clay. P-1 — P-5 and pCa(Mg)=subfacies.

(montmorillonite) mixed structure, kaolinite, sericite and X-ray amorphous precipitates. The carbonate content, determined by thermogravimetry, is 11.73—29.46 %, by Scheibler's calcimetry, 7.0—23.2 %. Its organic matter content is between 0.63—2.14 (thermogravimetric result) and 0.50—2.50 % (oxidimetric titration), respectively. TG parameters in respect of clay minerals are $H_2O(I)$ = 2.42— 4.17 %; $H_2O(II)$ = 1.30—1.43 %.

There were three types separated within the facies group corresponding to, at the same time, genetical categories as well.

CALCIUM-CARBONATIC PELITE FACIES TYPE (MARKED AS pCa)

Silts, sandy silts formed in the depressions between the sand mounds, containing relatively high amount of carbonates can be assigned to this group. Their basement and, often, their cover is composed of, typically, eolian sand with rounded grains. Their type section is represented by borhole Nr. 714, where their geochemical character could be studied best (*Fig. 2.*). Their thermoanalytical character is demonstrated on the graph marked A on *Fig. 5.* Indicator minerals of the sediments are dioctahedric clay mica (illite) and calcite, typical feature is low organic matter content. Total amount of iron oxides (Fe_2O_3/FeO) = 2—3 % (the ferro- and ferri-iron content of the rocks were not determined separately, because after preparation samples got oxidated in course of storing), Mn=50—100 ppm, Mg=0.5—1.5 %. Formations of this type were found on the NE Alföld region only in boreholes deepened in the region of the Nyírség.

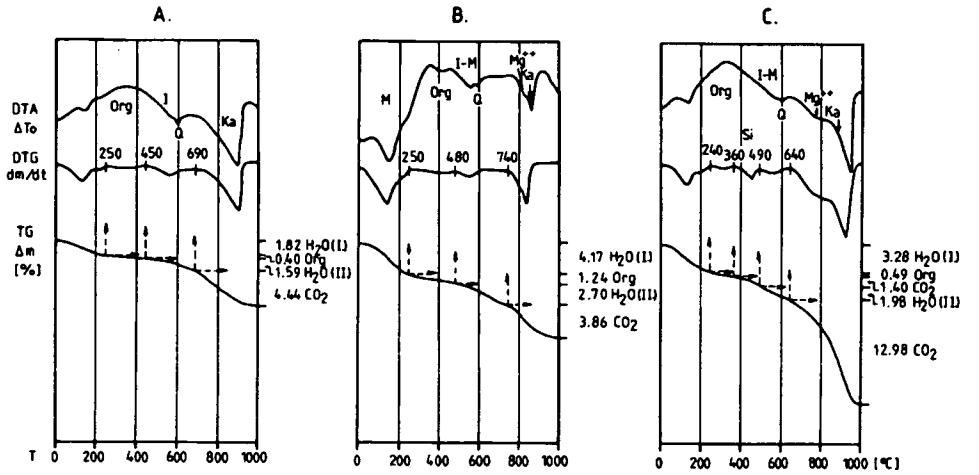

Fig. 5. Characteristic thermoanalytical curves and parameters of the carbonate-pelitic facies. A=pCa subfacies, borehole 714. 18.5—19.0 m B=pCa(Mg) subfacies, borehole 724. 5.5—6.0 m C=pCa(Fe) subfacies, borehole 724. 7.0—7.5 m Org=organic material, I=illite, I-M=illite-montmorillonite mixed layer, Q=quartz, Ka=calcite, Mg^{++}=protodolomite, magnesitocalcite, Si=siderite.

CALCIUM—MAGNESIUM—CARBONATIC PELITE FACIES TYPE (MARKED AS pCa/Mg)

Part of the riverine and riparion clayey silts belong to this group. Their basement is clay, containing very few or no carbonate, under which we find riverine sand. The characteristic but fairly varied sediments of this type are well represented by samples taken from the 14.5—15.0 m and 18.0—18.5 m phases of borehole Nr. 853. The carbonate content of theses samples is over 10 %. Their thermoanalytical characteristics are represented on the graph marked B on *Fig. 5.* Indicator minerals for this group comprise magnesito-calcite (proto-dolomite), illite-montmorillonite mixed structure and a considerable amount of organic matter. Total iron oxide content (Fe_2O_3/FeO)=4—5%, Mn = 500—750 ppm, MgO = 1.5—2.5 %.

Such sediments were found in boreholes deepened on the Szatmár Plain and in the Bodrogköz region as well.

SIDERITIC PELITE FACIES TYPE (MARKED AS pCa/Fe)

Light coloured yellowish grey, greyish green and bluish grey material formed at the border region of marshes, bogs in the oxidative environment of water inflows.

The basement and cover of these formations is composed of clayey layers containing no or very little carbonate with numerous plant fossils and Molluscan shell fragments.

The thermoanalytical characteristics of the subsurface are represented on graph marked C on *Fig. 5.* Indicator minerals are siderite, amorphous carbonates with Mg^{++} and Ca^{++} and calcite/magnesito-calcite. Characteristic clay mineral is illite-montmorillonite mixed structure. X-ray analysis could reveal the presence of sericite and chlorite as well. The facies is characterised by low organic matter content.

Total iron oxide content (Fe_2O_3/FeO)=5—7%, Mn = 1500—5000 ppm. MgO = 2.0—2.5 %.

On our area, only two boreholes exposed such type of sediments. Borehole Nr. 724 in the Nyírség, to the North of Mérk and borehole Nr. 852 in the Bodrogköz, to the North of Cigánd. This later sample contained some kaolinite as well.

LOW OR NO CARBONATE PELITE FACIES GROUP

The pelitic sediments exposed by the boreholes are, on the basis of their grain size composition, clayey silt or silty clay varieties. Their carbonate content is 5%, often with no carbonate at all. Their colour is varied, in air-dry state from greenish grey and brownish grey till dark grey, in some cases, stained by yellow and brown limonite, black manganese dioxide or blue vivianite. Mainly they are microlaminated or striped, occassionally with plant fossils, Molluscan shell fragments, manganese dioxide or limonite micro-concentrations. Constituents detected include montmorillonite, chlorite, sericite, illite, kaolinite, vivianite, amorphous pyrite, carbonate precipitate. Organic matter in the samples can be present in the form of macroscopically observable plant remains or intermittent material dispersed between the grains as well as huminelignine complexes. The indicator minerals

and characteristic geochemical composition is discussed in details at the specific description because of their widely variable values.

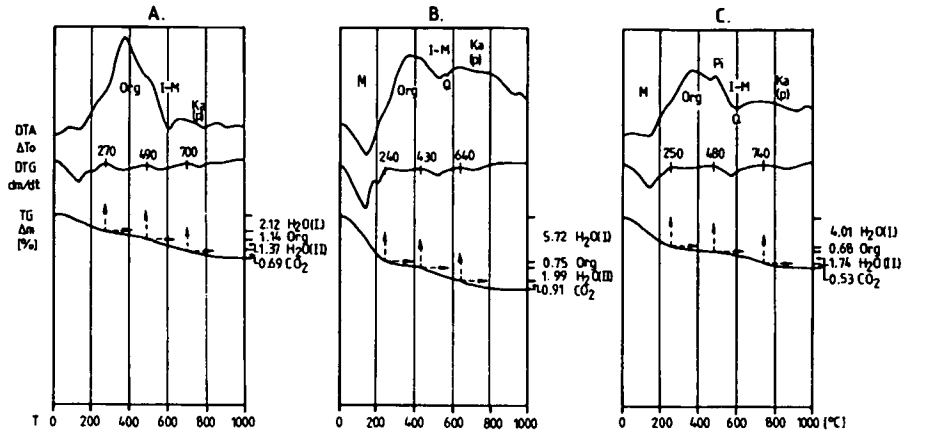

Fig. 6. Characteristic thermoanalytical curves and parameters of the low-carbonate /carbonate-free pelitic facies
A=P-1 subfacies, borehole 714. 10.0—10.5 m
B=P-2 subfacies, borehole 727. 2.0—2.5 m
C=P-3 subfacies, borehole 727. 4.5—5.0 m
Org=organic material, I-M=illite-montm. mixed layer,
Q=quartz, Pi=pyrite, Ka(p)=gel magnesite and calcite

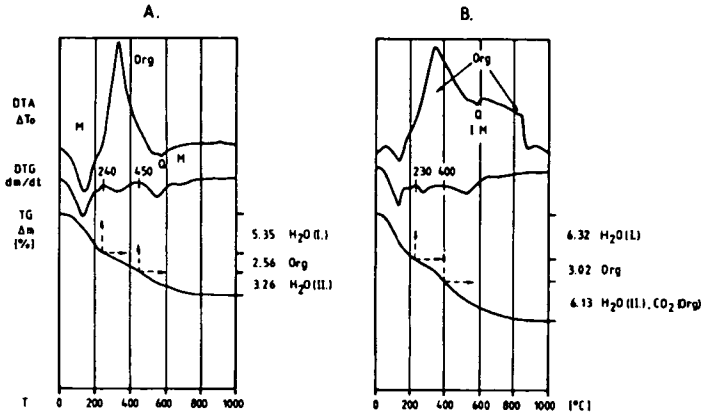

Fig. 7. Characteristic thermoanalytical curves and parameters of the low-carbonate /carbonate-free pelitic facies
A=P-4 subfacies, borehole 853. 11.0—11.5 m
B=P-5 subfacies, borehole 853. 17.0—17.5 m
Org=organic material, I-M=illite-montm. mixed layer, Q=quartz

LOESSY FACIES TYPE (MARKED AS P-1)

Silty sediments transported by the wind deposited quite often on temporarily wet surface (hydro-aerolite) belong to this group. They are typically yellow or

grey in their deeper layers. Their clay and fine silt content can reach 30—40%, but quite often, sand content can also reach as much as 20—30%. In the sequence of the borehole Nr. 714, the basal parts (20—27 m) are interrupted by two humic soil layers, 40 cms thick each. Its basement is eolic sand, the upper parts are carbonatised, gradually shifting into calcium-carbonatic pelite subgroup. Within the sections, this series can occur repeated several times. Typical sediments of this type can be studied in borehole Nr. 714 (*Fig. 2.*). Their thermoanalytical characteristics can be seen on the graph marked A on *Fig. 6.* Indicator minerals comprise illite-montmorillonite mixed structure, chlorite and carbonate precipitate. Parameters denoting clay-mineral content are: $H_2O(I)$=1.5—2.5 %, $H_2O(II)$=1.0—2.0 %. Organic matter content = 0.5—1.7% (oxidimetric titration). $CaCO_3$ content = 0.5—2.0 %. Chemical parameters:

Total iron oxide content (Fe_2O_3/Fe))=3—4 %, Mn = 50—100 ppm, P = 300—400 ppm, B/Ga = 2.0—2.5.

Sediments belonging to this type were exposed by boreholes deepened in the Nyírség region.

RIVERINE, RIPARIAN, HUMIC PELITE FACIES TYPE (MARKED AS P-2)

Sediments of this type are grey silt varieties, microlaminated, rich in micas, containing 20—30 % clay fraction with no Molluscan shells and plant fossils. They are void of carbonates or contain carbonate precipitates only. No amorphous pyrite was found in them. The most typical sample for this facies can be found in the sequence of borehole Nr. 727 (*Fig. 3*).

Its thermoanalytical characteristics are presented on graph B of Fig. 6. Its indicator mineral is the illite-montmorillonite mixed structure. X-ray analyses could detect the presence of chlorite and kaolinite as well.

Parameters denoting clay-mineral content are: $H_2O(I)$=3—6 %, $H_2O(II)$=2.0—4.0 %. Organic matter content = 1.50-5.00 % (oxidimetric titration). $CaCO_3$ content = 0.0—2.5%. Chemical parameters:

Total iron oxide content (Fe_2O_3/FeO)=5—6 %, Mn=500—1500 ppm, P = 500—1000 ppm, B/Ga = 2.0—3.0.

Sediments belonging to this facies were exposed by boreholes deepened in the Bodrogköz and the Szatmár Plains.

RIVERINE, RIPARIAN, LACUSTRINE, ENTROPHIC PELITE FACIES TYPE (MARKED AS P-3)

Clayey silts of dark grey, blackish gray, brownish grey colour can be assigned to this group. These sediments were probably formed in small eutrophic basins on the flood plains of the rivers in reductive environment. They often contain bluish knots of vivianite as well as blackish grey spots of humus. In the humic layers and spots we find no macroscopically observable plant fossils, but fairly frequently, there are fragments of Molluscan shells here. The clay mineral typical of the faces is an illite-montmorillonite mixed structure. Its disperged organic matter content is considerable, bound to the montmorillonite, just the same as its sulphur content present in the form of amorphous pyrite and in organic bounds. The samples contain no carbonate, at the maximum, a very small amount of carbonatic precipitate.

Typical example of this facies can be studied in the samples of borehole Nr. 727. Its thermoanalytical features are presented on graph C of *Fig. 6.*

Parameters denoting clay-mineral content are:

$H_2O(I)$ = 4—7 %, $H_2O(II)$ = 1.5—3.0 %. Organic matter content = 1.0—3.5 % $CaCO_3$ content = 0.0—1.5 %. Chemical parameters: Total iron oxide content (Fe_2O_3/FeO) = 4—6 %, Mn = 1200—5000 ppm, P = 500—1500 ppm, B/Ga = 3.0—4.0.

Sediments belonging to this facies can be found in the Bodrogköz region and the Szatmár Plains.

Pelite facies type of upfilling dead branches and sedimentary depressions on interfluvial regions (marked as P-4) and marshy (peat) pelitic facies (marked as P-5).

Clayey-sandy silts, silty-sandy clays filling up the former dead branches of rivers, flood plain depressions can be classified into this group. In these sediments, apart from 40—70 % of pelite content, we could find in almost each sample 15—25% of sand as well. These sediments are typically of greenish grey colour with spots of vivianite and plant remains. In the fluctuation zone of the soil waters they are yellow, with stains of ochre. Amorphous pyrite is not typical, it can mainly occur towards the cover of the sequence in the eutrophic subfacies (P-3). This type is typically void of carbonates or poor in carbonate, but the layers may form a transition towards the Mg-rich amorphous carbonatic facies (pCa/Mg).

Clay mineral typical of this facies is the montmorillonite, the organic matter is in finely disperged state (type P-4) or in the form of lignite (type P-5). These dark grey, dark brown clay stripes contain turfy matter. Their characteristics can be studied in borehole Nr. 853 (*Fig. 4*), their thermoanalytical features are presented on *Fig. 7.* Parameters denoting clay-mineral content $H_2O(I)$=5—7 %, $H_2O(II)$=3—6 %. Organic matter content, determined by titration, is 2—3 % for P—4 and 10—20 for P-5.

Chemical parameters: Total iron oxide content (Fe_2O_3/FeO)=4—8 %, Mn= 200—1500 ppm, P=400—1100 ppm, B/Ga = 4—7.

On *Fig. 8.*, the alternation of facies types in borehole Nr. 853 in function of depth is presented, compiled on a temperature scale of uniform intensity.

EVALUATION OF INDICATOR ELEMENTS, PAIRS OF ELEMENTS

Armed with knowledge on facies types presented above, a mathematical-statistical elaboration of the main components, trace elements and pair of elements were performed. Relation of several elements were studied including Al/Ti, K/Al, K/Na, Ca/Mg, Fe/Mn, V/Cr, Cr/Ni, Ba/Sr, B/Ga, Li/B, P/B ratios.

Independent of qualitative description of the rocks we have performed a linear regression analysis of the chemical parameters of all samples. The aim of our interest has been the description of basic geochemical correlations, revealing regional similarities and differences and studying the rules of the connection of elements. After computer assisted investigations, the following results seem to be valid and worth for publication.

On *Fig. 9.*, the investigation of the relation of the elements Al, K, B, and Ga proves the divergent geochemical character of the regions of the Norther Eastern part of the Great Hungarian Plain.

The Bodrogköz region (Zemplénagárd-Zalkod sections) is different from the Nyírség formations, on the basis of higher Al and K values of the former. In spite of the fact that the correlation of K and Al on both territories is very strong and

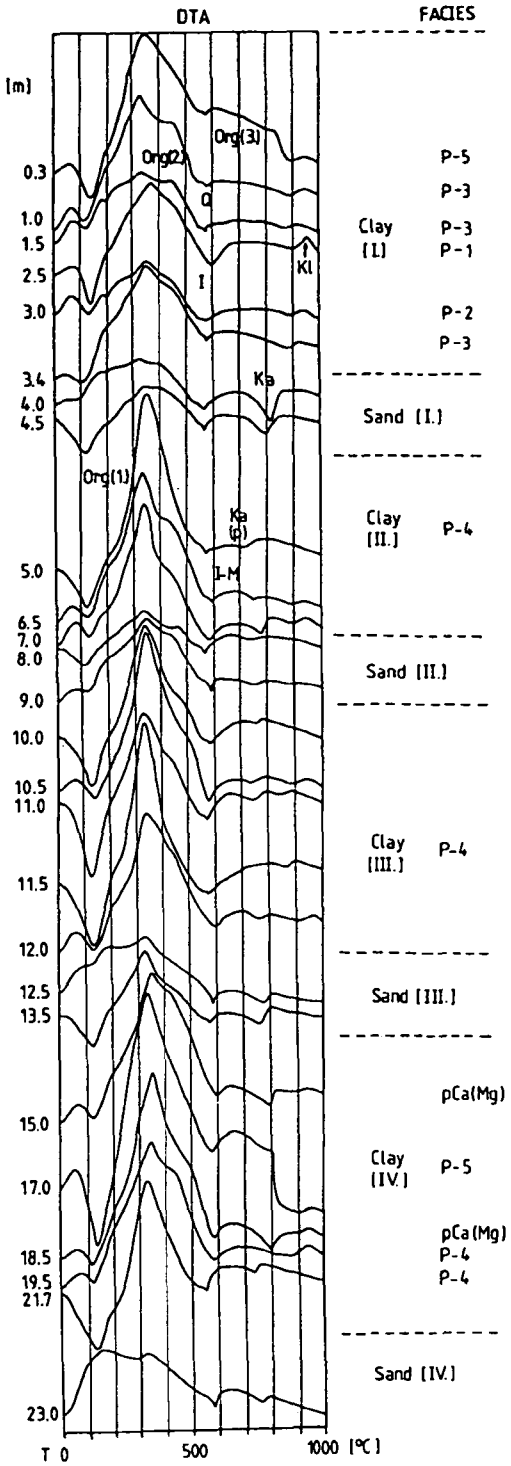

Fig. 8. **DTA** curves representing the change of the mineral-geochemical facies from sequence of the borehole 853.
Sand (IV)=sand from river channel; Clay (IV)=pelitic and peaty sediments from filling cut-off meander; Clay (III)=pelitic sediments deposited between river-branches; Sand[III] and [II]=river-sand, Clay[II]=pelitic sediments deposited between river-branches; Sand[I]=eolic redeposited sand of river-side; Clay [I]=eutrophic and "peaty" pelitic sediments of floodplains.
Org.(1.2.3)=organic materials, I=illite, I-M=illite-montm. mixed layer, Kl=kaolinite, Q=quartz, Ka=calcite, Ka(p)=gel magnesite and calcite.

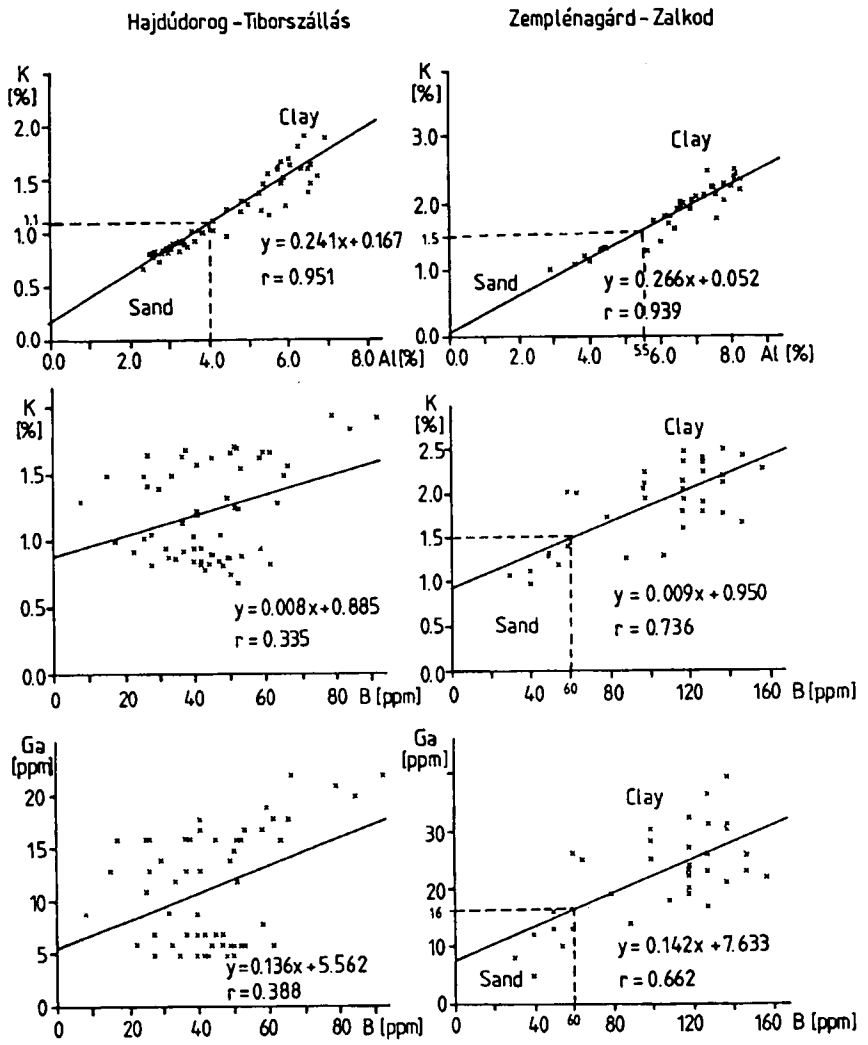

Fig. 9. Geochemical differentiation between pelitic sediments (Clay) and the grained under- and overlying beds (Sand) from boreholes of the sections Hajdúdorog-Tiborszállás and Zemplénagárd-Zalkod.

practically equal, there are considerable differences in the element pairs K/B, B/Ga in comparing the relevant regression coefficient values. Apart from obvious differences in the quality and quantity of the pelitic fraction, they are obviously connected with micromineralogical character as well.

Ca- and Mg- ions connected to, in the first place, hydrogene carbonates, were mostly dissolved from the clayey layers and precipitated in other clayey layers in the form of secondary carbonates. In the carbonate-free layers and those of low carbonate pelitic layers, the ratio of Ca/Mg ions is 1.0. Dolomitisation typical for the Danube-Tisza interfluvial region (MOLNÁR 1980; MOLNÁR and KUTI 1983)

cannot be demonstrated on the North-Eastern parts of the Alföld, proving the differences in sedimentation and diagenetic conditions.

The value of Mg content is roughly equal and, there is a close correlation in the values of Al, K, and Fe as well, but fairly independent of Ca (*Fig. 10*).

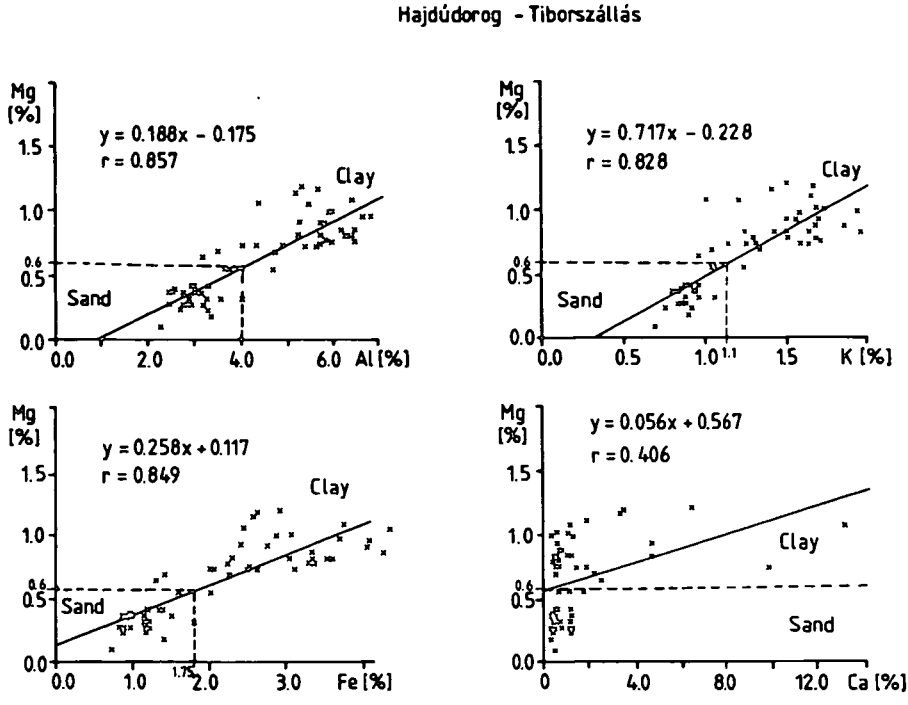

Fig. 10. Correlation between Mg and Al, Fe, K, Ca on the basis of the study of pelitic sediments (Clay) and grained over- and underlying beds (Sand) from boreholes of the section Hajdúdorog-Tiborszállás.

Accumulation of Mg took place in the formations examined as a result of the fine (bio)mass flourishing in the marshy environment.

Analysis of the carbonate-free and low carbonate content pelitic facies was performed on the most clayey samples selected from each borehole, most of them were absolutely void of carbonates, the rest containing < 3 % $CaCO_3$. Our primary aim was to distinguish between oxidative and reductive environments. Element relations between Al/Ti and Fe/Mn were most informative from this respect. Among more oxidative circumstances, coloured minerals with Ti content dissolve more intensively (hydrolise better). Thus, beside aluminium, more titanium is getting into solution, further promoted by the presence of sulphur compounds turned to sulphates in oxidative environment. This process takes place typically different for the different facies types. In case of P-1 (eolic) type and P-2, P-3 in case of river-side flood plain sediments organic matter and amorphous pyrite, in case of P-4, P-5 interfluvial depressions, bogs organic matter, amorphous pyrite and vivianite indicate a more reductive environment.

The separation of iron and manganese in sediments is also a process strictly dependent on facies relations.

By considerable organic matter content, in the presence of humine materials and in acidic pH, i.e., reductive environment, these ions enter into solution more intensively and are being transported in the form of hydrogene carbonates and, by a change in the pH getting into more oxidative conditions they are precipitated. These regularities can be studied on *Fig. 11.*

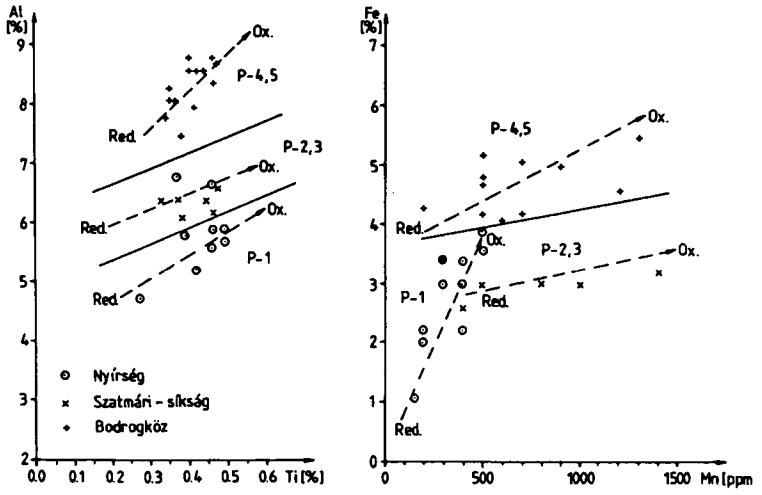

Fig. 11. Correlation between Al-Ti and Fe-Mn element pairs on the basis of the study of low-carbonate ($CaCO_3$ < 3 %) pelitic sediment from NE Tiszántúl (Transtibiscia). P-1, P-5= subfacies, oxidative (Ox.) and reductive (Red.) environments.

Finally, the chemofaciological analysis on the three boreholes presented above was performed. *Fig. 12* demonstrates the result of correlation studies on the basis of the element pairs K/B. The individual genetical units can be separated very well in the coordinate system. In field I., sediments of eolic reworked sands and inter-mound sediments resembling infusional loess are grouped. In field II.,

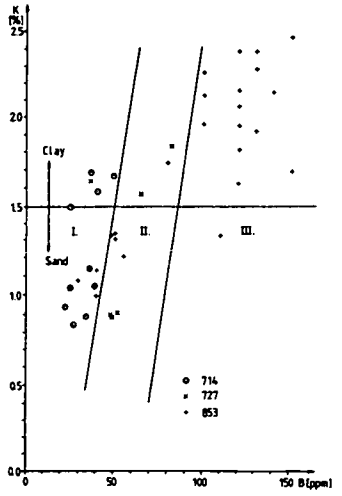

Fig. 12. Chemofacies-analysis of the clayey beds (Clay) and of the grained over- and underlying formations (Sand) from boreholes 714., 727., and 853. on the basis of the K/B ratio. I.=eolic, II.=fluviatilic, III.=lymnic (paludal) sediments.

riverine sands and riparian pelitic sediments, in patch III., upfilling of dead branches, limnic basins, marshes can be separated.

Our statistical analyses indicate that by the correlative evaluation of other pairs of elements we can trace the different areas of origin as well. This paper, however, does not aim at presenting this very complex evidence which can be studied only by detailed granulometric, grain-morphological and micromineralogical investigations.

ACKNOWLEDGEMENT

This work was supported by Foundation Grant of OTKA No. 154.

REFERENCES

BARTA, I., BALÁZS E., SÜMEGI P., SZÖÖR Gy. (1985): A Zemplénagárd-Nyírábrány, Zemplénagárd-Zalkod fúrásszelvények jellemző mintáinak ásványtani, geokémiai, malakológiai vizsgálata (Mineralogical, geochemical and malacological investigation of borehole sections from Zemplénagárd-Nyírábrány, Zemplénagárd-Zalkod). Manuscript, Research Report. HGS Archives. 1—134.

BARTA, I., SZÖÖR, Gy. (1983): Hajdúdorog-Tiborszállás közti szelvény fúrásmintáinak összehasonlító geokémiai vizsgálata és értékelése (Comparative geochemical investigation and evaluation of borehole section samples from the section between Hajdúdorog and Tiborszállás). Manuscript, Research Report. HGS Archives. 1—134.

BORSY, Z., CSONGOR, É., LÓKI, J., SZABÓ I. (1985): Recent results in the radiocarbon daating of wind-blown sand movements in the Tisza-Bodrog Interfluve. Acta Geogr. Debrecina. 5—16.

BORSY, Z., CSONGOR, É., LÓKI, J., SÁRKÁNY, S., SZABÓ I. (1981): A futóhomok mozgásának periódusai az Alföld ÉK részében. — (Periods of sand-blown movements in the NE parts of the Alföld region). Acta Geogr. Debrecina. 35—50.

BORSY, Z., FÉLEGYHÁZI, E., LÓKI, J. (1988): A Bodrogköz természetföldrajzi viszonyai. (Natural conditions in the Bodrogköz region). In: Bodrogköz. Ember — táj — mezőgazdaság. ed. FEHÉR Alajos. Publisher: MTA Miskolci Akadémiai Bizottság, Miskolc. 1—45.

CSONGOR, É., FÉLEGYHÁZI, E. (1987): Palaeohydrogeographic changes in the Bodrog-Tisza Interfluve (NE Hungary) in the past 20.000 years based on palynological studies and C-14 dating. In: Holocene environment in Hungary. 59—66.

DARÓCZY, S., PAPP, Z., SZÖÖR, Gy. (1990): Kőzetek béta-radioaktivitásának mérése és geokémiai fáciesanalitika alkalmazása. (Measurement of beta-radioactivity of rocks and its utilisation for geochemical facies analysis). Földt. Közl. (in press).

ERNST, W. (1970): Geochemical facies analysis. In: Series methods in Geochemistry and Geophysics. Elsevier. pp., 1—141.

KEITH, M. L., DEGENS, E. T. (1959): Geochemical indicators of marine and freshwater sediments. In: Researches in Geochemistry. Ed. by ABELSON, P.H. Wiley, N.Y. pp., 38—61.

KREJCI-GRAF, K. (1966): Geochemische Faziesdiagnostik. — Freib. Forschungsch. C. **224**, pp. 1—80.

MOLNÁR, B. (1980): Hiperszalin tavi dolomit-képződés a Duna-Tisza közén (Formation of hypersaline lacustrine dolomite in the Danube-Tisza Interfluvial Region) Földt. Közl. **110**, pp. 45—64.

MOLNÁR, B., FÉNYES, J., KUTI, L., NOVOSZÁTH L. (1988): A hagyományos és a pásztázó elektronmikroszkópos szemcsevizsgálati eredményeinek összehasonlítása (Comparison of the results of traditional and scanning electron microscopical grain examinations). Földt. Közl. **118**, pp. 27—48.

MOLNÁR B., KUTI L. (1983): Az ágasegyházi és orgoványi tavak kialakulása és limnológiai fejlődése (Formation and limnogeological evolution of the lakes at Ágasegyháza and Orgovány) Hidrológiai Közl. **113**, 225—237.

RÓNAI, A. (1985): Az Alföld negyedidőszaki földtana. (Quaternary geology of the Great Hungarian Plain) Geol. Hung. Ser. Geol. **21**, pp. 1—446.

Manuscript received, 22 November, 1990

Acta Mineralogica-Petrographica, Szeged, XXXII, 37—41, 1991

THE Eh-pH ENVIRONMENT OF DEPOSITION OF SOME SEDIMENTARY DEPOSITS FROM EGYPT

A. A. EL SOKKARY

Nuclear Materials Authority, Cairo*

ABSTRACT

Thirty four samples representing four types of sedimentary rocks from Egypt are subjected to laboratory determination of Eh-pH values in order to determine their environment of deposition.

The rock types under study are: (1) The Fe-Mn deposits associating Carboniferous rocks of West Central Sinai (2) Shales and clays usually covering the mentioned Fe-Mn ores of West Central Sinai (3) Phosphatic rocks from different localities in Egypt (4) Oligocene shales and clays from Gebel Qatrani in the Western Desert.

The environment of deposition of the Fe-Mn deposits of West Central Sinai is shown here to be shallow marine waters. Most of the shales and clays associating the Fe-Mn deposits of West Central Sinai have pHs indicating that their depositional environment is marine like the precipitating medium of the Fe-Mn ores. The few samples of these shales and clays that show pHs on the acidic side represent rocks subjected to bleaching effects by later acidic solutions.

Phosphatic sediments from different localities of the country have their pHs indicating typical marine environment of deposition.

Oligocene shales and clays of Gebel Quatrani in the Western Desert have pHs that range between acidic and alkaline media of deposition reflecting the fluviomarine origin of these sediments.

INTRODUCTION

The Eh-pH experimental data of some sedimentary deposits from Egypt are dealt with in the present communication in a trial to define the environment of deposition of these deposits. Four types of sedimentary deposits are subjected to experimental testing of their Eh-pH values, these are: (1) Fe-Mn depostis associated with Carboniferous rocks from West Central Sinai (2) Shales and clays overlying and underlying the mentioned Fe-Mn deposits of West Central Sinai (3) Phosphatic rocks from different localities from Egypt, and (4) Fluviomarine Oligocene shales and clays from Gebel Qatrani in the Western Desert of Egypt. Despite that the environment of deposition of these deposits is already worked out from different geological channels, yet it is the first time that the Eh-pH experimental method is applied to these deposits.

Special attention is given here to the problematic Fe-Mn deposits of West Central Sinai and their accompanying shales. The Eh-pH environment of deposition of these deposits was worked out on theoretical basis including the chemical constitution and mineralogical composition of the ores (ANWAR and EL SOKKARY 1972). Some genetical relations among the main ore-forming elements are studied by EL SOKKARY (1972).

* Cairo. Almaza, New Cairo. 57 Abdel Monem Hafez St., Egypt

The object of the present work is to determine the Eh-pH values of four types of sedimentary deposits from Egypt on experimental basis in the laboratory and to try to coordinate the obtained data with previous known environmental conditions of deposition of these deposits.

TECHNIQUE OF WORK

As already stated in the introduction, the studied samples are taken from four sedimentary deposits as follows: (1) Six samples representing the Fe-Mn deposits associated with Carboniferous rocks of West Central Sinai (2) Eight samples representing the shales and clays associated with the mentioned Fe-Mn deposits (3) Four phosphatic samples from different localities in Egypt (4) Sixteen samples representing Oligocene shales and clays from Gebel Qatrani in the Western Desert. Thus all the studied samples are 34 in number.

The location of phosphatic samples is as follows: Two samples from East Luxor phosphates, Nile Valley. One sample from Safaga phosphate, Eastern Desert. One sample from Qatrani phosphatized sandstone, Western Desert.

These samples are ground and made to pass sieve of 100 mesh size. Five gram portion of each powdered sample is transferred to a beaker to which 100 ml. of distilled water is added, the powder is stirred in water. This suspension is left for not more than 48 hours before actual measurements of Eh-pH values are taken, this is done in order to let equilibrium be established in the solid-liquid system.

The instrument used in Eh-pH measurements is a Pye Unicam pH meter, model Pye-292, with electrodes used in Ph measurements: glass electrode plus reference calomel electrode, and electrodes used in Eh measurements: platinum electrode plus reference calomel electrode. Two buffer solutions: one with pH=4 and the other with pH=9 are used to calibrate the instrument before pH measurements. Zobell solution (0.003 M pot. ferricyanide+0.003 M pot. ferrocyanide+0.1 M pot. chloride) with observed potential 0.183 volt is used to calibrate the instrument for Eh measurements.

In practice the measured voltage of the inert electrode-reference electrode pair is added algebraically to the potential of the reference electrode to get the Eh of the half cell reaction occurring at the platinum electrode (GARRELS 1960).

PRESENTATION OF DATA

Table 1 gives the experimental numerical data of the pH and Eh values of 34 samples of four sedimentary deposits from Egypt. The number of samples for each rock type is already given in the previous section on Technique of Work. The Eh values are reported in millivolts (mV).

Allover the 34 samples, pH ranges between 3.5—8.4 while Eh ranges between 307—635 mV. Water with pH value more than 7.0 is alkaline, while water with pH value less than 7.0 is acidic. Sea water is known to be faintly alkaline with pH 8.5 (MASON 1964).

Fig.1 is a graphic presentation of the Eh-pH relation of the 34 samples representing the mentioned four sedimentary deposits.

The relation is a straight line with slope 43.33 mV/pH. From this diagram the prevailing natural pH values of the studied samples range between 7.00—8.50 i.e. representing alkaline environment of deposition, while the prevailing Eh values range from 300—425 mV representing low-moderate oxidation potential.

TABLE 1.

Eh–pH values of some sedimentary rocks from Egypt

Serial No.	pH	Eh(mV)	Serial No	pH	Eh(mV)
Fe-Mn deposits of W. C. Sinai: Qatrani shales and clays					
1	7.78	350	19	7.20	385
2	7.50	375	20	8.15	355
3	7.72	355	21	7.95	365
4	8.12	355	22	7.38	385
5	7.10	405	23	8.20	355
6	7.80	365	24	8.15	345
Shales clays assoc. Fe-Mn ores:					
7	8.40	418	25	7.92	353
8	6.35	467	26	4.05	525
9	7.35	405	27	7.22	375
10	7.80	410	28	5.90	435
11	3.50	635	29	7.71	335
12	7.10	510	30	7.80	393
13	7.70	537	31	7.22	395
14	7.50	515	32	7.55	365
Phosphates from different loc.:					
15	7.63	375	33	4.85	455
16	7.90	335	34	4.20	513
17	7.70	325			
18	8.12	307			

DISCUSSION

Measured pH values of the Fe-Mn deposits of West Central Sinai range between 7.10—8.12, while measured Eh values of the same samples range between 350—405 mV. Thus the environment of deposition is alkaline with moderate oxidation potential indicating deposition in shallow water seas. It is therefore concluded that the Carboniferous Fe-Mn deposits of West Central Sinai are of marine origin. This ends the debate on the origin of these problematic ore deposits.

ANWAR and EL SOKKARY (1972) worked out the Eh-pH environment of deposition of the Mn-Fe deposits of West Central Sinai and deduced on theoretical basis that the depositional environment is most probably alkaline with moderate oxidation potential characterising shallow water seas. These authors (op. cit.) mentioned that higher oxidation potentials were not fully reached during deposition of the ore and the Eh is somewhere below 0.8 volts. It can be seen that these views worked on theoretical basis are in agreement with the present experimental Eh-pH data.

Table 1 shows that the various phosphatic samples under study have pH values that range between 7.63—8.12 and Eh values range between 307—375 mV. It is observed that the pH range is rather narrow pointing towards definite alkaline

medium of deposition with moderate oxidation potential which characterise typical marine environment of deposition. Again the pH-Eh ranges of the Fe-Mn deposits of West Central Sinai are close to those of the studied marine phosphatic deposits (being 7.10—8.12 for the pH range and 350—405 mV for the Eh range of the former) assuring that deposition of the Fe-Mn ores has taken place as well under definite marine facies.

The shales and clays associating the Fe-Mn deposits of West Central Sinai being overlying or underlying these deposits show somewhat different behaviour. Most of the samples (six out of eight) have alkaline tendencies with pHs that range between 7.10—8.40, however some of the samples (two out of eight) have their pHs on the acidic side being 3.50 and 6.35 respectively, yet the Eh range lies between 405—635 mV. Since most of the shale and clay samples have their pHs on the alkaline side which is very close to the same pH range of the Fe-Mn deposits themselves (being 7.10—8.12 for the latter), this indicates that the general environment of deposition of these shales and clays is marine, the same as the precipitating medium of the Fe-Mn ores.

However the few samples that show pHs on the acid side of the scale reflect that some parts of the shale and clay layers are subjected to bleaching acid solutions.

SHUKRI (1941) during a study on the use of pH values in determining the environment of deposition of some Liassic clays and shales of England mentioned that the bleached beds (affected by acid waters) are certainly poorer in booth carbonates and bases and they accordingly give a lower pH value.

Natural normal limits of Eh-pH among the investigated samples are shown in *Fig. 1* as represented by the rectangle in solid lines, these are as follows: the pH

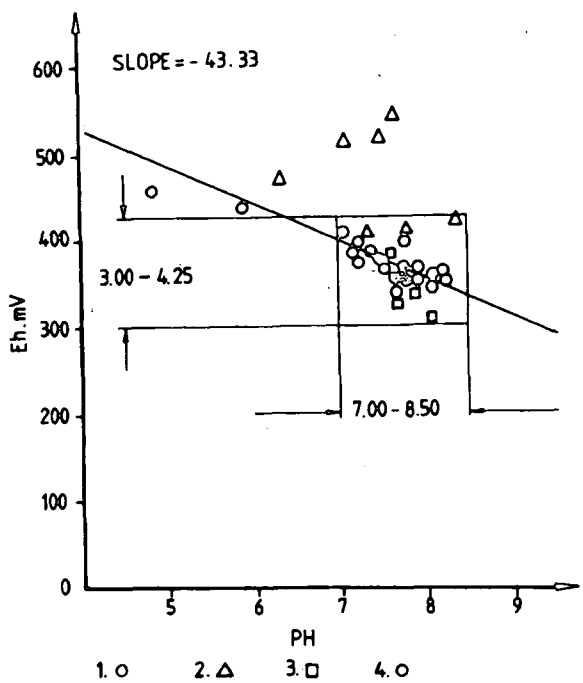

Fig. 1. Eh versus pH relation of the examined 34 samples.
1=Sinai Fe-Mn ores, 2=Sinai Fe-Mn shales, 3=phosphates, 4=Quatrani shales-clays.

range between 7.00—8.50 and the Eh range between 300—425 mV. Within this rectangle lie points representing phosphates with definite marine origin, the Fe-Mn ores and part of the shales and clays associating the mentioned ores. This gives more weight to the marine origin of the Fe-Mn ores and their accompanying shales-clays. Another part of the latter shales and clays lies above the defined frame i.e. they represent still alkaline medium of deposition but with somewhat higher Eh values up till about 540 mV. These might represent marine medium of deposition but with more oxidation potential i.e. more aeration and shallower waters.

With respect to Oligocene shales and clays of Gebel Qatrani, they show pHs that range between acidic and alkaline media. The general range of pH among these rocks is between 4.05—8.20. The majority of samples, 75 % of them, give pH values in the alkaline range between 7.20—8.20, while 25 % of the samples have their pHs in the acidic range between 4.05—5.90, Eh values on the other hand range between 335—525 mV.

That some Qatrani shales and clays are deposited from alkaline media and others appear to be deposited from acidic media assures the fluviomarine origin of these shales and clays. The moderate oxidation potential of these rocks indicates deposition from well aerated shallow waters.

CONCLUSION

It is revealed that the environment of deposition of the Fe-Mn deposits of West Central Sinai is alkaline with moderate oxidation potential indicating deposition in shallow water seas. With respect to shales and clays associating the Fe-Mn deposits of West Central Siani, most of them have their pHs on the alkaline side close to the same pH range of the Fe-Mn ores which indicates that their depositional environment is marine like the precipitating medium of the Fe-Mn ores. The few samples of these shales and clays that show pHs on the acidic side represent rocks subjected to bleaching action by later acidic solutions.

The various studied phosphatic samples have their pHs on the alkaline side of the scale referring to definite alkaline medium of deposition with moderate oxidation potential which characterises typical marine environment of deposition.

The Oligocene shales and clays of Gebel Qatrani in the Western Desert have pHs that range between acidic and alkaline medium of deposition. This assures the fluviomarine origin of these sedimentary rocks.

REFERENCES

ANWAR, Y. M. and EL SOKKARY, A. A. (1972): Geochemical and paragenetic studies of the Mn-Fe ores of West Central Sinai, Egypt. Bull. Faculty of Science, Alex., Vol. X.

EL SOKKARY, A. A. (1972): Statistical geochemical studies on the Mn-Fe ores of West Central Sinai. Proc. of Egypt. Acad. Sci., Vol. XXV.

GARRELS, R. M. (1960): Mineral equilibria at low temperature and pressure. Pub. Harper and Brothers, N.Y.

MASON, B. (1964): Principles of geochemistry. Pub. John Wiley and Sons, Inc., N.Y.

SHUKRI, N. M. (1941): The use of pH values in determining the environment of deposition of some Liassic clays and shales. Bull. Fac. Sci., Fouad I Univ., Cairo, Vol. No. 24.

Manuscript received, 27 June, 1991.

Acta Mineralogica-Petrographica, Szeged, XXXII, 43—47, 1991

PRELIMINARY ZIRCON FISSION TRACK RESULTS IN THE KŐSZEG PENNINIC UNIT, W. HUNGARY

A. DEMÉNY and I. DUNKL

Laboratory for Geochemical Research,
Hungarian Academy of Sciences*

ABSTRACT

Zircon fission track ages were determined in quartzphyllite samples of the Hungarian side of the Kőszeg-Rechnitz Penninic series. The data scatter between 15.1 and 18.5 My, showing a slight areal variability which calls attention to different uplift rates in the unit. The results agree well with literature data gathered from far-lying Penninic units, that means, that the uplift of the Penninic Bündnerschiefer series might have taken place in the same time interval throughout the whole Alps.

KEYWORDS: zircon fission track, Penninic unit, Kőszeg-Rechnitz series.

INTRODUCTION

The relationship between the Kőszeg-Rechnitz metamorphic series and other Alpine Bündnerschiefer units was discussed first by SCHMIDT (1956), but direct evidence for the Mesozoic age of the Kőszeg-Rechnitz unit was provided by SCHÖNLAUB (1973). Beside these studies, a great number of authors has dealt with comparisons between the Kőszeg-Rechnitz series and other Alpine Penninic terranes. Similarities in the evolution history of the Tauern window and the Kőszeg-Rechnitz window were discussed by KOLLER (1985) from the side of metamagmatites and by DEMÉNY and KREULEN (1989) from the side of metasediments. These studies dealt with rock formation and metamorphic processes, but there has been no comparison regarding the age of uplift. While an extensive data set exists for the Tauern window (e.g. CLIFF *et al.* 1985), GRUNDMANN and MORTEANI 1985, STAUFENBERG 1987, *etc.*), only one author (KUBOVICS 1983) presents data for the Kőszeg-Rechnitz series. In this latter paper a 12 my whole rock K/Ar age was mentioned which figure is slightly lower than those of the Tauern window. As the K/Ar age data can be affected by deformation events, we intended to use a method independent of this effect.

This paper presents preliminary results of zircon fission track studies in the Kőszeg-Rechnitz series and correlations with other Penninic terranes.

* 1112 Budapest, Budaörsi út 45, Hungary

GEOLOGICAL BACKGROUND AND SAMPLES

The Kőszeg-Rechnitz unit belongs to the Alpine Bündnerschiefer series (SCHMIDT 1956, SCHÖNLAUB 1973) and consists of metamagmatites and metasedimentary rocks (BANDAT 1932, KISHÁZI and IVANCSICS 1976, 1984, KOLLER and PAHR 1980). The ophiolitic origin of the former rock type was discussed by KUBOVICS (1983) and KOLLER (1985). KOLLER (1985) correlated the series with the Glockner nappe of the Tauern window.

The metasediments are mainly phyllites with varying amount of carbonate, mica and quartz, and contain a significant quantity of detrital material as indicated by occurrences of conglomerate bodies (KOLLER and PAHR 1980). The origin of this detrital fraction has been discussed by DEMÉNY (1988) and DEMÉNY and KREULEN (1989).

The series has been affected by three metamorphic events: an oceanic hydrothermal, a subduction-related HP/LT type and a Tertiary metamorphism. The latter had the most extensive effect reaching 400 °C temperature and 2—3 kbar pressure. The conditions of these metamorphic imprints have been thoroughly studied by LELKES-FELVÁRI (1982), KOLLER (1983) and DEMÉNY (1990).

The zircon grains studied in this paper were separated from quartzphyllite samples of the Hungarian part of the Kőszeg-Rechnitz window (*Fig. 1.*). All but one (sample V) derived from drill-cores (see Table 1. for depths), while sample V was collected from a roadcut. The rocks consist dominantly of quartz, muscovite and chlorite, while opaque minerals, tourmaline, zircon, rutile and apatite appear as accessoric components.

TABLE 1.

Fission track results on detrital zircon crystals of quartzphyllites near Kőszeg

Samples	No. of data	Ns	Ni	Ps	Pi	FT AGE	+- 2s Poiss.	Uran. (ppm)
						Million years		
Velem, outcrop	4/4	245	449	12.9	35.6	18.5	+- 3.2	227
V—9 / 102.9*	27/27	1356	1353	26.6	26.4	18.5	+- 1.9	282
K—6 / 6.1	31/31	3134	3937	22.7	26.5	15.1	+- 1.2	283
K—6 / 120.3	33/33	2050	2350	23.9	26.7	16.1	+- 1.7	235
K—7 / 40.4	17/16	1157	1411	17.3	20.3	15.1	+- 1.4	286

No. of data: Crystal or field number investigated/concerned for the results.
Ns, Ni: Number of spontaneous and induced tracks.
Ps, Pi: Spontaneous and induced track density (10^5 tracks/cm^2).
Uran. (ppm): Uranium content of investigated crystals.
*: Depths (m)

The zircon grains on which fission track ages were measured reach 0.1 mm and show evidences for preserving the original crystal morphology in spite of their detrital origin. Since fission track dating does not give formation age, but the time of cooling to a certain temperature, we could use our data to estimate the age of uplift after the Tertiary metamorphism.

EXPERIMENTAL METHODS

The zircon crystals were embedded in FEP-teflon. The spontaneous fission tracks were etched after polishing by eutectic melt of NaOH-KOH-LiOH at somewhat lower temperature (190 °C) than suggested by the prescriptions of ZAUN and WAGNER (1985). Etching was carried out for different durations in each preparate (38 to 49 hours). Neutron irradiation was made at the reactor of the Technical University of Budapest. The neutron fluence was determined using the NBS SRM 962a uranium glass standard. As the external detector method was applied (GLEADOW 1981), a mica external detector was put onto the preparates and the standard and after irradiation the induced fission tracks were etched by HF for 40 to 60 min.. Counting of spontaneous tracks was made in oil immersion under a Zeiss NU2 microscope, with a magnification of 1600. In case of the mica detectors dry optics of 800-time magnification were used. To compensate the different track registration geometry ($2\ \pi/4\ \pi$) between the external detector and the dated minerals, the geometry factor of 0.5 determined by GLEADOW and LOVERING (1977) was applied.

The ages were calculated on the basis of the weighted average of the measured track density proportions by the zeta method (HURFORD and GREEN 1983). The limits of error are given by the classical procedure, i.e. by the double Poisson dispersion (GREEN 1981).

RESULTS AND DISCUSSION

The results listed in Table 1. are shown together with sample localities in *Fig. 1.* The data scatter between 15.1 and 18.5 my indicating an areal variability. Samples lying close to each other (e.g. samples V and V9) give similar ages, which calls attention to a possible areal difference in uplift. Future work will aim establishing such variability throughout the whole window.

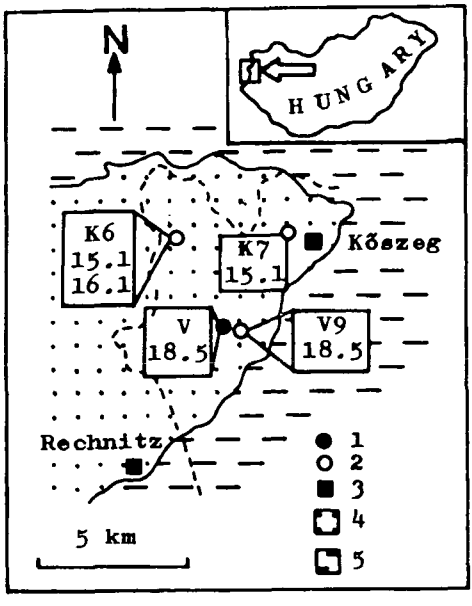

Fig. 1. Sample localities and fission track age results. 1. Sample from the surface, 2. Samples from drilling cores, 3. Settlements, 4. Penninic rocks, 5. Tertiary cover.

The next question is the comparison between our data and results on other Alpine Penninic units. The farest Bündnerschiefer series from which uplift data have been gathered is the terrane of the Lepontin Alps. HURFORD (1986) determined 11—19 My zircon fission track ages for uplift and cooling of this unit.

More information exists for the Tauern window, although the possible fission track ages can only be estimated from results of other dating methods. HURFORD (1986) discussed the possibilities of such estimation and gave blocking temperatures for various age determination methods. Following his approach we can derive the theoretical zircon fission track ages from Rb/Sr, K/Ar and apatite fission track results of RAITH *et al.* (1978), CLIFF *et al.* (1985), GRUNDMANN and MORTEANI (1985), STAUFENBERG (1987) and BLANCKENBURG *et al.* (1989). It can be concluded from these data that the Bündnerschiefer series of the Tauern window cooled to about 200 °C (zircon fission track blocking temperature) 10 to 20 My ago. This time gap agrees well with the zircon fission track data of HURFORD (1986) and with our results.

It is apparent from the above data series that although there are large distances between these far-lying Bündnerschiefer units, the uplift took place in almost the same time interval throughout the whole system.

ACKNOWLEDGEMENTS

The authors are indebted to late I. BÉRCZI for the irradiation experiments. A. Pahr is also gratefully thanked for the kind help he provided in the field work.

REFERENCES

BANDAT, H. (1932): Die geologische Verhältnisse des Kőszeg-Rechnitzer Schiefergebirge. Földtani Szemle. **I.2.** 140—186.

BLANCKENBURG, F. V., VILLA, I. M., BAUR, H., MORTEANI, G., STEIGER, R. H. (1989): Time calibration of a PT-path from the Western Tauern Window, Eastern Alps: the problem of closure temperatures. Contributions to Mineralogy and Petrology. **101**, 1—11.

CLIFF, R. A., DROOP, G. T. R., REX, D. C. (1985): Alpine metamorphism in the south-east Tauern Window, Austria: 2.Rates of heating, cooling and uplift. J. Metamorphic Geol., **3**, 403—415.

DEMÉNY, A. (1988): Determination of ancient erosion by zircon morphology and investigations on zoned tourmaline in the Kőszeg-Rechnitz Window (Western Hungary). Acta Mineralogica-Petrographica, Szeged. **XXIX**, 13—26.

DEMÉNY, A. (1990): Mineralogical, geochemical and stable isotope studies in Penninic rocks of Hungary: comparison between the Kőszeg-Rechnitz series and the Tauern window. Thesis. Eötvös Loránd University of Budapest. 100 pp. (In Hungarian).

DEMÉNY, A., KREULEN, R. (1989): Carbon isotopic compositions of graphites in the Penninic windows of Eastern Austria and Western Hungary and the Tauern Window. TERRA Abstracts, 1, pp. 332.

GLEADOW, A. J. W. (1981): Fission track dating methods: What are the real alternatives? Nuclear Tracks. **5**, 3—14.

GLEADOW, A. J. W., LOVERING, J. F. (1977): Geometry factor for external detectors in fission track dating. Nuclear Track Detection. **1**, 99—106.

GREEN, P. F. (1981): A new look at statistics in fission track dating. Nuclear Tracks. **5**, 77—86.

GRUNDMANN, G., MORTEANI, G. (1985): The young uplift and thermal history of the central Eastern Alps (Austria/Italy), evidence from apatite fission track ages. Jb. Geol. B.-A., **128**, 197—216.

HURFORD, A. J. (1986): Cooling and uplift patterns in the Lepontine Alps, South Central Switzerland and an age of vertical movement on the Insubric fault line. Contributions to Mineralogy and Petrology. **92**, 413—427.

HURFORD, A. J., GREEN, P. F. (1983): The zeta age calibration of fission-track dating. Chem. Geol., Isot. Geosci. Sect., **41**, 285—312.

KISHÁZI, P., IVANCSICS, J. (1976): Standardized investigations on metamorphic rocks in Western Hungary. II. The Rechnitz Metamorphic Complex. Hung. Geol. Survey, internal report. Manuscript. (In Hungarian)
KISHÁZI, P., IVANCSICS, J. (1984): Guide-book to the geology of the Kőszeg schist series. Hung. Geol. Survey, internal report. Manuscript. (In Hungarian)
KOLLER, F. (1985): Petrologie und Geochemie der Ophiolite des Penninikums am Alpenostrand. Jb. Geol. B.-A., **128**, 83—150.
KOLLER, F., PAHR, A. (1980): The Penninic ophiolites of the Eastern end of the Alps. Ofioliti. **5**, 65—72.
KUBOVICS, I. (1983): Petrological characteristics and genetic features of the crossitite from Western Hungary. Földtani Közlöny. **113**, 207—224. (In Hungarian with English abstract)
LELKES-FELVÁRI, GY. (1982): A contribution to the knowledge of the Alpine metamorphism in the Kőszeg-Vashegy area (Western Hungary). N. Jb. Geol. Palaont. Mh., **1982. 5**, 297—305.
RAITH, M., RAASE, D., KREUZER, H., MÜLLER, D. (1978): The age of the alpidic metamorphism in the western Tauern Window, Austrian Alps, according to radiometric dating. In: CLOSS, H., ROEDER, D. H., SCHMIDT, K. (eds): Alps, Apennines, Hellenides. Inter-Union commission on Geodynamics, Scientific Report No. **38**, 140—148., Stuttgart, 1978.
SCHÖNLAUB, H. P. (1973): Schwamm-Spiculae aus dem Rechnitzer Schiefergebirge und ihr stratigraphischer Wert. Jb. Geol B.-A., **116**, 35—48.
SCHMIDT, W. (1956): Die Schieferinseln am Ostrand der Zentralalpen von Rechnitz, Bernstein und Möltern. Mitt. Geol. Gesellschaft in Wien., **47**, 360—365.
STAUFENBERG, H. (1987): Apatite fission-track evidence for postmetamorphic uplift and cooling history of the Eastern Tauern Window and the surrounding Austroalpine (Central Eastern Alps, Austria). Jb. Geol. B.-A., **130**, 571—586.
ZAUN, P. E., WAGNER, G. A. (1985): Fission track stability in zircon under geological conditions. Nuclear Tracks. **10**, 303—307.

Manuscript received, 26 November, 1990

Acta Mineralogica-Petrographica, Szeged, XXXII, 49—57, 1991

THE THERMAL BEHAVIOUR OF SOME FELDSPARS FROM EGYPT

A. A. EL SOKKARY

Nuclear Material Authority, Cairo*

ABSTRACT

A new and sensitive Hungarian derivatograph is used in studying the thermal behaviour of six feldspars from Egypt and U.S.A., its temperature range is up till 1200 °C. Four endothermic peaks could be noted in the *dta* curves of the studied feldspars. These are: **P1** at 225—330 °C, **P2** at 425—600 °C, **P3** at 695—860 °C and **P4** at 940—980 °C.

The first peak **P1** is partly correlated with loss of adsorbed water and partly with loss of constitutional water of certain hydrated silicate minerals like clays present as alteratic n product of feldspar. This peak can express the extent of alteration of the feldspar. The second peak **P2** is shown to be correlated with the miscibility of the two feldspars forming the perthite or antiperthite under study. Moreover, it is shown to be empirically correlated with temperature of formation. The third and fourth peaks **P3** and **P4** are transition temperatures of plagioclase and microline to the high temperature forms respectively. The last two reaction temperatures are particularly useful as petrogenetic indicators.

INTRODUCTION

The study of the thermal behaviour of feldspars, particularly the alkali feldspars, is of paramount importance. In the first place it gives an idea about the miscibility or homogenization temperature of exsolved perthites and antiperthites. Secondly, phase transitions can be followed and the structural states of feldspars with their temperature changes can be worked out. This turn will help, at least partly, to decipher the crystallization history of the feldspar. A matter which will throw some light on the genesis of the fledspar and hence the enclosing rock whether igneous (like granite or pegmatite) or metamorphic (like gneiss).

Available literature on the subject of thermo-analysis of feldspars are not quite common. Among the contributors are: GOLDSMITH and LAVES 1954 (HEIER 1957), ROSENQVIST 1954 and KOHLER and WIEDEN 1954 (DEER *et al.* 1963). However, recent development in the manufacture of derivatographs has greatly increased the sensitivity of the instrument and made it possible to detect minor thermal reactions and accurately define the temperature of the reaction, besided losses or grains in weight can be estimated. Thus it became essential to reinvestigate the thermal behaviour of feldspars on the light of modern sophisticated equipment.

The present work is an investigation of the thermal behaviour of some feldspars separated from their granites or pegmatite occurring in the basement rocks of the Eastern Desert of Egypt.

Speculation is made concerning the temperature of formation of the enclosing acid rocks.

* Cairo, Almaza, New Cairo, 57 Abdel Monem Hafez St., Egypt

TECHNIQUES OF WORK

The used instrument in thermoanalysis is a Hungarian derivatograph with instrumental settings mostly used as follows: weight of sample around 0.5 g, crucible platinum, **TG** 20, **DTA** 1/2, **DTG** 1/5, heating rate 10 °C/min. **HGB** 100, **DGB** 100, spindle 3, stabilization volt 95, temperature range up till 1200 °C, furnace 2. Sometimes duplicate runs are done for each sample. Dry heat treatment is used. It is to be noted that interpretation of the differential thermal analysis curve (*dta*) is aided by both the derivative thermogravimetric (*dtg*) and thermogravimetric (*tg*) curves (KHALIL and EL SOKKARY 1976). The temperature rise curve (*t*) is shown as well together with these three curves.

The feldspars are separated from their corresponding granitic rocks in a high state of purity (above 95 %) by a method which is described in detail by EL SOKKARY (1970). Briefly, the method starts with grinding the rock, the powder is made to pass mesh sieve ranging between 80—100. Slimes are removed and then the powder is subjected to bromoform separation. The light fraction is then subjected to separation by a mixture of bromoform and decalin. Finally the desired feldspar is taken and run through a Frantz Isodynamic separator in order to remove the last traces of ferromagnesian minerals.

Six samples are prepared for thermoanalysis. Five of them with sample numbers (1—5) from the central and southern parts of the Eastern Desert of Egypt, while the last one (sample 6) is from U.S.A. Table 1 lists the analysed samples, their host rocks and localities.

TABLE 1.

Analysed feldspar samples with host rocks and localities.

Sample No.	Host rock	Locality	Separated Feldspar
1	Pink granite	G. Kadabora	Microline microper.
2	Pink porph. granite	Aswan	Microline microper.
3	Amazonite peg.	Um Groof	Amazonite perthite
4	White granite peg.	Hafafit	Microline perthite
5	Garnet peg.	W. Gemal	Oligoclase antiper.
6	---	U.S.A.	Orthoclase crystals

PRESENTATION OF DATA

Table 2 gives the most important reaction temperatures (four in number) of the six feldspars under study beside the total loss in weight of each sample expressed as per cent of sample weight. The first peak **P1** is an endothermic peak that ranges between 225—330 °C and is mostly due to loss of loosely absorbed water.

The second peak **P2** is an endothermioc peak that ranges between 425—600 °C and most probably represents the miscibility or mixing of the two alkali feldspars forming the perthitic or antiperthitic feldspar under study.

The third peak **P3** which is an endothermic peak ranging between 695—860 °C is due to phase transition of the plagioclase feldspar to some high form. The fourth peak **P4** is as well an endothermic peak ranging between 940—980 °C and is due to phase change of microcline to a high form. *Fig. 1* gives the *t*, *dta* and

dtg curves of one of the analysed feldspars No. 5, while *Fig. 2* gives the *dta* curves of the six studied feldspars from Egypt and U.S.A.

TABLE 2.

Reaction temperatures in centigrade (°C) of some feldspars from Egypt

Sample No.	P1	P2	P3	P4	Total loss %
1	280	580	860	980	1.09
2	330	560	695	970	0.86
3	250	580	720	955	0.30
4	310	520	825	>825	0.38
5	225	600	805	940	0.75
6	240	425	800	-	0.45

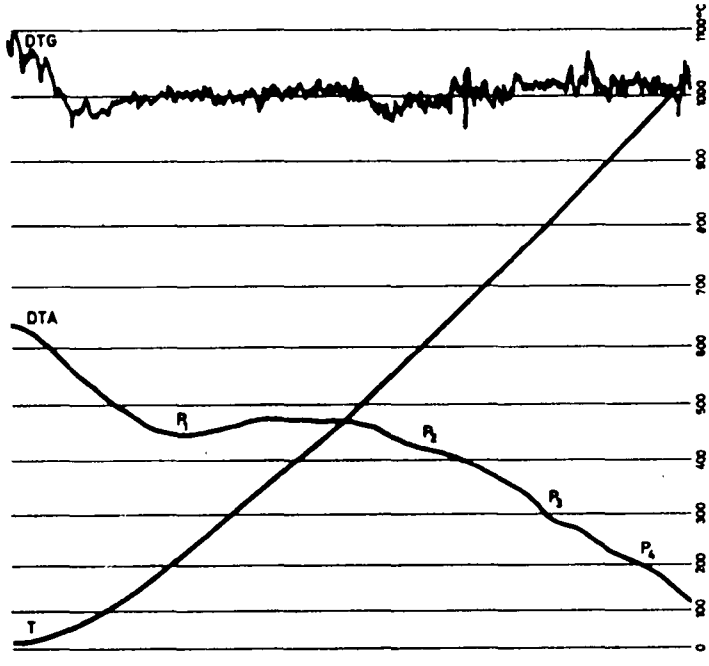

Fig. 1. T, DTA and DTG curves of one of the analysed feldspars, No. 5.

DEER *et al.* (1963) in their rock-forming minerals, the volume on framework silicates mentioned that the *dta* curves for alkali feldspars have generally been reported to show neither endo- nor exothermic peaks, though ROSENQVIST, 1954 noted in some cases a small endothermic peak at about 900 °C which he tentatively intepreted as representing a phase change. KOHLER and WIEDEN 1954 recorded a sharp endothermic peak at 820 °C for an albite from Rischuna, Switzerland.

HEIER (1957) reported that by dry heat treatment of microcline, a number of states with intermediate triclinicities are produced at 1050 °C, and after 720 hours

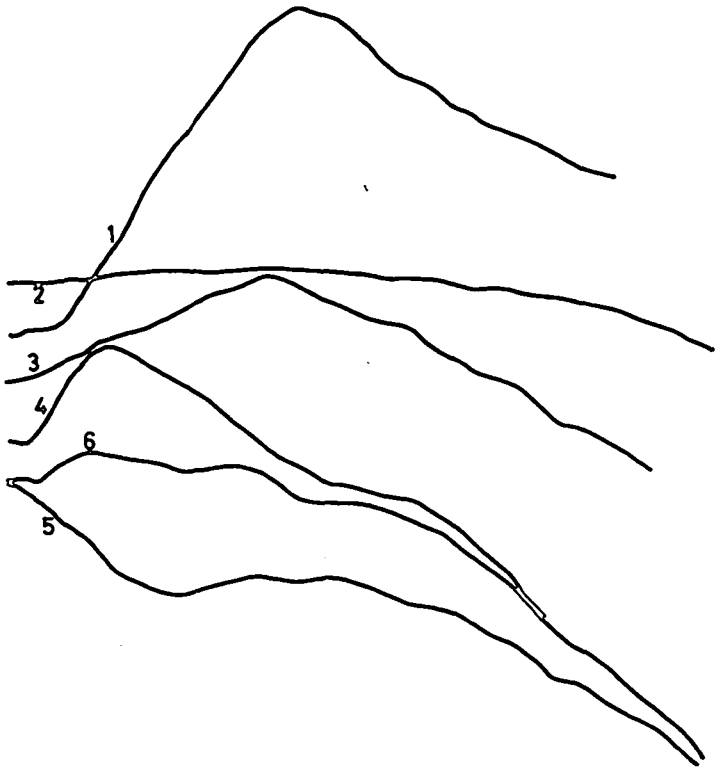

Fig. 2. DTA curves of the six studied feldspars from Egypt and USA.

of exposure at this temperature the monoclinic form is developed, GOLDSMITH and LAVES 1954.

Thus for alkali feldspars whether potassic or sodic some phase change occure between 900—1050 °C and for plagioclases (according to DEER *et al.* 1963) some change occurs at between 780—820 °C correlated with the change to the high temperature form.

THERMAL BEHAVIOUR OF EGYPTIAN FELDSPARS

As already stated in the previous section on presentation of data, four endothermic peaks are noted in the *dta* curves of the studied feldspars from Egypt. The first peak P1 takes the range 225—330 °C and is thought to be due to loss of loosely adsorbed water. As a matter of fact adsorbed water is supposed to be lost at temperature range 100—110 °C. Since the obtained endothermic peak occurs at certainly higher temperature range (225—330 °C), this gives some doubt that this peak is due only to loss of adsorbed water on the feldspars. Tentatively loss of interlayer water or constitutional OH of certain clay minerals or hydrated silicate minerals present as alteration product of feldspars may be postulated.

DEER *et al.* (1972) stated that: The dehydration of halloysite (member of the kaolinite group) proceeds in a number of stages. Some of its adsorbed water (surface and interlayer) is lost on heating to 110 °C as with any other mineral, but

the remainder comes off gradually and is not completely expelled until about 400 °C. The same reference (op. cit., p. 262) mentions that *dta* curves of illite show three endothermic peaks, one between 100—200 °C representing loss of loosely held water. Adsorbed water therefore can be driven off at temperatures greater than 110 °C according to the mentioned reference.

Thus the endothermic peak occurring at the temperature range 225—330 °C of the analysed feldspars may be partly due to loss of loosely adsorbed water and partly due to loss of combined water of certain alteration products of the feldspars. The more weathered the feldspar is, the more is its total loss of water as in the case with the feldspar sample No. 1 from Kadabora which gives 1.09 % total loss of weight.

Unmixing or miscibility temperature of the analysed Egyptian feldspars whether perthites or antiperthites range between 425—600 °C as denoted by the endothermic peak P2 on the *dta* curves. Evidence that this peak is correlated with miscibility of the two feldspars forming the perthite or antiperthite under study will be given later. The relation between feldspar composition, miscibility temperature and formation temperature will be dealt with as well in some detail in the next section.

The third endothermic peak that appears on the *dta* curves of the studied feldspars from Egypt ranges between 695—860 °C and is correlated with phase change to some high form of the present plagioclase feldspar whether constituting perthite or antiperthite.

It is to be noted that the analysed perthites and antiperthites behave as if they were mixtures of both potassic feldspar (microcline or orthoclase) and plagioclase feldspar (albite or oligoclase). This can account for the presence of the two endothermic peaks responsible for transition of plagioclase and microcline respectively to the high disordered forms. It seems that grinding the feldspar samples to below 100 mesh sieve size aided in liberating some extent the two feldspars (forming the perthite or antiperthite under investigation) from each other*. Thus the *dta* curve could show the transition temperature of both microcline and plagioclase to the high forms in one and the same curve.

The fourth endothermic peak P4 on the *dta* curves of these feldspars ranges between 940—980 °C, being concerned with the transition of microcline to high forms with intermediate triclinicities.

Consideration of feldspar sample No. 5 which is an oligoclase antiperthite with microcline as the included feldspar does not clearly record the high transition temperature peak P4 on the *dta* curve which is supposed to result from the included microcline, this may be due to its low content in the studied antiperthite. On the other hand feldspar sample No. 6 which is an orthoclase perthite from U.S.A. does not show this high transition peak because itself represents the high disordered form which is monoclinic orthoclase in this particular case.

Thus the present study on the thermal behaviour of some alkali feldspars from Egypt showed the presence of four endothermic peaks at the following temperature ranges: P1 at 225—330 °C, P2 at 425—600 °C P3 at 695—860 °C and P4 at 940—980 °C. This is to be compared with DEER *et al.* (1963) who stated that the *dta* curves for alkali feldspars have generally been reported to show neither endo- nor exothermic peaks.

* Particularly the pegmatite perthite samples No. 3 and 4 in which the two feldspars forming perthite are visible to the naked eye.

Table 3 gives the composition of four of the studied feldspars expressed in Or, Ab and An weight per cent, besides the same table lists the miscibility temperature of these feldspars as noted from the present *dta* curves and the formation temperature deduced from BARTH diagram relating the composition of the coexisting feldspars to their temperature of formation (DEER *et al.* 1972). The composition of the first three feldspars with sample Nos. 1, 2 and 3 is taken from EL SOKKARY (1970), while the composition of the fourth feldspar with sample No. 4 is also taken from EL SOKKARY (1975).

TABLE 3.

Composition of some studied feldspars in wt. % as related to miscibility temperature (M.T.) and formation temperature (F.T.) in centigrade (°C)

Sample No.	Or	Ab	An	M.T.	F.T.
1	57.5	40.4	2.1	580	680
2	64.2	34.0	1.8	560	600
3	61.5	36.6	1.9	580	620
4	67.8	30.9	1.3	520	580

Fig. 3. is a plot correlating the composition of the coexisting feldspare with their miscibility temperature as directly taken from the *dta* curves. The figure

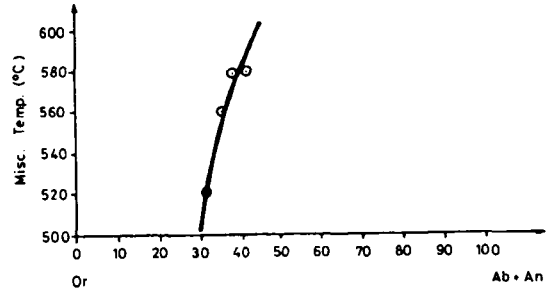

Fig. 3. Miscibility temperature vs. plagioclase content (Ab+An %) in some of the studied feldspars.

shows that this relation is a linear systematic one i.e. there is proportional systematic relation between the composition of coexiting feldspars and the miscibility temperature noted from peak **P2** of the *dta* curves. This assured that the endothermic peak **P2** on the *dta* curves of the studied feldspars is due to miscibility of the two feldspars forming the perthite or antiperthite under study.

Fig. 3. is correlated as well with isobaric equilibrium diagrams for the alkali feldspars in dry melts and at various pressures of water. This figure is to be compared here with *Fig. 4* taken from DEER *et al.* (1972) and represents the isobaric equilibrium relation for alkali feldspars at water pressure=5000 bars. The last curve shows that at a particular feldspar composition (1 Or : 2 Ab), the miscibility temperature becomes nearly the same as the liquifaction temperature at 5000 bars H_2O and equals 695 °C. In this particular case the position of the

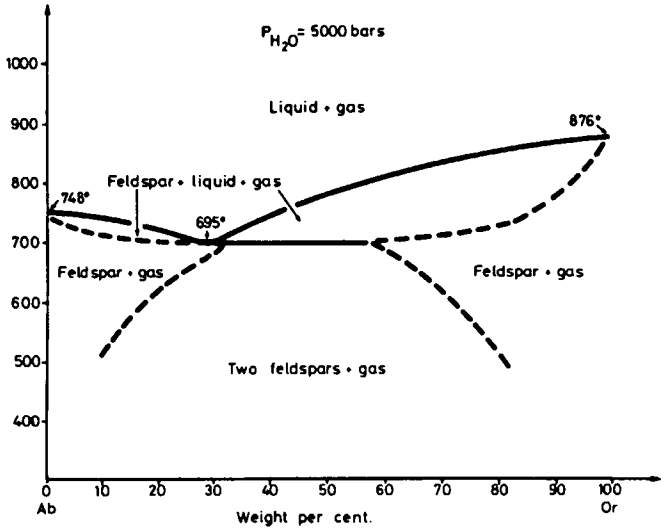

Fig. 4. Composition of feldspar in terms of Or and Ab per cent vs. temperature at 5000 bars H_2O pressure (DEER *et al.* 1972. p. 304).

solvus or unmixing curve directly underlines the solidus and liquidus curves without a gap in between.

Fig. 5. on the other hand gives the relation between formation temperature and miscibility temperature in some Egyptian feldspars. However, this relation is tentative since the curve is drawn with four points only, nevertheless it is promising. Thus the miscibility temperature as taken from the *dta* curve of the analysed feldspar can express its temperature of formation through the binary relation between these two temperatures.

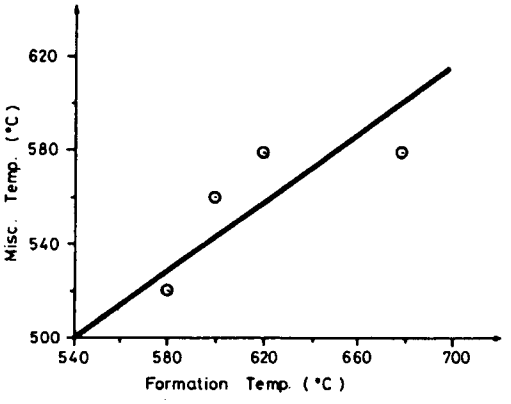

Fig. 5. Miscibility temperature vs. formation temperature in some of the studied feldspars.

DISCUSSION

Four endothermic peaks are noted in the *dta* curves of the analysed feldspar. The first peak P1 occurs at temperature range 225—330 °C. It can be correlated with weatherability or alteration of the feldspar sample i.e. the extent of this peak can be taken as a measure expressing the extent of alteration of the studied feldspar.

The second peak P2 occurring at temperature range 425—600 °C and is presumably due to miscibility of albite in microcline forming perthite or the reverse forming antiperthite. Evidence that this peak is correlated with miscibility of the two feldspars forming perthite or antiperthite under study is given. This evidence stems out from the fact that there is proportional systematic relation between the composition of coexisting feldspars and the miscibility temperature as noted from the *dta* curves. At a certain feldspar composition 1 Or : 2 Ab the miscibility temperature becomes nearly the same as the liquifaction temperature at 5000 bars of H_2O. Moreover, the miscibility temperature as it taken from the *dta* curve of the feldspar can express its formation temperature.

The third endothermic peak P3 ranges between 695—860 °C and represents transition temperature of plagioclase feldspar to the high form. Meanwhile, the fourth endothermic peak P4 ranges between 940—980 °C is concerned with the transition of microcline to high form.

Thus the study of the thermal behaviour of some feldspars from Egypt proved to be useful. This study can throw some light on the extent of weathering or alteration of the studied feldspar. Miscibility temperature of the two feldspars forming perthite or antiperthite is noted as well from the *dta* curves of the analysed feldspars. This miscibility temperature is shown to be correlated with temperature of formation of the feldspar. Transition temperatures of both plagioclase and microcline to the high forms are noted from the *dta* curve of the analysed feldspar which is useful as petrogenetic indicator.

HEIER (1957) could correlate the triclinicity (including low and high forms) of potash feldspars with their temperature of formation. It is already mentioned (EL SOKKARY 1970) that K- feldspars with low triclinicity (high monoclinic form or orthoclase) characterise metasomatic rocks or rocks undergoing chemical change or local redistribution to form porphyroblasts.

Thus the change from low feldspar forms to high ones or the reverse as indicated from the *dta* curves, has its bearing on the genesis of the enclosing rocks of feldspars.

ACKNOWLEDGEMENT

The writer would like to thank in particular Dr. A. M. ABDEL REHIM, Faculty of Science, Alexandria University for running some of the feldspar samples with the derivatograph.

REFERENCES

DEER, W. A., HOWIE, R. A. and ZUSSMAN, J. (1963): Rock Forming Minerals. Vol. 4: Framework Silicates. John Wiley and Sons, Inc.

DEER, W. A., HOWIE, R. A. and ZUSSMANN, J. (1972)$ An Introduction to the Rock Forming Minerals. Pub. Longmans, London.

EL SOKKARY, A. A. (1970): Geochemical studies of some granites in Egypt, U. A. R. Unpublished Ph. D. Thesis. Alex. Univ.

EL SOKKARY, A. A. (1975): Mineralogy and chemistry of a pegmatitic feldspar from Hafafit, Eastern Desert, Egypt. Arab J. Nucl. Sci. & Applic. **8.** 111—118.
HEIER, K. S. (1957): Phase relations of potash feldspar in metamorphism. J. Geol. **65**, No. 5.
KHALIL, S. O., EL SOKKARY, A. A. (1976): An yttrian spessartine from a pegmatite in the South Eastern Desert, Egypt. Bull. Fac. Sci. Alex. **XI**, No. 2.

Manuscript received, 30 October, 1991

Acta Mineralogica-Petrographica, Szeged, XXXII, 59—63, 1991

ORIGIN OF SOME MINERALS FROM THE CRYISTALLINE BASEMENT OF SZEGHALOM, EAST HUNGARY

T. M. TÓTH

Department of Mineralogy, Geochemistry and Petrology, József Attila University*

ABSTRACT

There are some minerals having unknown origin in the joints of the cryistalline basement at Szeghalom. The origin of them may have been attached either to a postvolcanic effect or a very low grade metamorphism. Based on mineralogical and geochemical investigations as well as tectonic considerations the priority of Laramian progressive metamorphism is proved.

INTRODUCTION

Hydrocarbon reservoirs, belonging to the Szeghalom Unit of crystalline basement of the Great Hungarian Plain have become very important for a few years in Hungary. These metamorphic rocks are strongly fractured and covered by undisturbed Neogene basin sediments. They consist mostly of gneisses, amphibolites and mica-schists. A fairly large part of the joints are filled by some unknown origin minerals, like zeolites, calcite and pyrite. The development of these minerals can be attributed to a very low grade metamorphism, perhaps some kind of postvolcanic effect, or sedimentary (diagenetic) events. It would be very important to know the real conditions of their origin, because these processes could involve certain changes in the permeability, porosity and other rock-physical features. The aim of this paper is to solve these problems, and giving an accaptable age of origination. The examined rock samples were collected from 9 boreholes (*Fig. 1*). In addition the description of 3 further borholes were utilized.

A REVIEW OF THE CRYSTALLINE BASEMENT AT SZEGHALOM

Szeghalom Unit can be found in the area of so called Biharian Autochton, at the northern border of the Hungarian part of Codru Nappe system. The rocks of the unit had suffered polymetamorphic effects. The first important event was a Barrow type, medium grade metamorphism (about 320—330 My ago) (SZEDERKÉNYI 1984). The main rock types related this effect are amphibolite, amphibole gneiss, biotite gneiss and biotite mica schist. Gneisses and mica schists have a sedimentary origin, like everywhere in Tisza Unit.

* H—6701 Szeged, P.O.Box. 651, Hungary

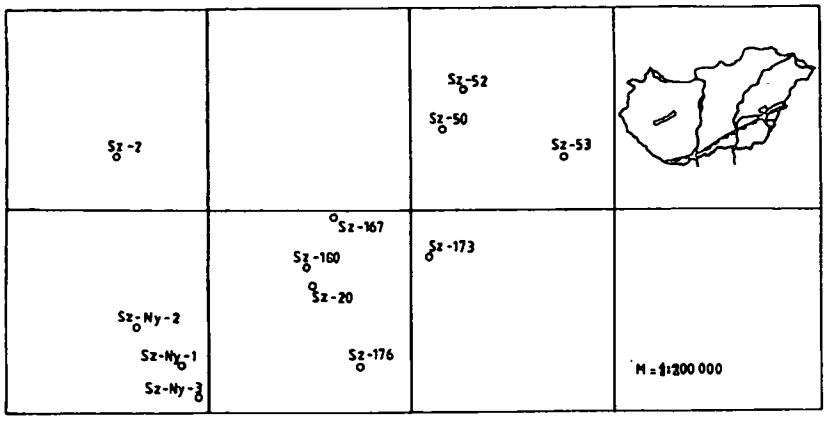

Fig. 1. The map of examined boreholes

During and after Variscan orogenesis a cosiderable portion of metamorphites was eroded, due to the fast uplifting. This elevation was attached of course to retrograde effects.

The third metamorphic event in the unit took place during the Alpine orogenesis; first of all in its Laramian phase. The maximum grade of this metamorphism can be characterized by greenschist facies, without any conspicuous alteration of the medium grade older metamorphic rocks.

After the Upper Cretaceous epoch this area was covered by the sea. The period of the transgression is not known exactly, but based on palinological data it can be ranged between Upper Cretaceous and Lower Miocene.

Several other important features of the rocks originated from the examinated boreholes are also observed, as followes:

— The main rock types are gneiss and mica schist with few intercalated amphibolites.
— The directions of the joints are about vertical, without any movement along them. The most of them are filled by intact minerals (without renewal). That is why the joint system is regarded to be a result of a single tectonic event.
— The joints don't continue in the overlying Paleogene and younger clastic basin sediment cover, at all. So, the tectonic effect must have followed by the erosion, which may have ranged between Upper Cretaceous and Lower Miocene.
— The joints are filled up with different minerals showing possibility of a hydrothermal origin. The recognized paragenesis is chlorite, illite, two habits of calcite, laumontite, pyrite and quartz.

MINERALOGICAL STUDY OF THE VEINLETS

I could not find any unexpected minerals neither with X-ray diffraction nor with infrared spectroscopy. However the listed minerals can offer several kind of suggestions about the origin.

The succession of minerals seems to be fix. The most important one from the wall-rock of the joint is illite —calcite — laumontite — pyrite. Some component from the succession may sometimes be missing. E.g. illite may has been replaced by chlorite. One can seldom find pyrite — laumontite — pyrite and quartz —

calcite — quartz paragenesis, too. But the first one seems to be widespread, thus the origin of the minerals must have attributed to the same effect.

All zeolites examined by X-ray diffraction or infrared spectroscopy turned out to be laumontite. (*Fig. 2.* and *3*). So the mineralization must have been attached to a postvolcanic effect or a very low grade metamorphism, because other environments where zeolites can be found, have been ruled out by paleogeogprahic setting, or there doesn't originate any laumontite. (MUMPTON 1981). The stability area of laumontite shows, that the real temperature of mineralization must have been between 150 and 280 °C. (*Fig. 4.* COOMBS 1959).

Fig. 2. IR spectra of laumontite

Pyrites, having a hydrothermal origin always contain characteristic trace elements, like Ni, Cu, Co, Zn, Au, Ag, Pb and As. Measuring of the abundance of these elements in the pyrites can be found in Szeghalom, it showed the absence or very low level of them, suggesting a not magmatic origin. Trace elements in the grey calcites are represented by Fe and Mn only, which have not any indicator roles.

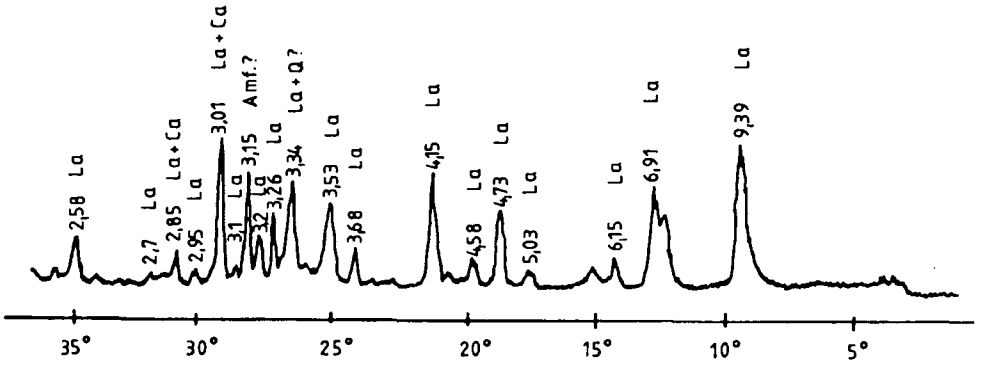

Fig. 3. X-ray spectra of laumontite
La — laumontite; Ca — calcite; Q — quartz; Amf — amphibole

Using crystallographic characters of the calcite and quartz it was tried to specify their forming temperature. There have been two types of calcite in the

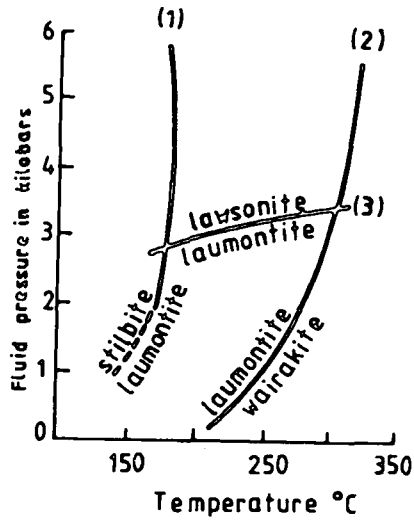

Fig. 4. The stability area of laumontite (after COOMBS 1959)

paragenesis: a romboeder habit and a lamellar one. Together with the characteristic shape of the quartz crystalls they suggest that the temperature of the origin may have been located into the upper levels of the hydrothermal interval, i.e. 200—280 °C.

THE POSSIBLE TERM OF THE ORIGIN

As one could see before, the origination of the joint system must have preceded the mineralization. It may have been linked either with nappe movements, had taken place during the Upper Cretaceous, or with the Neogene pull-apart movements.

There are some boreholes in the so called "Bihar Autochtonous Group" where Jurassic and Cretaceous sediments lie under the crystalline rocks, e.g. Endrőd-7, Füzesgyarmat-7, and -9 boreholes about 10 kilometres far from the Szeghalom Unit. These patterns suggest, that the "autochton" was in motion, and it took part in the Alpine nappe movements. So this phase must have had an effect on the metamorphic rocks of the Szeghalom Unit.

The main tectonic character of the Pannonian basin is determined by strike-slipe type faults during the Miocene. But the joint system of the basement at Szeghalom couldn't be followed in the neogene sediments. So, the tectonic effect, produced the fissures preceded the Miocene, sometimes Pre-Lower Miocene sedimentation, like other parts of the Hungarian Plain (HORVÁTH *et al.* 1988). So, the most possible age of the joint system may be Upper Cretaceous in relation to the Laramian phase of Alpine orogenesis.

CONCLUSION

The joint system of the metamorphic rocks at Szeghalom is filled up by minerals related to an exact paragenesis, which consists usually of illite, calcite, laumontite and pyrite. The precipitation of the minerals can be attached to a single phase after origination of the joint system, the temperature of it may have been located between 200 and 280 °C. Based on abundance of trace elements all magmatic effect may be ruled out with no doubt. The acceptable age of origination is probably the Laramian phase of Alpine orogenesis. So the proper reason of mineralization was the very low grade metamorphism and fracturing followed by a hydrothermal front related to the Laramian phase.

REFERENCES

COOMBS, D. S., ELLIS, A. J., FYFE, W. S., TAYLOR, A. M. (1959): The zeolite facies; with comments on the interpretation of hydrothermal syntheses. Geochim. Cosmochim. Acta pp. 53—108.

HORVÁTH, F., DÖVÉNYI, P., SZALAY, A., ROYDEN, L. H. (1988): Subsidence, Thermal, and Maturation History of the Great Hungarian Plain. AAPG Memoir, **45**, Oklamoha/Budapest pp. 355—373.

MUMTON, F. A., ed. (1981): Minerlogy and geology of natural zeolites. Mineralogical Soc. of America, Chelsea

SZEDERKÉNYI, T. (1984): Az Alföld kritályos aljzata és földtani kapcsolatai (The crystalline basin of Hungarian Plain, and its geological connections). D. Sc. Theses. Library of Hung. Ac. Sci. Budapest

Manuscript received, 10 November, 1991

Acta Mineralogica-Petrographica, Szeged, XXXII, 65—75, 1991

MINERALOGICAL CHARACTERISTICS OF THE WESTERN NILE DELTA COAST SEDIMENTS

N. M. EL-FISHAWI and A. A. BADR

Geol. Dept., Institute of Coastal Research*

ABSTRACT

In this paper, results of 3 years of heavy mineral investigations are presented. Fourteen annual nearshore profile samples were collected along the coast between Rosetta and Burullus. Each profile includes backshore, beach and nearshore samples up to 6 m depth. Coastal dune samples from east of Burullus are also studied.

The sediment of the Rosetta headland are characterized by the greatest concentration of heavy minerals. It declines in the central part and then relatively increases towards Burullus. The heaviest minerals decrease normal to the shoreline while the lighter ones increase.

High concentration of the heavy mineral at Rosetta and Burullus sediments may be related to:
(1) Contribution from offshore old sediments of classic Nile branches rather than the present Nile.
(2) Contribution from the land itself, where the dunes and backshore contain great amount of these minerals.
(3) These minerals are concentrated during severe coastal erosion.

INTRODUCTION

The heavy minerals are among the minerals of the parent rock surviving destruction. It may be supposed that the processes operating during transport of sediment would modify the composition by selective sorting. The selective transport of the heavy minerals plays an effective role in concentration and distribution of these minerals along the coast.

Previous studies of the mineralogy of the Nile Delta coastal sediments include those of SHUKRI (1950), NAKHLA (1958), MESHREF (1962), ANWAR and EL-BOUSIELY (1970), COASTAL EROSION STUDIES (1973), FRIHY (1975), RASHED (1978), EL-NOZAHY and BADR (1986), EL-FISHAWI and MOLNAR (1985) and AL-ASKARY and FRIHY (1987). Some of these pervious studies were carried out on whole samples.

The mineralogy of the nearshore profile sediments has been investigated. This study delineates the results of mineralogical examinations of the 14 annual nearshore profiles collected along the coast between Rosetta and Baltim (*Fig. 1*) during 1984—1986. Each profile includes backshore, beach and nearshore samples up to 6 m depth.

The mineralogical examination was also carried out on 5 sample series collected during 1987 from coastal dunes between Burullus and Baltim. Each series includes beach, windward side, top and leeward side samples.

The aims of the present study were:

* 21514 Alexandria, 15 Farana Street, El-Shallalat

(1) To investigate the distribution of the heavy minerals during the three years.
(2) To evaluate the changes of nearshore profile sediments along and normal to the shore.
(3) To trace the direction of sediment movement.
(4) To differentiate between coastal environments.

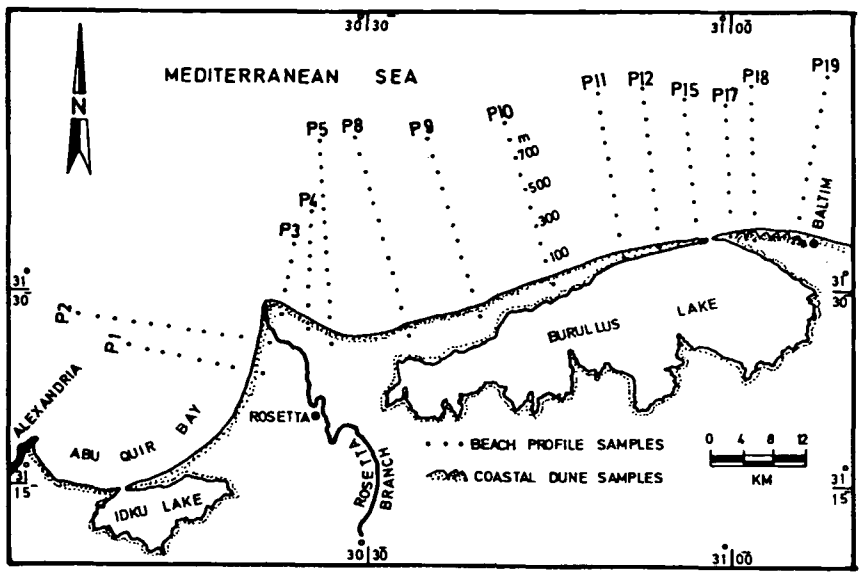

Fig. 1. Location map of the study area showing beach profile and coastal dune samples.

METHODS AND TECHNIQUES

The mineral analysis was applied on 3 Φ and 4 Φ size fractions (250 — 125 and 125 — 63 μm) which contain the highest heavy mineral residues. The samples were washed by stannous chloride and hydrocloric acid (10 %) to remove the iron oxide coatings on grains and carbonates. The heavy minerals were obtained by using bromoform (sp. gr. 2.89) separation technique, taking into consideration the precaution given by CARVER (1971) in order to obtain a satisfactory separation. The obtained heavy mineral fraction was washed by alcohol, dried, weighed and heavy mineral contents were calculated for each sample. The heavy mineral fraction was mounted in Canada balsam on a glass slide for microscopic investigation. Counting was carried out for 400 grains for each sample by a line-counting method. The frequency percentages of heavy mineral individuals were calculated.

HEAVY MINERAL RESIDUES

Table 1 shows the weight percent of heavy mineral residue of nearshore profile sediments and the total average in the 3 and 4 Φ fractions. It is observed that total average weight percent in the 3 Φ fraction ranges between 9.37 % and 17.89 %, while it is 42.42 % and 72.40 % in the 4 Φ fraction. This indicates that heavy minerales are more concentrated in the finer fraction.

TABLE 1.

Average weight percent of heavy mineral residues normal to the shoreline

Distance (m)	Weight percent of heavy minerals							
	3 Φ				4 Φ			
	1984	1985	1986	Average	1984	1985	1986	Average
Backshore	17.62	18.51	11.45	15.86	79.49	66.76	70.95	72.40
Beach	12.00	12.93	15.34	13.42	70.10	74.62	55.19	66.64
100	08.27	12.48	07.80	09.52	64.43	66.26	47.11	59.27
200	08.59	08.39	11.13	09.37	47.76	61.61	45.31	51.56
300	12.05	15.57	12.24	13.29	58.44	59.49	32.64	50.19
400	14.72	11.01	12.19	12.64	57.30	46.16	30.81	44.76
500	12.72	10.04	13.53	12.10	48.58	43.16	38.53	43.42
600	14.23	13.69	12.19	13.37	47.07	43.27	41.01	43.78
700	19.31	11.05	11.25	13.87	46.95	43.12	37.20	42.42
800	09.92	14.83	12.28	12.34	36.36	43.06	49.72	43.05
900	24.40	15.63	11.34	17.12	45.05	56.80	54.55	52.13
1000	20.57	—	15.21	17.89	43.67	—	48.21	45.94

Depending upon the weight percent of heavy minerals along the shore (*Fig.* 2), the studied area can be subdivided to:

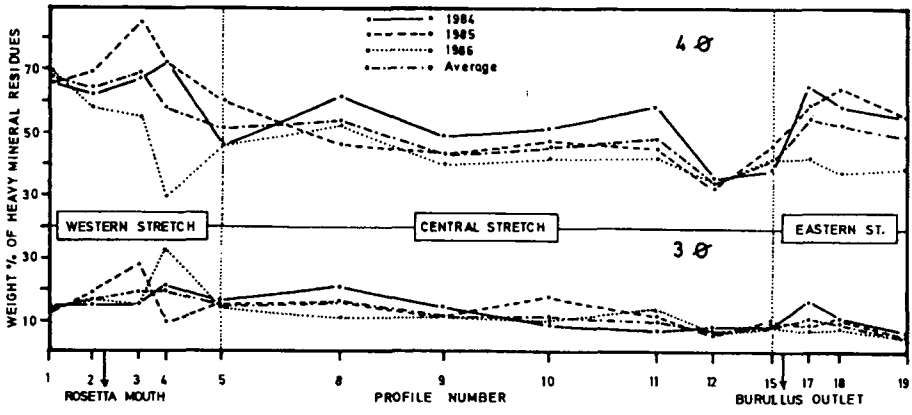

Fig. 2. The average percent of heavy mineral residues of the nearshore profile sediments.

Western stretch. It lies astride Rosetta mouth and contains profile Nos 1, 2, 3 and 4. The average weight percent of heavy minerals ranges between 52.41 % and 72,87 % in the 4 Φ fraction. The backshore, beach and the surf zone sediments are characterized by high concentrations of heavy residue. The reason for this high concentration may be related to the modification caused by the underflow action of the waves and sorting according to density and size during transportation and deposition.

The greatest concentration of heavy minerals is found towards the western stretch than the eastern one. The reason may be related to the westward dominate

littoral current (57 %; FANOS 1986). Furthermore; the relict bottom sediments of the old Canopic branch may have played an effective role in increasing the concentration of heavy minerals in the western side.

Central stretch. It extends between Rosetta mouth and Burullus outlet and includes profile Nos. 5, 8, 9, 10, 11, 12 and 15. This stretch is characterized by the lowest amount of heavy residues where the percent of heavy minerals ranges between 43.09 % and 49.09 % for the 4 Φ fraction.

The weight percent of heavy minerals shows high concentrations in the backshore, beach and the surf zone, then it fluctuates seaward. Some peaks of high concentrations are observed seaward.

Eastern stretch. It extends east of Burullus outlet and indcludes profile Nos 2, 17, 18 and 19. The weight percent of heavy minerals in the 4 Φ fraction ranges between 40.07 % and 60.34 %. The heavy residue indicates higher concentration in this stretch than in the central one.

An attempt was made to indicate the relationship between accretion or erosion and the weight percent of heavy mineral residue of the nearshore profile sediments. The western stretch (*Fig. 2*) has been subjected to severe erosion in 1985. Conditions during 1986 lead to minor erosion with some accretion (EL-FISHAWI and BADR, 1989). The effect of these features is reflected on the heavy mineral residues where high percents are recorded in 1985. The central stretch shows a higher rate of accretion in 1986 than in 1985. As a result, the percent of heavy mineral residues in 1985 is higher than that in 1986. This phenomenon is also observed in the eastern stretch. This leads to the conclusion that higher concentration of heavy minerals is recorded at the severely eroded beaches while low concentrations are encountered at less eroded or accreted beaches.

When the sea attains its maximum high level, the powerful waves constantly act on the submerged beach. The waves sort out light and heavy minerals which are not accessible during periods of low sea level. When the sea level reaches its original lower position, the lighter minerals have been carried out seaward while the heavier owner are left on the beach. It is observed that the beach erosion at Rosetta and Burullus areas plays a significant role in concentrating the heavy minerals in coastal sands. This is in agreement with RAO (1957) and COASTAL EROSION STUDIES (1973).

The distribution of weight percent of heavy mineral residues normal to the shoreline is illustrated in Table 1. For the 4 Φ fraction, the average weight percent of heavy residues of the backshore, beach, breaker zone (100—300 m distance) and seaward sediments of about 1000 m distance is found to be 72.40 %, 66.64 %, 50.19 % and 45.94 %, respectively. Therefore, the weight percent of heavy residues generally decreases seaward due to decreasing effect of the hydrodynamic forces.

COASTWISE VARIATION OF HEAVY MINERALS

The recorded heavy mineral constituents of the coastal sediments are composed of a great variety of minerals. The most common of which are opaques, amphiboles, pyroxenes, epidote, garnet, zircon, tourmaline, rutile, apatite, kyanite, monazite, staurolite, biotite, chlorite, glauconite and altered minerals.

Fig. 3. shows the frequency distribution for various heavy minerals in fractions 3 and 4 Φ. The following is a brief account on the distribution and behaviour of some indicative heavy minerals on the coastal sediment:

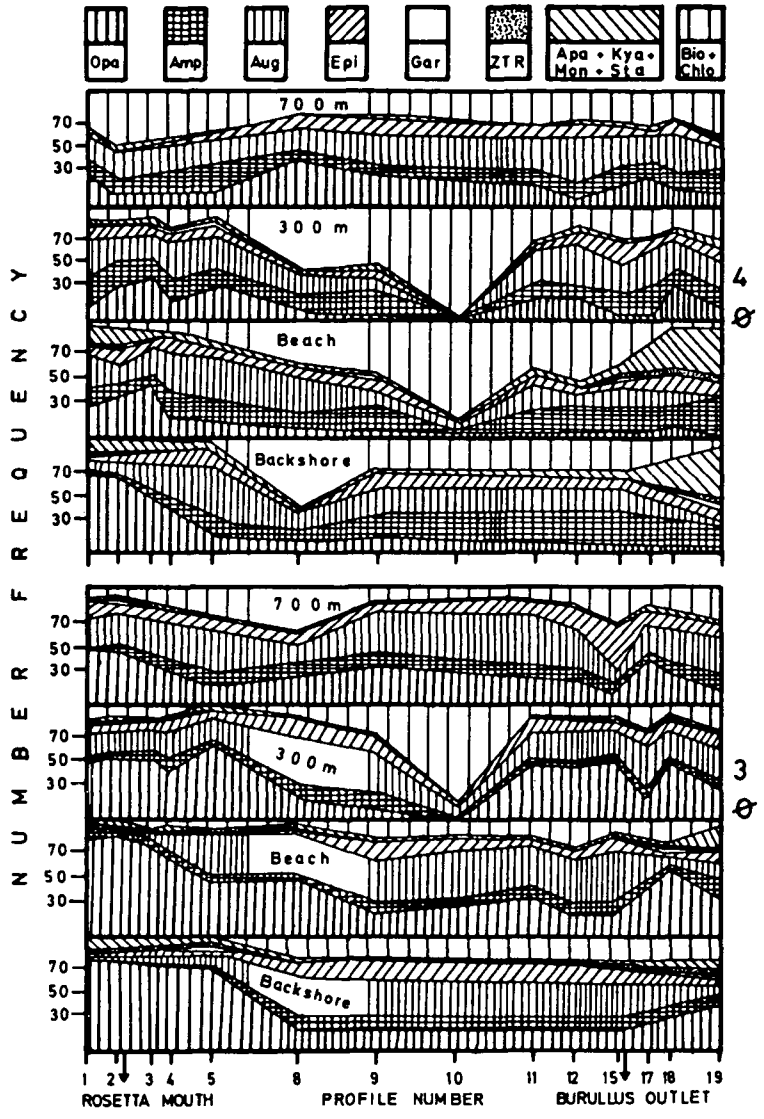

Fig. 3. Heavy mineral variations along the nearshore profile sediments, 1985.

The average percent of opaques ranges between 16.79 % and 35.13 % in the 3 and 4 Φ fractions, respectively which indicates high concentration in the finer size grade. The maximum concentration of opaques is observed astride Rosetta mouth (50.83 %) and decreased eastward attaining 34.62 % in the central stretch then it increases again attaining 40.12 % in the eastern stretch. The average percent of opaques decreases with time where it is found to be 19.85 %, 17.69 % and 12.83 % in the 3 Φ fraction and 39.72 %, 36.99 % and 28.69 % in the 4 Φ fraction of 1984, 1985 and 1986, respectively.

The average percent of amphiboles ranges between 18.82 % and 9.53 % in the 3 and 4 Φ fractions. This indicates that amphibole contents increase in the coarse fraction. It is observed that amphiboles increase eastward and westward from Rosetta mouth. In the 3 Φ fraction during 1986 amphiboles of the western, central and eastern stretches are found to be 16.62 %, 19.12 % and 22.74 %, respectively. This indicates that the content of amphiboles increases in a down drift direction. Such behaviour of amphiboles is the reverse of that of opaques. Similar trends were arrived at by PETTIJOHN and RIDGE (1933), LANGFELDER *et al.* (1968), RASHED (1978), EL-FISHAWI and MOLNAR (1985) and EL-NOZAHY and BADR (1986).

Average augite in the three stretches is higher in the finer fraction (4 Φ) than in the coarser one (3 Φ), being 24.30 % and 21.27 %, respectively. Augite concentrates astride Rosetta mouth and increases westward and eastward. The central stretch is characterized by higher concentrations around profiles 10 and 18 which are very near to the trace of the old Saitic and Sebennetic branches.

The average percent of garnet ranges between 0.46 % and 0.52 %. The garnet content in beach sands is higher than that in the nearshore area. Similar to opaques, the concentration of garnet decreases in a down-drift direction. The percent of garnet decreases with time where it is found to be 0.75 %, 0.50 % and 0.32 % in the 3 Φ fraction and 0.65 %, 0.41 % and 0.32 % in the 4 Φ fraction during 1984, 1985 and 1986, respectively.

The average percent of zircon + tourmaline + rutile (ZTR) ranges between 1.00 % and 1.38 % in the size 3 and 4 Φ fractions. These minerals are considered to be of the heaviest ones which increase shoreward. It is observed that these minerals decrease westward and eastward from Rosetta mouth. The average percent of ZTR decrease with time, being 1.59 %, 0.88 % and 0.52 % in the 3 Φ fraction and 2.39 %, 1.04 % and 0.71 % in the 4 Φ fraction during 1984, 1985 and 1986, respectively.

The percent of biotite and chlorite minerals ranges between 27.96% and 15.02% in the size 3 and 4 Φ fractions, respectively. Biotite and chlorite increase gradually away from Rosetta mouth, i.e., the minimum concentration is found astride Rosetta mouth. The reason may be related to the effect of the littorial current on sediment available for transportation. The concentration of biotite and chlorite in the central stretch is higher than those of eastern and western stretches. The reason may be related to the fact that these minerals are flaky and have not been able to be deposited in turbulent conditions but are carried away with currents and deposited in more calm areas. Similar result is arrived at by ANWAR and EL-BOUSEILY (1970), RASHED (1978), EL-FISHAWI and MOLNAR (1985) and EL-NOZAHY and BADR (1986). The average percent of biotite and chlorite increases with time, being 22.97 %, 25.67 % and 35.23 % in the 3 Φ fraction and 11.87 %, 14.84 % and 18.36 % in the 4 Φ fraction during 1984, 1985 and 1986, respectively.

VARIATION OF HEAVY MINERALS NORMAL TO THE COAST

Under the effect of waves and wind induced currents the deposition and concentration of heavy minerals are subjected to sorting processes. Therefore, an attempt was made to study the distribution of heavy minerals normal to the shoreline in fractions 3 and 4 Φ during the three years. Opaque and translucent heavy minerals vary significantly normal to the shoreline. *Fig. 4* shows the number frequencies for some indicative minerals.

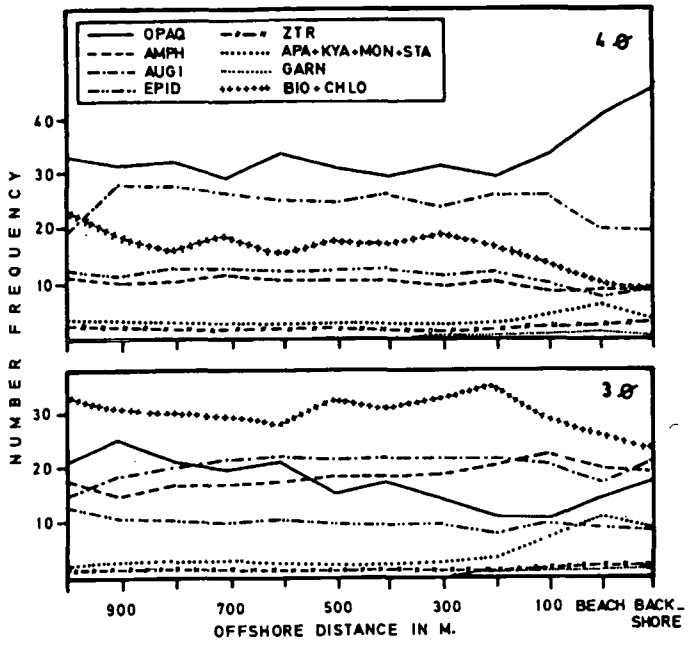

Fig. 4. Heavy mineral variations normal to the shoreline, 1984-1986,

Generally, the heaviest minerals increase in the beach and decrease seaward. For example, it is observed that the concentration of opaque minerals in size grade 4 decrease seaward. The average content of opaque minerals for backshore, beach, breaker zone (100 m distance) and nearshore zone (900 m distance) being 47.1 %, 41.7 %, 34.1 % and 31.2 %, respectively.

On the other hand, the concentration of opaque minerals in the 3 Φ fraction decreases from the backshore to the breaker zone, then it increases gradually seaward. The average content of opaque minerals in backshore, beach, breaker zone and nearshore zone is found to be 17.1 %, 14.2 %, 10.2 % and 24.4 %, respectively.

Generally, the biotite, chlorite, amphibole, augite and epidote minerals increase seaward with some fluctuations (*Fig. 4*). For example, the average content of biotite and chlorite minerals in the 3 Φ fraction for the backshore, beach, breaker zone (100 m distance) and nearshore zone (900 m distance) being 22.0 %, 23.2 %, 28.5 % and 37.7 %, respectively. The breaker zone sediments reveal a higher content of amphiboles and augite and a lower content of opaques, garnet and ZTR than in the beach sediments. Such a sorting may be related to the action of breakers which tend to concentrate the less heavies with the coarse sands. In the natural separation, the heaviest minerals (opaques, garnet and ZTR) were left on the beach surface due to the action of waves on the surf zone. This is in agreement with SWIFT *et al.* (1971), RASHED (1978), EL-FISHAWI and MOLNAR (1985) and EL-NOZAHY and BADR (1986). The low abundance of biotite and chlorite on the beach and breaker zone is due to their hydraulic properties which prevent their settling in the high energy condition. Similar result was arrived at by MOHAMED (1968).

An attempt was made to differentiate between windward, top and leeward side of the coastal dunes between Burullus and Baltim and to correlate between their average heavy mineral contents with that of the nearshore zone. The variation of the heavy mineral content along the coastal dunes is shown in *Fig. 5* while *Fig. 6* shows the frequency number of heavy minerals.

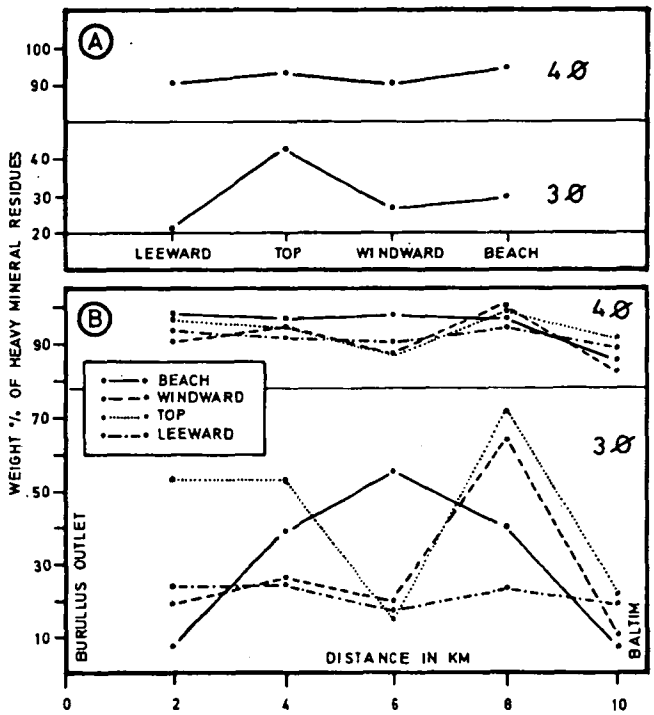

Fig. 5. The average percent of heavy mineral residues of the coastal dune sands. A. Variation normal to the shoreline. B. Variation along the shoreline.

Like in case of nearshore sediments, it is found that the weight percent of heavy mineral contents is higher in the size 4 Φ than in the 3 Φ. The weight percent of heavy mineral contents in beach, windward, top and leeward side of dunes are 29.78 %, 27.57 %, 42.75 % and 21.55 % in the 3 Φ fraction and 94.03 %, 90.08 %, 93.21 % and 90.56 % in the 4 Φ fraction, respectively. It is indicated that the heavy mineral content in the 3 Φ fraction increases from the beach to the top of dunes, where it attains the maximum values. Then it decreases in the leaward side (*Fig. 5*).

The percent of opaque, ZTR, augite and epidote minerals in the 4 Φ fraction is higher than that of the 3 Φ fraction. On the other hand, the percent of garnet, (apatite + kyanite + monazite + staurolite), (biotite + chlorite) and amphibole minerals increases in the 3 Φ fraction.

It is desirable to compare between the heavy minerals of the eastern nearshore stretch with those of the nearly dunes. The dune sands have higher contents of the total heavy residue, opaque, garnet, ZTR and (apatite + kyanite + monazite + staurolite) minerals than those of the backshore, beach and nearshore sands. This

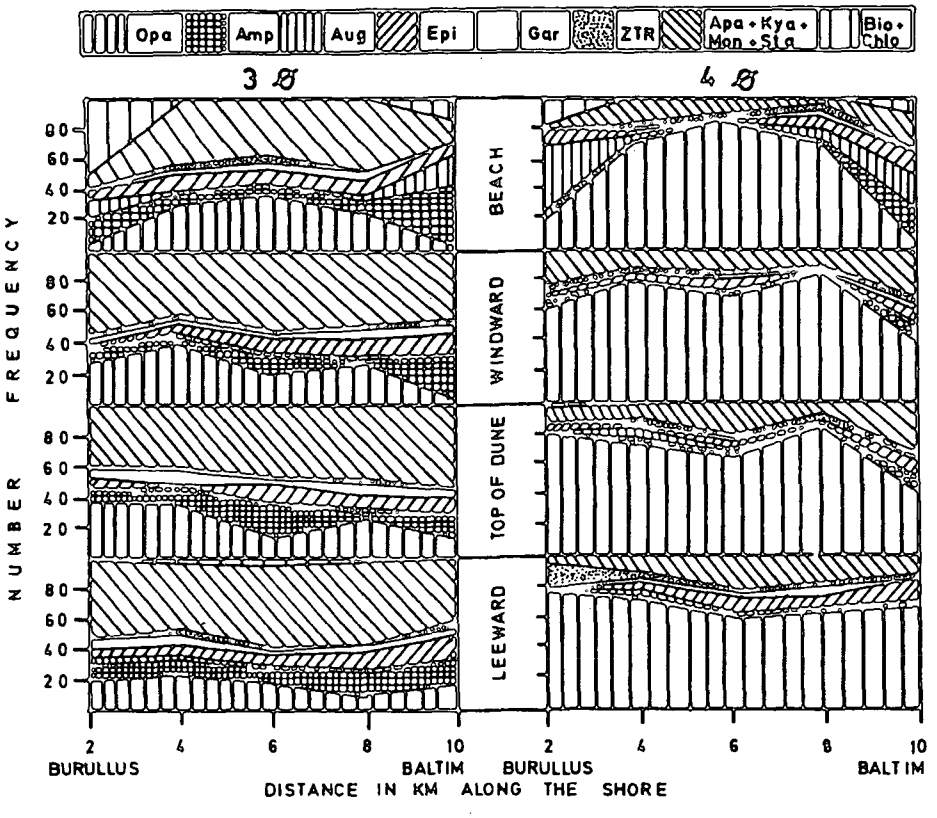

Fig. 6. Heavy mineral variations along the coastal dune sediments, 1987.

can be explained in such a way that the heavy minerals of the dunes may represent the lag concentrate, due to wind working over the dunes more than the beach and backshore, where wetness prevents much wind action. During this reworking the wind picks up the light minerals, which are largely removed, leaving the heaviest behind on the dunes. This is in agreement with STEWART, (1956), SHEPARD and YOUNG (1961), GILES and PILKEY (1965) and EL-FISHAWI and MOLNAR (1985).

CONCLUSIONS

(1) The longshore drift between Rosetta and Baltim, which is the principal mechanism of sediment supply, is towards the east. In that direction, the heaviest minerals (opaque, garnet and ZTR) decline while lighter ones (biotite, chlorite, amphibole, augite and epidote) generally increase.

(2) It is indicated that the severe beach erosion at Rosetta and Burullus areas plays a significant role in concentrating the heavy minerals in eroded beaches. On the other hand, high concentration of heavy minerals astride Burullus outlet may be related to the offshore supply of the sediments related to the old Nile branches (Saitic and Sebennitic).

(3) In the natural separation the heavy minerals vary significantly normal to the shoreline. The heaviest minerals increase in the beach surface due to the action of waves. On the other hand, the lighter minerals increase seaward due to their settling in a gradual decrease of energy levels.
(4) The breaker zone sediments reveal a higher content of less heavies and lower content of more heavies than in the beach sediments. Such a sorting may be related to the action of breakers which tend to concentrate the less heavies with the coarse sands. On the other hand, the low abundance of biotite and chlorite in the breaker zone is due to their hydraulic properties which prevent their settling in high energy conditions.
(5) The heavy mineral content increases from the beach to the top of dunes, where it attains the maximum values, then it decrease in the leeward side. The dune sands have higher contents of heaviest minerals that the backshore, beach and nearshore sands. The heavy minerals of the dunes may represent the lag concentrate, due to the fact that the wind working over the dunes more than the beach and backshore, where wetness prevents much wind action. During this reworking the wind picks up the light minerals which are largely removed, leaving the heaviest minerals behind on the dunes.

REFERENCES

ANWAR, Y. M. and EL-BOUSEILY, A. M., (1970): Subsurface studies of the black sand deposits at Rosetta Nile mouth, Egypt. Part II: Mineralogical studies. Bull. Fac., Alex. Univ. **10**, 141—150.

CARVER, R. E., (1971): Heavy minerals seaparation. In: Carver, R. E., ed., Procedures in Sedimentary Petrology. Wiley-Interscience, New York. 427—452.

COASTAL EROSION STUDIES, (1973): Detailed Technical Report. Project 70/581, UNDP/UNESCO/ASRT, Alex., 259 p.

EL-ASKARY, M. A. and FRIHY, O. E., (1987): Mineralogy of the subsurface sediments at Rosetta and Damietta promontories, Egypt. Bull. Inst. Oceano. Fish., Egypt. **13 (2)**, 111—120.

EL-FISHAVI, N. M. and BADR, A. A., (1989): *Volumetric changes of nearshore sediments between* Rosetta and Burullus, Egypt. International Union for Quarternary Research, INQUA, **11**, 39—42.

EL-FISHAWI, N. M. and MOLNAR, B., (1985): Mineralogical relationships between the Nile Delta coastal sands. Acta Miner. Petr., Szeged, **27**, 89—100.

EL-NOZAHY, F. A. and BADR, A. A., (1986): Mineralogy of the continental shelf sediments of Abu-Quir Bay, Northern coast of Egypt. Geojournal, **13 (4)**, 347—358.

FANOS, A. M., (1986): Statistical analysis of longshore current data along the Nile Delta coast. Water Science, Water Research Center, Cairo. **1**, 45—55.

FRIHY, O. E., (1975): Geological study of Quarternary deposits between Abu Quir and Rashid. M. Sc. Thesis, Fac. Sci., Alex. Univ. 103. p.

GILES, R.T. and FILKEY, O. H., (1965): Atlantic beach and dune sediments of the southern U.S. Jour. Sed. Pet. **35**, 900—910.

LANGFELDER, J., STAFFORD, D. and AMEIN, M., (1968): A reconnaissance of coastal erosion in North Carolina. Dep. of Civil Eng., North Carolina State Univ. Raleigh, 172 p.

MESHREF, W. M., (1962): Mineralogical and radiometric study for some black sand depostis on the Mediterranean coast. M.Sc. Thesis Fac. Sci. Ain Shams Univ.

MOHAMED, M. A., (1968): Continental shelf sediments of the Mediterranean Sea north of the Nile Delta in U.A.R. M. Sc. Thesis, Fac. Sci., Alex. Univ. 90 p.

NAKHLA, A. A., (1958): Mineralogy of Egyptian black sand and its application. Egyptian Jour. Geol. **2 (1)**, 1—22.

PETTIJOHN, F. J. and RIFGE, J. D., (1933): A mineral variation series of beach sands from Cedar Point, Ohio, Jour. Sed. Pet. **3**, 92—94.

RAO, C. B., (1957): Beach erosion and concetnration of heavy mineral sands. Jour. Sed. Pet. **27 (2)**, 143—147.

RASHED, M. A., (1978): Sedimentological and mineralogical studies of the coastal samples of Abu-Quir Bay, Alexandria. M.Sc. Thesis, Fac. Sci., Alex. Univ., 157 p.

SHEPARD, F. P. and YOUNG, R., (1961): Distinguishing between beach and dune sands. Jour. Sed. Pet. **31**, 196—214.

SHUKRI, N. M. (1950): The mineralogy of some Nile sediments. Quatr. Jour. Geol. Sci. London **105**, 511—534.
STEWART, H. B. (1956): Sediments and the environments of deposition in a coastal lagoon. Ph. D. Thesis, Calif. Univ. 355 p.
SWIFT, D. J. P., HILL, C. E. and MCHOME, J., (1971): Hydraulic fractionation of heavy mineral suites on an unconsolidated retreating coast. Jour. Sed. Pet., **41** (3), 683—690.

Manuscript received, 16 June, 1991

Acta Mineralogica-Petrographica, Szeged, XXXII, 77—83, 1991

CORRELATION BETWEEN COASTAL SEDIMENTS ALONG BURULLUS — DAMIETTA STRETCH, EGYPT

N. M. EL-FISHAWI

Geology Dept., Institute of Coastal Research*

ABSTRACT

The most conspicuous physiographic features of Egypt are the Nile Valley and the Nile Delta coast. The present study investigates the relationship between the coastal environments of the Nile Delta. The area of study lies between longitudes 30° 55' and 31° 52' E. It extends for about 87 km along the coast between Burullus and Damietta mouth. The coastal area could be subdivided into 5 environments according to the geomorphology and the nature of sediments. Coastal dunes, backshore, beach, breaker and nearshore are well developed here and extend in narrow strips up and down the length of the coast.

The coastal sediments are evaluated depending upon:

1. Mean grain size statistical parameter.
2. Correlation coefficient of mean grain size.
3. Shape measurement for sand grains (roundness value).
4. Number frequency for some species of heavy minerals.

The sediment characteristics of the coastal environments indicated strong relationship normal to the shoreline in moving from littoral to eolian environments. The dynamic forces effecting the coast play an effective role in sorting processes within each coastal environment.

INTRODUCTION

Sedimentary petrographers have attempted to use grain size determine sedimentary environments. A survey of the extensive literature on this subject illustrate the steady progress that has been made toward this goal. Many excellent contributions have been made, each providing new approaches and insights into the nature and significance of grain size distributions such as bivarian plot technique (MASON and FOLK 1958; FRIEDMAN 1967; MOIOLA and WEISER 1968; GINDY *et al.* 1982), log-probability curve technique (FULLER 1961; SPENCER 1963; VISHER 1969) and CM diagram technique (PASSEGA 1964).

One of the major problems in distinction between environments is that the same sedimentary processes occur within a number of environments and the consequent textural response is similar. In fact, the textural studies do not need to stand alone, but can provide a separate line of evidence to aid in identifying sedimentary environments.

The aim of the present study, therefore, is to determine quantitatively the same properties occur within the coastal sedimentary environments. Grain size, roundness and heavy minerals were used to investigate the relationship normal to the shoreline.

* 15 Faraana St., Alexandria 21514, Egypt

SAMPLING AND TECHNIQUES

The area under investigation lies between longitudes 30° 55' and 31° 52' E (*Fig. 1*). It extends for about 87 km along the eastern coast of the Nile Delta between Burullus outlet and Damietta mouth. During April 1980, the coast was surveyed and samples were collected at 3 km intervals. The sample net consisted of 28 transects at right angles to the coast. Each profile contained samples from coastal dune, backshore, beach, breaker and nearshore (6 m depth).

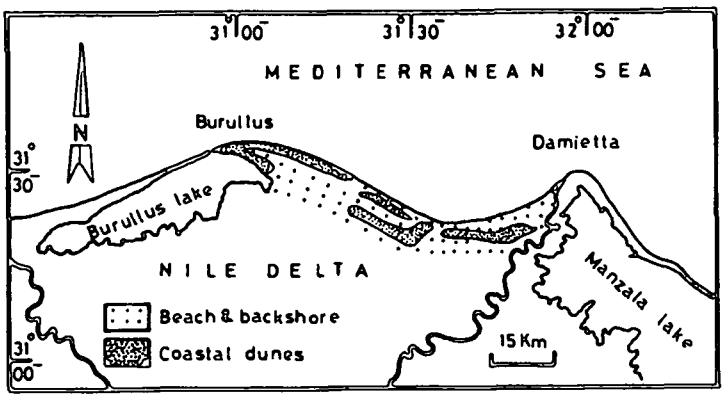

Fig. 1. Location map for the studied area.

Grain size analysis was carried out by the conventional sieving method with screens placed at one-phi intervals. About 50 g of sands was taken for analysis, using a mechanical shaker with a sieving time of 15 minutes. The sieve meshes give the class intervals -1, 0, 1, 2, 3, and 5 phi. Mean grain size proposed by FOLK and WARD (1957) was then obtained by using a suitable computer programme.

Quantitative expression of grain shape was used. BOGGS (1967) describes the use of grain photographs and the Zeiss electronic particle size analyzer (Zeiss TGZ 3) in the analysis of grain roundness. The roundness values of the present investigation were calculated according to this technique on grain sizes between -1 and 5 phi. About 100 grain photographs for each sample were used.

Fractions lying between 2 and 4 phi were used for heavy mineral study. The heavy minerals were separated by using the well-known bromoform separation technique. About 400 grains were counted in Canada Balsam for each sample. Number frequency was obtained for opaque, amphibole, pyroxene, zircon, tourmaline and rutile.

RELATIONSHIP BETWEEN COASTAL ENVIRONMENTS

The coastal area between Burullus and Damietta was chosen as a testing ground to determine the relationship among coastal sands of various environments. It represents 5 environments according to the geomorphology and the nature of the sediments. Coastal dunes, backshore, beach, breaker and nearshore are well developed here. All the coastal environments are normally sharply distinguished and extend in narrow strips up and down the length of the coast.

Mean grain size, roundness and heavy minerals for each environmental sands were averaged to represent a single profile in order to trace the variation normal to the shoreline.

Mean grain size:

The investigation of the data can be made by plotting the mean grain size with each environment normal to the shoreline (*Fig.* 2). A visual inspection of the mean size can be used as a preliminary interpretation of the energy conditions within each environment. It is generally true that the grain is coarser where the energy is greater.

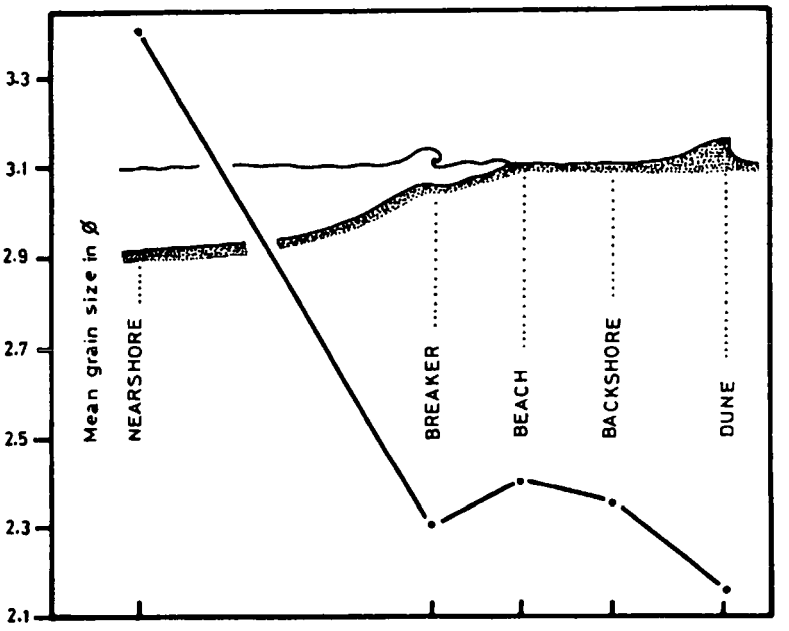

Fig. 2. Mean grain size relationships for coastal environments.

Finest mean grain size is occurred at the nearshore sediments. The mean size of 3.4 Φ indicates quite energy conditions up to 6 meter depth. In moving from the nearshore through the breaker to the beach, there is steady increase in the mean size. Mean grain size of 2.3 Φ shows a high energy levels where the waves break. Beach sediments become slightly finer (2.4 Φ) than the breaker sediments due to decreasing energy. On the other hand, backshore and dune sediments subject to the wind action. The mean grain size becomes coarser in moving from the beach through the backshore (2.35 Φ) and up to the dune (2.15 Φ). The wind action tends to select the coarser grains from the beach to be added to the backshore and dune sediments. So, it can be said that the energy conditions and levels play an effective role in relating the mean grain size to each coastal environment.

Correlation coefficient

EL-FISHAWI (1983) calculated the correlation coefficient of the mean grain size for each pair of some coastal sands. In the present investigation, this correlation coefficient is analysed after adding that of the nearhore sands. The correlation coefficient is calculated to measure the correspondence of the mean size to the fitted equation.

The relationship between coastal environments depends upon the presence of agreement or disagreement between adjacent or not adjacent environments which can be reflected from the value of the correlation coefficient. The sketch diagram in *Fig. 3* illustrates the results.

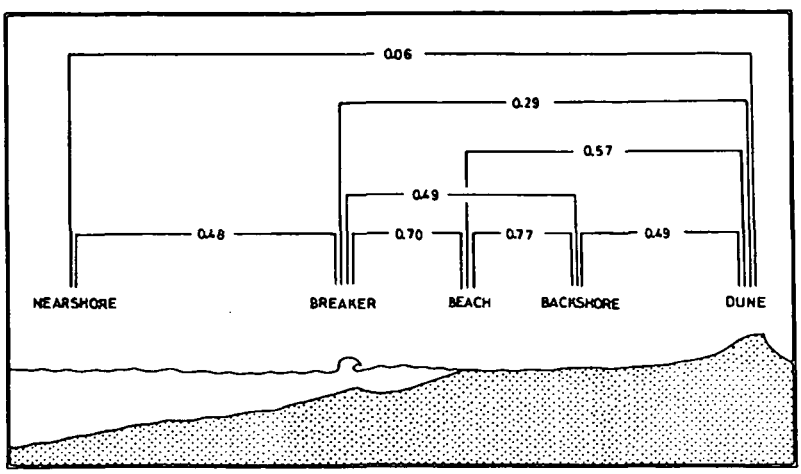

Fig. 3. Correlation coefficient relationships between each pair of mean grain size for coastal sands.

The correlation coefficient of the mean grain size for each pair of coastal environments provides a general view about the nature of the relationship. A relatively significant correlation coefficient is found between the adjacent environments; it ranges from 0.70 to 0.77 for the relations beach-breaker and beach-backshore. Insignificant correlation is appeared for the backshore-dune relation. In fact, the backshore is normally flooded with sea water. A distance of about 800—1000 m separating breaker from nearshore may explain the insignificient correlation between them. On the other hand, the relationship between each pair of separated environments is often weak; the correlation coefficient for the breaker-dune, breaker-backshore and beach-dune relations ranges from 0.29 to 0.57. At last, there is no relationship between nearshore and dune environments (r= 0.06) where the dynamic forces effecting them are totally different.

Grain shape:

Definite correlation between roundness and coastal environmental sands is established (*Fig. 4*). The line connecting the mean roundness for each environment indicates a marked increase in roundness in moving from nearshore (0.36) through breaker (0.45), beach (0.50), backshore (0.52) and up to dune sands (0.58).

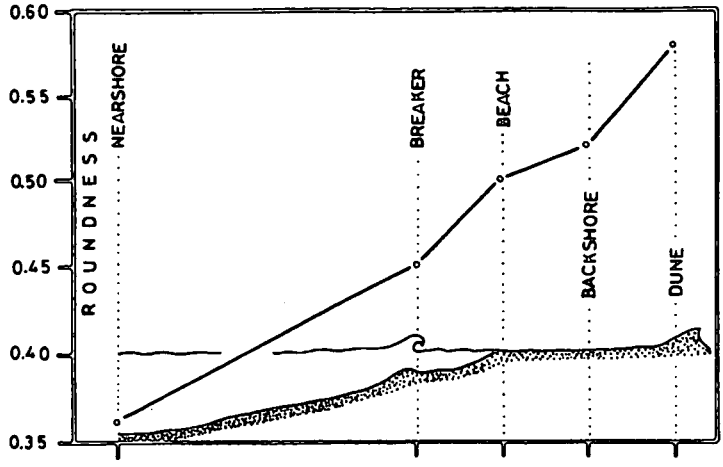

Fig. 4. Roundness variations normal to the shoreline.

Higher roundness in beach sands than in both nearshore and breaker sands may be due to the action of waves and swash in selecting the more rounded grains to be added to the beach. On the other hand, the improvement of roundness from the beach to the eolian sands may be related to the sorting processes of the wind action. The wind can select the more rounded grains from the beach to be rolled and finally added to the dune sands. Therefore, during the sediment transport normal to the shoreline, dynamic forces tend to sort the grains according to their shape. Moreover, it can be simply stated that the eolian action is more effective in shape-sorting processes than the wave action where the dune sands are rounder than the littoral sands.

Heavy minerals:

Number frequency for opaques, amphiboles, pyroxenes and zircon + tourmaline + rutile (ZTR) was examined as shown in *Fig. 5.* It is interesting to note that the number frequencies for opaques and amphiboles are inversely related to each other; as the opaques increase, the amphiboles decrease.

In moving from the nearshore landwards, opaque frequency decreases from 26.18 % to 14.49 % at the breaker and then increases with fluctuations to the beach (23.88 %), the backshore (18.06 %) and up to the dune (28.62 %). At the same direction, amphiboles and pyroxenes show inverse relation. Number frequency for zircon + tourmaline + rutile indicates a progressive increase from the nearshore (0.46 %) through the breaker (0.76 %), the beach (4.64 %), the backshore (1.77 %) and up to the dune (3.53 %).

High amphibole and low opaque contents at the breaker sands may be related to the action of breakers in concentrating the less heavies with the coarse sand. Wind action plays an effective role in concentrating the more heavies in dune sand. Lower content of amphibole and higher content opaque and ZTR in the eolian than in the littoral sands may be related to the fact that the wind working over the dunes more than the beaches; where wetness prevents much wind action.

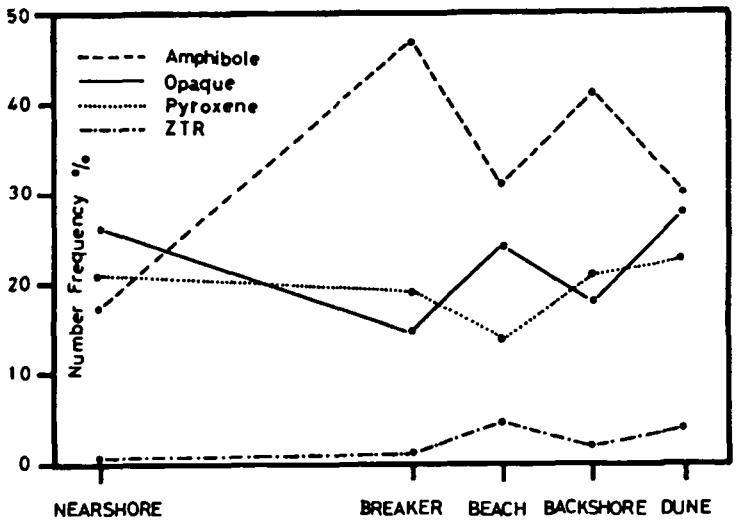

Fig. 5. Heavy mineral variations normal to the shoreline.

CONCLUSIONS

The sedimentary environments of the Nile Delta coasts display a strong correlation normal to the shoreline. The results of the mean grain size, roundness and heavy minerals analyses indicate a significant trend in moving from the littoral environments (nearshore, breaker and beach) to the eolian ones (backshore and dune). In moving from nearshore through breaker, beach, backshore and up to dune environments, it was found:

1. A progressive increase in mean grain size.
2. A strong relationship between each pair of adjacent environments and weak or no relationship between the separated environments.
3. A marked improvement of roundness value.
4. An increase of opaque and zircon + tournaline + rutile and a decrease in amphibole with some fluctuations.

Wave and surf actions in the littoral environments tend to select the coarser, the rounder and the heaviest mineral grains to be added to the beach. On the other hand, wind action in the eolian environments usually continue the sorting processes up to the sand dunes which contain the coarsest grains, the highest roundness value and high concentration of the heaviest minerals. Eolian action is more effective in sorting processes than the littoral action.

REFERENCES

BOGGS, S., 1967. Measurement of roundness and sphericity parameters using an electronic particle size analyzer. Jour. Sed. Pet., **V. 37**, pp. 908—913.

EL-FISHAWI, N. M., 1983. Sedimentary processes of the present Nile Delta coast sediments. Ph. D. thesos, József Attila Univ., Szeged, Hungary, 139 p.

FOLK, R. L. and WARD, W. C., 1957. Brazos River bar, a study in the significance of grain size parameters. Jour. Sed. Pet., **V. 27**, pp. 3—27.

FRIEDMAN, G. M., 1967. Dynamic processes and statistical parameters compared for size frequency distributions of beach and river sands. Journ. Sed. Pet., **V. 37**, pp. 327—354.
FULLER, A. O., 1961. Size characteristics of shallow marine sands from Cape of Good Hope, South Africa. Jour. Sed. Pet., **V. 31**. pp. 256—261.
GINDY, A. R., EL-ASKARY, M. A. and EL-FISHAWI, N. M. 1982. The skewness-median environmental discriminator for some recent and ancient sediments from Egypt. N. Jb. Geol. Palaont. Mh., Stuttgart. **H. 12**, pp. 705—722.
MASON, C. C. and FOLK, R. L., 1958. Differentiation of beach, dune and aeolian flat environments by size analysis, Mustan Island, Texas. Journ. Sed. Pet., **V. 28**, pp. 211—226.
MOIOLA, R. J. and WEISER, D., 1968. Textural parameters: an evaluation. Jour. Sed. Pet., **V. 38**, pp. 45—53.
PASSEGA, R., 1964. Grain size representation by CM patterns as a geological tool. Jour. Sed. Pet., **V. 34**, pp. 830—847.
SPENCER, D. W., 1963. The interpetation of grain size distribution curves of clastic sediments. Journ. Sed. Pet., **V. 33**, pp. 180—190.
VISHER, G. S., 1969. Grain size distributions and depositional processes. Jour. Sed. Pet., **V. 39**, pp. 1074—1106.

Manuscript received, 27 May, 1991

Acta Mineralogia-Petrographica, Szeged, XXXII, 85—90, 1991

GRINDING OF MECSEK COALS IN PRESENCE OF ADDITIVES, II.

É. SZÉKELY, R. SZÉKELY

Hungarian Hydrocarbon Industrial Research and Development Institute*

ZS. GYÖNGYÖS-RADNAI

Mecsek Coal Mining Co. Research Center**

ABSTRACT

Authors present the grinding experiments of refuses with coal in presence of additives at the Pécs Thermal Plant. They have examined the relation of the quantity of fine fractions and grain sizes during the process of crushing, as well as their changes as a function of the grinding time taking into consideration a mass proportion of coal-grinding body of 1:1 and 1:3.

INTRODUCTION

In power plants operating with pulverized coal the energy demand for the crushings of the fuel to be burned means a significant amount of costs, and that is the case with the Pécs Thermal Plant as well. The production of the fine grain fraction of about 74 μm in the process of the so-called drying grinding is carried out in ball crushers with high performance.

From the types of coal to burned at the Pécs Thermal Plant, i.e. /1/ slurry from Pécs, /2/ pulverized coal from Komló, /3/ rice call type "B" from Komló, and /4/ coal with refuse, we have dealt in the first part of this study with the grinding experiments in presence of additives of three different quality of coals. In the second part of this study we have investigated the refuse with coal applied for the appropriate adjusting of the caloritic value.

THE EXPERIMENTS

The grinding tests were carried out in laboratory mills simultanously, in five mills in presence of additives, in other five mills without additives. The mills were equipped with revolution adjusting device and with a counting system. We have performed the measurements with a mass proportion of coal: grinding body of 1:1 and 1:3, and with a revolution of 80 1/min. (The present revolution number corresponds to the optimal revolution number of the mill). The structure of the raw refuse with coal > 200 mm, therefore it is crushed (on a crusher type VEB Spezial

* H—2443 Százhalombatta, P.O.Box. 32. Hungary
**H—7629 Pécs, Keller J. u. 5. Hungary

Maschinenbau 46 typ 214) bellow the grain size of 2.5 mm. We have considered this size as standard.

The auxiliary material for grinding was dispersed on the surface of the air dry coal with spraying of a 10 % ($\frac{m}{m}$) water solution; the auxiliary material in this case was the sodium salt of the alkil-benzosulfonate — its trade name is: Evatriol, manufacturer Egyesült Vegyiművek. The concentration of the utilized auxiliary material was always 0.05 % ($\frac{m}{m}$) referring to the mass of the air dry coal.

The grain structure of all samples has been determined before grindings. This step was followed by an experimental grinding by changing the time and the mass porportion of coal:grinding body. The samples have been crushed for 5, 10, 20, 40 and 60 minutes. After the grinding time the grinding bodies were separated from the grinded material by means of a funnel fitted with filter. We have determined the grain structure distribution of the grinded material.

THE PROCESSING OF THE MEASUREMENT RESULTS

The measurement data were processed by means of regression analysis of grain size distribution according to ROSIN-RAMMLER-SPERLING-BENETT (RRSB) (2, 3).
The relation RRSB

$$R(x)=e^{-\left(\frac{x}{x}\right)^{n_e}} \tag{1}$$

taking into consideration

$$Y_i = \ln \ln \frac{1}{R_i} \tag{2}$$

$$X_i = \ln x_i \tag{3}$$

by correlation that is (X_i; Y_i) a linear regression can be applied to the pair (x_i; R_i) (it is the serial number of the measuring points), and for the new variable;

$$Y = a_d + bX \tag{4}$$

From the comparison results that:

$$n_e = b \tag{5}$$

$$X_0 = e^{-\frac{a_d}{n_e}} \tag{6}$$

$$a_d = \ln x_0^{-n_e} \tag{7}$$

On the basis of the relations (1)—(7) we have carried out the calculations by means of a program written for a computer PC-1500

$$B = 1 - \frac{f(x_i) - R_i^2}{R_i^2 - \frac{1}{N}(R_i)^2} \cdot 100$$

where the B value was denominated the linear accuracy of the measurement which is the square value of the correlation coefficient calculated by means of non logarithmic values of the corresponding points of the regression and measurement data. We have calculated furthermore the standard error of the linear regression on the basis of the relation:

$$S_f = \frac{f(X_i) - e_i^2}{N - 1} \tag{9}$$

The results are shown in Tables 1 and 2, where

n_e the factor of uniformity
a_d axis section
x_0 the characteristic grain size (mm)
B_{lin} the accuracy of determination (%)
S_f the standard errors of measurements (%)

belonging to given revolution number (n), mass proportion of coal grinding body (m_{COAL}/m_{BALL}) and grinding time (t).

TABLE 1.

Data of the regression analyses of grainsize distribution according to ROSIN, RAMMLER, SPERLING, BENETT
Model: refuse with coal

n $\left(\frac{1}{min}\right)$	$\frac{m_{COAL}}{m_{BALL}}$	t (min)	n_e	a_d	x_0 (mm)	B_{lin} (%)	S_f (%)
88	1 : 1	5	1.011	0.128	0.987	96.20	6.31
		10	0.989	0.094	0.909	96.10	6.25
		20	0.990	0.174	0.838	96.30	6.21
		40	0.988	0.285	0.749	97.27	5.35
		60	1.006	0.351	0.705	97.20	5.35
88	1 : 3	5	0.981	0.226	0.793	97.44	5.10
		10	0.967	0.324	0.714	97.50	5.06
		20	0.885	0.386	0.647	96.95	5.38
		40	0.847	0.424	0.606	97.17	5.05
		60	0.859	0.511	0.551	97.46	4.80

Figures 1, and *2,* show the dependence of the grinding time (t) and the factor of uniformity of coal:grinding body mass proportion of 1:1 and 1:3. It can be observed that n_e which characterizes the dispersity of the grinded material changes abruptly with the time during grinding in presence of additive (EVATRIOL).

Figures 3. and *4.* show the axis section (a_d) deriving from the distribution functions in function of the grinding time (t). The value of (a_d) is charcteristic for the proportion of the fine grain fraction of the grinded material. During the grinding with additive the fine grain fraction exceeds significantly the values obtained at the standard measurement both in case of mass porportion of coal:grinding body of 1:1 and 1:3.

TABLE 2.

Data of the regression analyses of grainsize distribution according to ROSIN, RAMMLER, SPERLING, BENETT

Model: refuse with coal + E

$n\left(\frac{1}{min}\right)$	$\frac{m_{COAL}}{m_{BALL}}$	t (min)	n_e	a_d	x_0 (mm)	B_{lin} (%)	S_f (%)
88	1 : 1	5	1.044	0.148	0.868	96.71	6.21
		10	1.067	0.232	0.804	96.48	6.33
		20	1.036	0.350	0.714	96.09	6.59
		40	0.974	0.424	0.647	96.19	6.45
		60	0.937	0.487	0.595	96.12	6.44
88	1 : 3	5	1.025	0.450	0.644	97.06	5.68
		10	0.981	0.498	0.602	97.02	5.58
		20	0.891	0.597	0.511	97.42	4.89
		40	0.853	0.650	0.466	97.19	4.96
		60	0.798	0.828	0.354	97.03	4.83

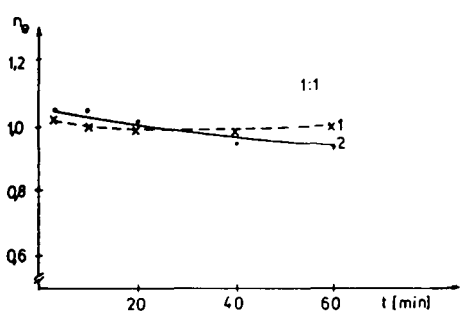

Fig. 1. Changes of the uniformity factor in function of the grinding time in case of refuse with coal

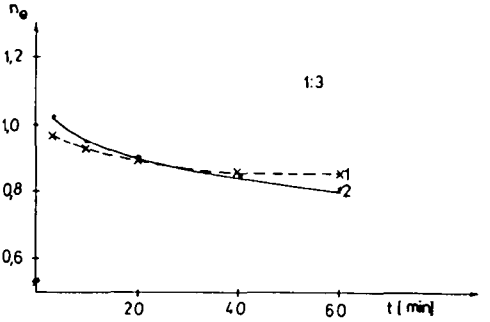

Fig. 2. Changes of the uniformity factor in function of the grinding time in case of refuse with coal

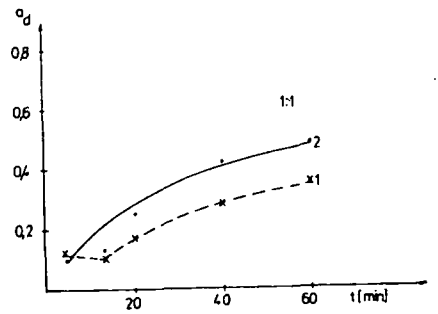

Fig. 3. Changes of a_d in function of the grinding time

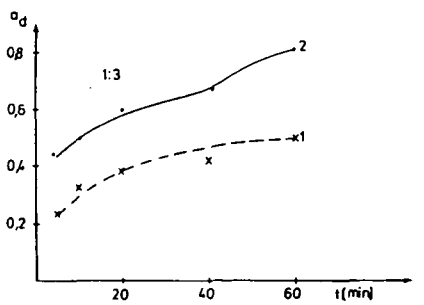

Fig. 4. Changes of a_d in function of the grinding time

Figures 5. and *6.* show the dependence of the grinding time for characteristic grain sizes (X_0). The effect of the surface active material is obvious in case of this comparison as well: the grain size is lower in each measuring point than in the case of standard grinding, namely the use of Evatriol increases the efficiency of the crushing.

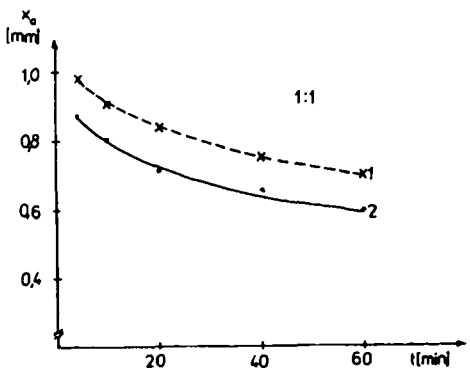

Fig. 5. Changes of the characteristic grain size in function of the grinding time

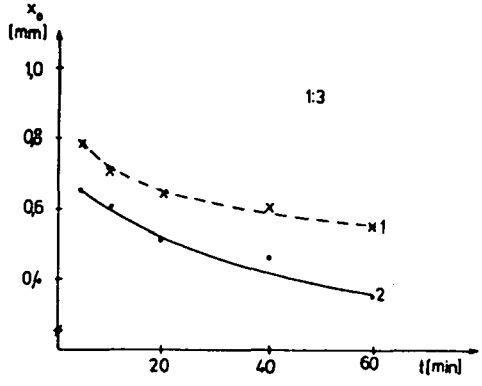

Fig. 6. Changes of the characteristic grain size in function of the grinding time

We have investigated the modification of grain size compared to the standard (ΔX_0) in function of the grinding time in case of grinding with additive. The relation obtained is shown in *Fig. 7.* On the basis of the diagram we have stated that in case of grinding with refuse with coal in presence of additive and with a mass porportion of coal:grinding body of 1:1 the decrease of grain size ranges from 13 to 20%, in case of a proportion of 1:3 from 18 to 55% during a given grinding interval.

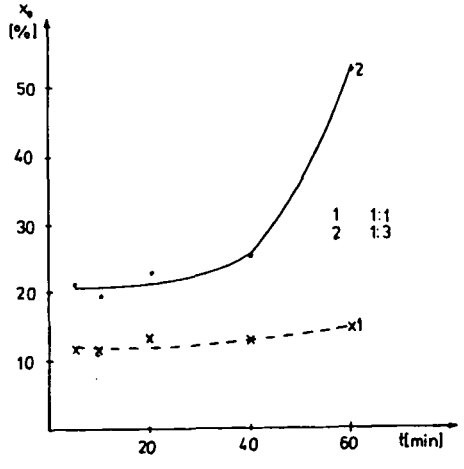

Fig. 7. Changes of the grain size compared to the standard grinding in function of the grinding time.

SUMMARY

In the second part of this paper we have presented the experiments carried out at Pécs Thermal Plant related to the grinding of refuses with coal in presence of additives. Furthermore we have investigated the distribution of grain size of the grinded material, the relation of the quantity of fine fractions during the crushing as well as the grain sizes and their changes function of the grinding time with a mass proportion of coal:grinding body of 1:1 and 1:3.

On the basis of our measuring results we have stated that in case of using Evatriol, an anion surface active material, the effect is favourable in comparison with the standard grinding without additive. During the same grinding time it is obtained a higher proportion of fine fraction and lower grain sizes, which show the increase in efficiency of the crushing.

When applying a mass proportion of coal:grinding body of 1:3 the results are more favourable in each case, however the capacity factor is more advantegous in case of a mass proportion of 1:1.

REFERENCES

SZÉKELY, É., SZÉKELY, R., GYÖNGYÖS-RADNAI, ZS. (1990): Grinding of Mecsek coals in presence of additives I. Acta Miner. Petr., Szeged. XXXI, (in press)

ROSIN, P., RAMMLES, E., SPERLING, K. (1933): Bericht 52 des Reichkohlenrats. Berlin.

BEKE, B. (1963): Apritáselmélet (Crushing-theory). Akadémia Press. Budapest. (in Hungarian)

Manuscript received, 28 December, 1990